

23/3/78

THE ORIENTATION OF SOLUTES IN STRETCHED POLYMER FILMS.  
ITS MECHANISM AND APPLICATION IN STUDYING THE  
ELECTRONIC TRANSITION MOMENT DIRECTIONS OF  
SOME PYRIMIDINES AND PURINES.

by CLIFTON C. BOTT

Department of Physical and Inorganic Chemistry,  
University of Adelaide.

Thesis presented for the degree of Doctor of Philosophy

January 1977

To the best of my knowledge and belief, this thesis contains no material previously published or written by another person, nor any material previously submitted for a degree or diploma at any University, except where due reference is made.

CLIFTON C. BOTT,

Department of Physical and Inorganic Chemistry,  
University of Adelaide.

January 1977

### ACKNOWLEDGEMENTS

I wish to thank Dr. T. Kurucsev for the opportunity of carrying out this research project in his laboratory.

The financial assistance of a Commonwealth Postgraduate Award is acknowledged.

I would also like to acknowledge financial assistance from the Department of Physical and Inorganic Chemistry, which enabled me to attend the 10th Australian Spectroscopy Conference.

I am grateful to Mrs. Del Hewish for typing the thesis, and Mrs. Judy Laing for drawing the diagrams.

C.C.B

Adelaide

January, 1977

## SUMMARY

The thesis consists of a general discussion of the orientation of aromatic molecules dispersed in stretched polymer films, followed by a study of the orientational properties and electronic transition moment directions of some pyrimidine and purine compounds in poly(vinylalcohol) films, as revealed by their infrared and ultraviolet linear dichroic spectra.

An analysis was made of the properties of average solute orientation through which the absorption dichroism is related to the electronic transition moment directions. Then, on the basis of results for some model compounds, the dependence of the average solute orientation on that of the polymer itself, and on the repulsive, electrostatic and dispersion interactions between solute and polymer was discussed. It was concluded that both dispersion and repulsive interactions contribute to orientation, but that the latter are not of significance unless solute molecules are elongated in shape along a clearly defined axis. Using a London approximation for the solute-polymer dispersion potential, a theoretical treatment of the solute orientation was given, and relationships between the molecular orientation and polarisability properties were derived.

The remainder of the work was concerned with the interpretation of the infrared and ultraviolet dichroic spectra of some derivatives of uracil, cytosine and xanthine. Preliminary studies were necessary to establish the assignment of the infrared carbonyl vibrational bands to specific vibrational modes, and to establish the molecular polarisability properties so that the observed and predicted orientation properties could

be compared. The orientational properties of the compounds were derived from the infrared dichroism of their carbonyl bands, and the moment directions of the lower electronic transitions from the ultraviolet dichroism below  $45000\text{ cm}^{-1}$ . The ambiguity in the interpretation of dichroism which is an inherent limitation in the stretched film method was resolved by comparison of the results for the electronic moment directions with the results of other spectroscopic techniques, and of molecular orbital calculations. Discussions were given of the relationship of the molecular polarisability properties to the observed orientation characteristics and of the efficiency of molecular orbital calculations of the PPP-CI and CNDO-CI types in describing the electronic transition characteristics of pyrimidine and purine molecules.

## CONTENTS

### CHAPTER ONE: INTRODUCTION

1

- 1.1 Molecular Transition Moments
- 1.2 Methods of Determining Transition Moment Polarisation
- 1.3 The Stretched Film Method

### CHAPTER TWO: DICHROISM AND ORIENTATION

15

- 2.1 Dichroism and Molecular Orientation
- 2.2 Orientation of Symmetric Molecules
- 2.3 Polymer Orientation
- 2.4 Empirical Models of Solute Orientation
- 2.5 Orientation Mechanisms

### CHAPTER THREE: EXPERIMENTAL AND MOLECULAR ORBITAL

#### CALCULATIONS

47

- 3.1 Materials
- 3.2 Preparation of Films
- 3.3 Spectroscopic Measurements
- 3.4 Experimental Errors and Difficulties
- 3.5 Aggregation
- 3.6 Molecular Orbital Calculations

### CHAPTER FOUR: CARBONYL STRETCHING VIBRATIONS OF

#### PYRIMIDINES AND PURINES

55

- 4.1 Carbonyl Stretching Modes
- 4.2 Solvent Effects

CHAPTER FIVE: POLARISABILITY PROPERTIES OF PYRIMIDINES

AND PURINES

65

- 5.1 Lorentz-Lorenz Equations for Isotropic and Anisotropic Media
- 5.2 Unit Cell and Molecular Polarisability Properties
- 5.3 Molecular Polarisabilities

CHAPTER SIX: ORIENTATION AND TRANSITION MOMENTS

OF URACIL AND CYTOSINE DERIVATIVES

73

- 6.1 Observed and Calculated Transitions of Uracil and Cytosine Derivatives
- 6.2 Dichroic Spectra
- 6.3 Orientation Axes and Orientation Parameters
- 6.4 Transition Moment Directions
- 6.5 Discussion

CHAPTER SEVEN: ORIENTATION AND TRANSITION MOMENTS

OF XANTHINE DERIVATIVES

93

- 7.1 Observed and Calculated Transitions of Xanthine Derivatives
- 7.2 Dichroic Spectra
- 7.3 Orientation and Transition Moments

APPENDICES

100

- A.1 Resolution of a Dichroic Spectrum into Components Polarised Along Orthogonal Axes
- A.2 Derivation of Equation 2.9
- A.3 Derivation of Series Expansions of the Functions A and B
- A.4 Proof of Some Identities Resulting from Equation 2.2

REFERENCES

107

CHAPTER ONEINTRODUCTION1.1 Molecular Transition Moments

The electric dipole transition moment relating the energy eigenstates  $\psi_1$  and  $\psi_2$  of a molecule is defined by the following integral

$$\underline{m}_{12} = \langle \psi_1^* | \sum_i e_i \underline{r}_i | \psi_2 \rangle$$

where  $e_i$  and  $\underline{r}_i$  are the charge and position operator of particle  $i$  of the molecule.

The measured intensity of an electric dipole induced transition between the two states, 1 and 2, is related to the transition moment  $\underline{m}_{12}$  (in esu) as follows (Kauzmann, 1957; Murrell, 1963):

$$4.319 \times 10^{-9} \int \epsilon d\bar{\nu} = f_{12} = 4.703 \times 10^{29} \bar{\nu}_{12} (\underline{e} \cdot \underline{m}_{12})^2 \quad (1.1)$$

where  $\epsilon(\bar{\nu})$  is the molar absorptivity at wavenumber  $\bar{\nu}$ ,  $f_{12}$  is the oscillator strength of the transition,  $\bar{\nu}_{12}$  is the energy difference between states 1 and 2 (in reciprocal centimetres), and  $\underline{e}$  is a unit vector in the direction of the electric field of the interacting radiation. The numerical factors incorporate various fundamental constants. In order to derive an expression for  $\underline{m}_{12}$  of practical use in dealing with electronic spectra, it is necessary to separate the contribution of electronic and nuclear motion. When the states are non-degenerate, this is achieved by means of the Herzberg-Teller expansion where the moment of a transition from the ground state to vibrational level  $\mu$  of electronic state  $i$  is represented as a sum of contributions from "pure electronic" moments (Ballhausen and Hansen, 1972; Hochstrasser, 1966)

$$\begin{aligned} \underline{m}(i,\mu; 0,0) = \underline{m}(i,0) \langle \lambda_{i,\mu} | \lambda_{0,0} \rangle + \\ \sum_{j \neq i} \frac{\underline{m}(j,0)}{\bar{v}_{0j} - \bar{v}_{0i}} \sum_{\eta} v_{\eta}^{j,i} \langle \lambda_{i,\mu} | Q_{\eta} | \lambda_{0,0} \rangle \end{aligned} \quad (1.2)$$

The  $\underline{m}(j,0)$  are "pure electronic" transition moments, evaluated for a fixed nuclear configuration (normally the ground state equilibrium configuration), the  $\lambda_{i,\mu}$  are vibrational wave functions,  $Q_{\eta}$  is the position operator of the  $\eta$ th vibrational normal mode and the  $v_{\eta}^{j,i}$  are the electronic matrix elements of the operator  $\partial V / \partial Q_{\eta}$ ,  $V$  being the potential energy term in the molecular Hamiltonian. The crude adiabatic approximation, in which nuclear motion is neglected, gives only the zeroth order term in eqn 1.2. For vibronic transitions where the zeroth order term vanishes, either because the electronic transition is forbidden, or because  $\lambda_{i,\mu}$  is non-totally symmetric, the contribution from the first order terms, if sufficiently large to be observed in the spectrum, comes from terms  $\underline{m}(j,0)$  having a different polarisation to  $\underline{m}(i,0)$ , and as a result an electronic band observed in toto, may be found to have mixed polarisation. Such vibronic coupling effects are not rare, and an excellent example is provided by an analysis of the stretched film dichroic spectrum of dibenzofuran by Bree et al. (1974).

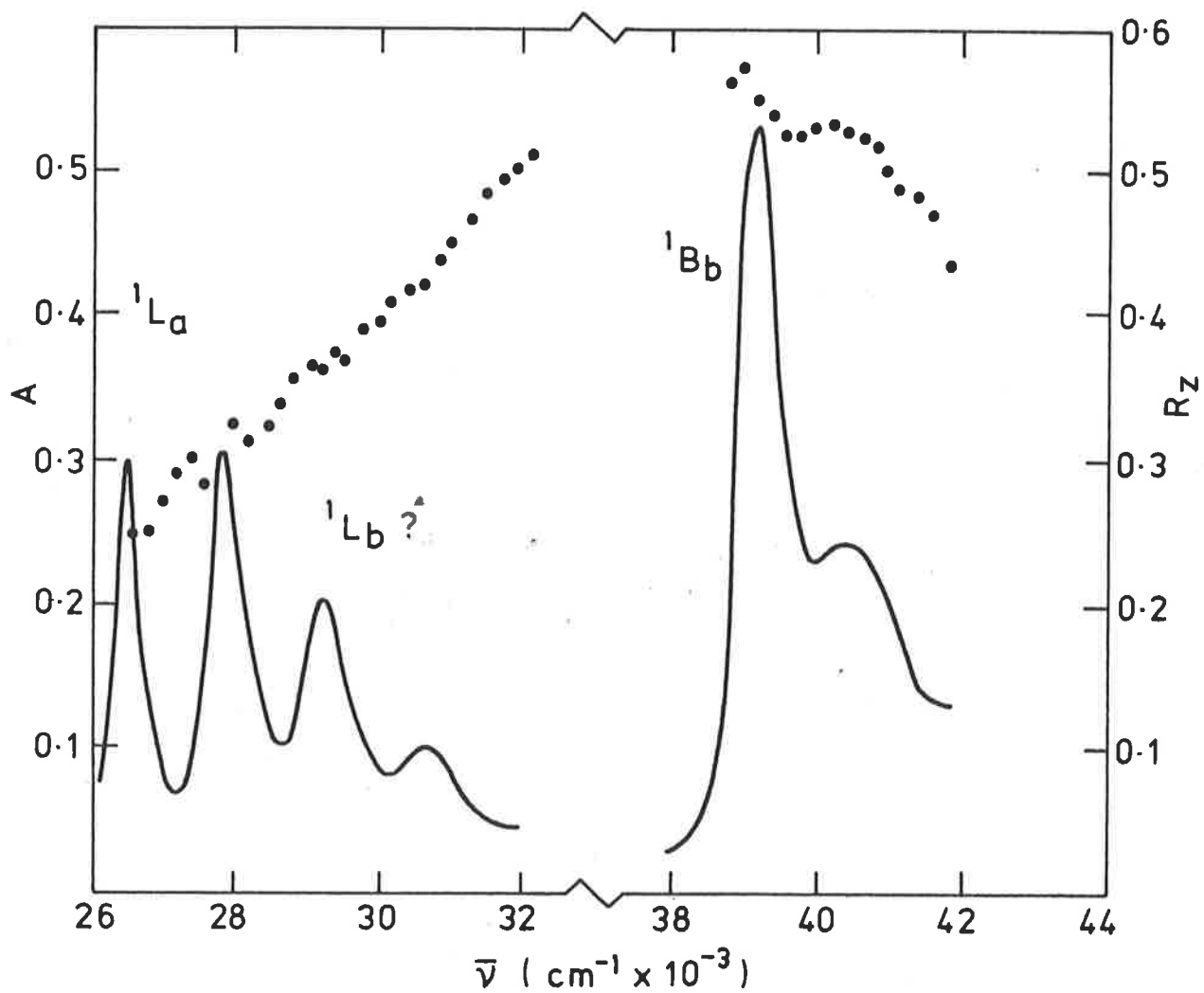
The molecules whose transition polarisations have been most thoroughly investigated belong to the  $C_{2v}$  or  $D_{2h}$  point groups, and their  $(\pi^*, \pi)$  (in-plane) transition moments are either parallel to the  $C_2$  axis, or perpendicular to it. For these molecules, the electronic transition moment,  $\underline{m}(i,0)$ , has the same polarisation at the observed vibronic origin,  $\underline{m}(i,0; 0,0)$ . On the other hand, polarisation of the  $(\pi^*, \pi)$

transitions of aromatic molecules with only  $C_s$  point symmetry, into which category come the pyrimidine and purine molecules studied, are symmetry determined only in that they are parallel to the plane of the molecule. Coupling can occur between  $\underline{m}(i,0)$  (of eqn 1.2) and all other  $(\pi^*,\pi)$  transitions  $\underline{m}(j,0)$ , through any in-plane vibration of the molecule. In such cases, therefore, the observed polarisation of a transition can be taken as representing the polarisation of a particular "pure electronic" transition only to the extent that vibronic coupling with other states can be neglected.

Changes in dichroism within electronic bands have frequently been adduced as evidence of "hidden" electronic transitions predicted by calculations, without a suitable investigation of vibronic coupling as an alternative explanation. Controversy over the dichroic spectrum of anthracene in the region 26000 to 32000  $\text{cm}^{-1}$  (fig 1.1) provides a good illustration. Calculations predict the presence of a weak electronic transition (labelled  ${}^1L_b$ ) at about 29000  $\text{cm}^{-1}$ , with the same polarisation as the intense  ${}^1B_b$  transition, and the large increase in dichroism observed in this area has been put forward as evidence of its existence (Inoue et al., 1971; Davidsson and Norden, 1972). However Michl, Thulstrup and Eggers (1974) concluded, after a thorough analysis of the available evidence, that the effect is due to a vibronic progression arising from coupling of the  ${}^1L_a$  and  ${}^1B_b$  electronic transitions by a non-totally symmetric vibration.

The importance of experimental determination of transition moment polarisations to molecular spectroscopy in general has been emphasised by Albrecht (1961) and Doerr (1966). Because they are directly connected with the symmetry or nodal properties

FIG 1.1 DICHROIC SPECTRUM OF ANTHRACENE IN POLY(ETHYLENE)



of transitions, they provide a good yardstick for the success of SCF-LCAO calculations in giving qualitative descriptions of electronic wave-functions. Transition energies and intensities are not informative in this regard.

There is additional interest in the transition moment directions of the pyrimidine and purine bases because of their importance in theoretical interpretations of nucleic acid spectra, and because of the importance of such interpretations in investigating the structure and function of nucleic acids. The hypochromism of absorption, the circular dichroism (CD) and optical rotatory dispersion (ORD) spectra of nucleic acids and simpler oligomers, and the degenerate exciton coupling in dinucleotides are all related to molecular conformation. In theories of hypochromism (Devoe, 1965; Rhodes and Chase, 1967), optical activity (Tinoco, 1967; Johnson and Tinoco, 1969) and degenerate exciton coupling (Joyce and Kurucsev, 1974), this relationship is expressed in equations involving the vector properties of the electronic transition moments of the constituent pyrimidine and purine bases. Therefore in order to test the validity of the theories by comparison with experiment, and in order to apply them to interpreting the spectroscopic measurements, it is first necessary to elucidate the transition moment polarisations of the bases.

A knowledge of transition moment polarisations also makes possible the use of linear dichroism as a means of studying the anisotropic interactions between molecules. Of interest in this laboratory is the binding of various acridine derivatives and "reporter" molecules to DNA. By measuring the linear dichroism of absorbance it has been possible to establish

the relative orientations of the nucleic acids and those acridine molecules whose transition moments are determined by symmetry, and draw conclusions on the nature of the binding (Kelly and Kurucsev, 1976). Interpretation of results for the non-symmetric molecules is contingent on the development of a method of determining their transition moment polarisations.

### 1.2 Methods of Determining Transition Moment Polarisations

It is seen from eqn 1.1 that, for a sample of molecules of fixed orientation, the integrated absorptivity associated with a vibronic transition gives a measure of the angle between the direction of the transition moment and the polarisation of the light beam. If the orientation of the molecules in relation to the experimental system is known, the magnitude of the direction of the transition moment in relation to the molecule may be derived, although the sign may be ambiguous because the geometric term in eqn 1.1 is quadratic, and it is usually not possible in experimental situations to adjust the polarisation direction  $\epsilon$  in order to maximise the scalar product.

In general, it is not possible to measure the integrated absorptivity of a vibronic band of an oriented sample of molecules. For practical purposes, eqn 1.1 is put into a form where ratios of integrated intensities only appear, and it is assumed that these may be adequately replaced by ratios of absorbances at a suitable wavenumber.

The most common, and successful, method of determining transition moment directions involves measurements on single crystals (PSCS). In principle, because the crystals can be aligned with high accuracy relative to the optical system, the

transition moment directions can be determined from absorbance measurements if the orientation of the molecules in relation to the external form of the crystal is known. Where crystals with a sufficiently small cross-section cannot be prepared, it is the practice to measure instead polarised reflectance spectra, absorbance being derived either by means of formulae from classical electron theory (Callis and Simpson, 1970), or by a Kramers-Kroenig transform (Chen and Clark, 1969). Another alternative, which has not been applied to pyrimidines or purines, involves use of mixed crystals (Bridge and Gianneschi, 1976). The range of compounds which can be studied by PSCS is limited to those whose crystals are sufficiently large and well-formed for spectrophotometry. Furthermore, it has been emphasised by Devoe (1971), that transition moment directions of the unit cell can be considerably dependent upon exciton coupling, and it is therefore uncertain to what degree PSCS measurements reflect the properties of isolated molecules which are desired.

The method of photoselection (Albrecht, 1961) is also frequently used in studying transition polarisations. The "photoselected" molecules are excited by polarised radiation, and polarisation of emission at a particular wavenumber is monitored for a spectrum of exciting radiation. The relative polarisations provide a measure of the relative directions of the absorbing and emitting transition moments. The results are qualitative (Callis and Simpson, 1970) because considerable randomisation of molecular orientations occurs during the lifetime of the excited states.

Other techniques, with the exception of the stretched film

method which is discussed in the next section, have not had wide application: bibliographies have been given by Doerr (1966) and Thulstrup, Michl and Eggers (1970). The use of nematic liquid crystals as orienting solvents (Sackmann and Moehwald, 1973) is of interest, owing to its similarity to the stretched film method. In both cases, solute orientation arises from anisotropic interaction with an oriented matrix and as a result, there is a useful similarity in theoretical treatments of orientation in the two media.

Numerous calculations of the SCF-LCAO type (Roothaan, 1951) have been made for aromatic molecules, and the increasing elaboration of such calculations is a major impetus for experimental work. The important types of calculation can be put into three categories, in increasing order of complexity: PPP-CI, CNDO-CI and "ab initio" calculations. The PPP calculations (Parr, 1964) make use only of the p atomic orbitals which contribute directly to the pi-electron system of the molecule; the CNDO-CI calculations (Pople and Beveridge, 1970) use all valence atomic orbitals. The singly excited ( $v \leftarrow \mu$ ) configurations consist of Slater determinants of the molecular orbitals as follows:

$$\Phi_{SE} = 2^{-\frac{1}{2}} \{ |\phi_1 \bar{\phi}_1 \dots \phi_\mu \bar{\phi}_\nu \dots \phi_n \bar{\phi}_n| - |\phi_1 \bar{\phi}_1 \dots \bar{\phi}_\mu \phi_\nu \dots \phi_n \bar{\phi}_n| \}$$

Configuration interaction (CI) consists of further variational calculations to find optimum wave functions which are linear combinations of the  $\Phi_{SE}$  states, and significantly improves the success of CNDO calculations in predicting electronic spectra (Hug and Tinoco, 1973).

Ab initio calculations make use of a full set of occupied Gaussian atomic orbitals (Snyder et al., 1970). Although they are more satisfactory in that all matrix elements involved in

the calculation are evaluated explicitly rather than by "semi-empirical" means, extensive CI is not possible for complex molecules because of the enormous length of the calculations required, and as a result the calculated transition energies are excessively high.

All three methods of calculation employ a fixed molecular geometry, and as such are at the level of the crude adiabatic approximation. Recently vibronic calculations for benzene (Ziegler and Albrecht, 1974) and some aza-analogues (Chappell and Ross, 1976) have been published, and calculations for more complex molecules are in progress (Ross et al., 1976). The results indicate that the effects of nuclear motion are considerable. Since a knowledge of the normal modes of vibration of the molecule is required for such calculations, they are not at present applicable to pyrimidines and purines, whose normal modes are unknown.

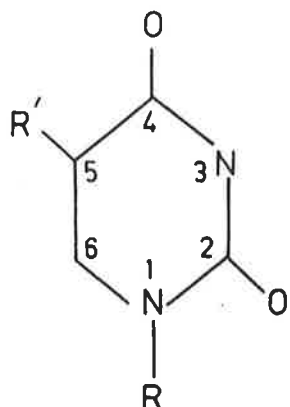
Evaluation of the performance of calculations in predicting transition moment directions has been hampered until recently by the lack of experimental data. A considerable body of data has now become available from stretched film dichroism measurements involving molecules of moderate complexity consisting of aromatic hydrocarbons (Kole and Michl, 1974; Thulstrup, Case and Michl, 1974; Thulstrup et al., 1975), derivatives having one or two amino-substituents (Downing and Michl, 1972; Michl, Thulstrup and Eggers, 1974; Thulstrup et al., 1976) and heterocyclic analogues containing one or two hetero-atoms (Muller et al., 1974; Michl and Eggers, 1974). Results of PPP-CI calculations in these cases were in satisfactory agreement with experimental results.

Results of PSCS and photoselection determinations of transition moment directions of pyrimidines and purines are summarised in table 1.1. The angles quoted are defined according to a generally accepted convention (Devoe and Tinoco, 1962) which is illustrated in fig 1.2. The second observed transition of uracils is labelled "III" for reasons discussed in Chapter Six. Fig 1.2 shows also the structures of the derivatives of uracil, cytosine and xanthine of interest in this work. Apart from one exception, discussed in Chapter Seven, the tautomeric forms of the compounds are as shown. These molecules are of greater complexity than those discussed in the paragraph above: double bonded substituents are present on the aromatic system and in the case of the purines there are four hetero-atoms. The reliability of calculated transition moment directions in such cases has not been evaluated, and will be discussed in Chapters Six and Seven in conjunction with the experimental results.

### 1.3 The Stretched Film Method

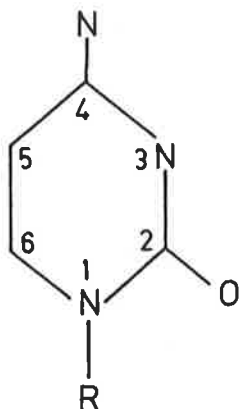
In stretched film experiments, a sample of the compound to be studied is dispersed in a rectangular strip of polymer material, either by soaking the strip in a solution of the compound in a suitable solvent or by casting the strip from a solution containing both polymer and solute. Polyethylene (PE) and poly(vinylalcohol) (PVA) are the polymers most commonly used. The film is clamped at opposite ends and stretched to three or four times the original length, which induces an anisotropic orientation distribution of both polymer and solute molecules. The stretched film is mounted in a spectrophotometer

FIG 1.2 PURINE AND PYRIMIDINE STRUCTURES AND THE "DEVOE-TINOCO" CONVENTION



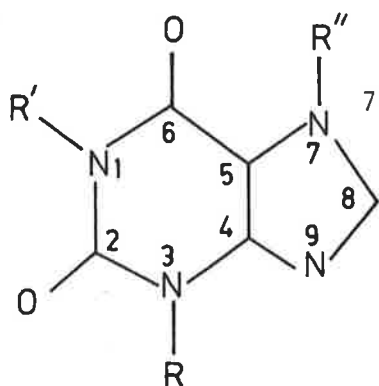
URACIL  
 THYMINE  
 1-METHYLTHYMINE  
 URIDINE  
 THYMIDINE

$R = R' = H$   
 $R = H; R' = CH_3$   
 $R = R' = CH_3$   
 $R' = H; R = D\text{-ribose}$   
 $R' = CH_2; R = D\text{-2-deoxyribose}$



CYTOSINE  
 CYTIDINE  
 5'-CMP

$R = H$   
 $R = D\text{-ribose}$   
 $R = D\text{-ribose-5'-phosphate}$



7-H-XANTHINE  
 1-METHYLXANTHINE  
 3-METHYLXANTHINE  
 THEOBROMINE  
 THEOPHYLLINE  
 CAFFEINE

$R = R' = R'' = H$   
 $R = R'' = H; R' = CH_3$   
 $R' = R'' = H; R = CH_3$   
 $R' = H; R = R'' = CH_3$   
 $R'' = H; R = R' = CH_3$   
 $R = R' = R'' = CH_3;$

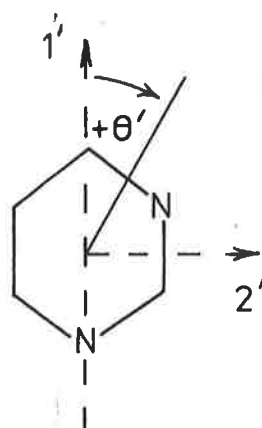
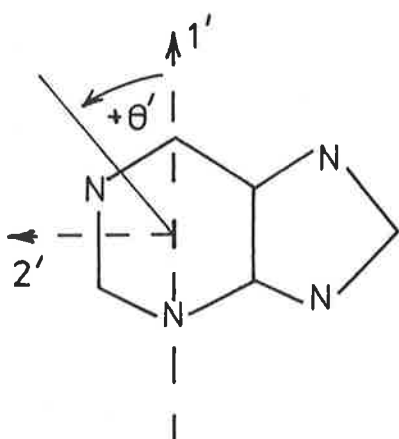


TABLE 1.1

TRANSITION MOMENT DIRECTIONS OF PYRIMIDINES AND PURINESAS DETERMINED BY PSCS AND PHOTOSELECTION

Compound	Method*	$\theta'_I$ (degrees)	$\theta'_{II}$ or $\theta'_{III}$	Reference
1-Methylthymine	A	-19±2	~70	Stewart and Davidson (1963)
	R	-19±2		Callis and Simpson (1970)
1-Methyluracil	A	0±2 or 7±2	~90	Eaton and Lewis (1970)
6-Azaauracil	R	9	-35	Brown et al. (1974)
Cytosine	A	14±1	-5±3	Lewis and Eaton (1971)
Cytosine + 1-Methylcytosine (average)	R	12±3	-1±10	Callis and Simpson (1970)
5-Methylcytosine	P	$ \theta'_I - \theta'_{II} $	= 40±15	Callis and Simpson (1970)
Purine**	R	48	51	Chen and Clark (1969)
Adenine.HCl**	R	-28	-70	Chen and Clark (1973)
9-Methyladenine	A	-3±3	~90	Stewart and Jensen (1964)
9-Ethylguanine	R,P	44±5 or -14±5	and and -65±10 -85±10	Callis et al. (1971); (1964)
Caffeine	P		$ \theta'_I - \theta'_{II} $ 71	Lancelot (1975)

\* A: absorbance; R: reflectance; P: photoselection

\*\* results quoted for two lowest ( $\pi^*$ ,  $\pi$ ) transitions only

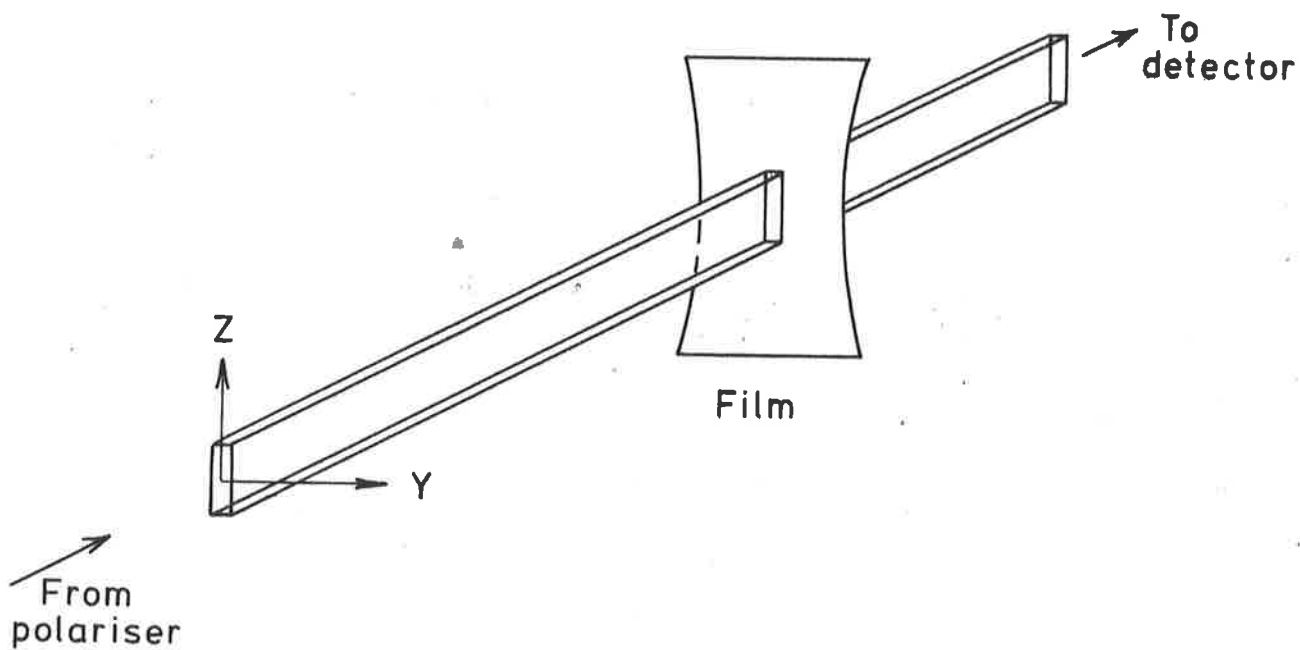
equipped with polariser, in such a way that the light beam travels along an axis (X) perpendicular to the plane of the film (fig 1.3). The dichroic spectrum consists of two sets of measurements of absorbance as a function of wavenumber ( $\bar{\nu}$ ), denoted  $A_Z(\bar{\nu})$  and  $A_Y(\bar{\nu})$ . For the first, the polarisation of the light beam is such that the electric field is parallel to the axis of stretch (Z) of the film, whilst for the second, polarisation is in a perpendicular direction (Y). The stretched film method is superior to PSCS in that it is experimentally much simpler, and as the solute is unimolecularly dispersed, degenerate exciton coupling is absent. On the other hand it is disadvantaged by the fact that the solute orientation is not well defined, with the result that accurate information on transition moment directions cannot normally be extracted from the measured dichroic absorbances. Whilst in crystals there are usually no more than two optically distinct molecular orientations, which have a known relationship to the external form of the crystal, the orientations of solute molecules in stretched films are distributed over all possible values according to a distribution function of unknown form. As will be shown in section 2.1 the principal axes and values\* of a symmetric second rank tensor K of order three must be determined in order to completely analyse the dichroism data.

As a result of the orientation problem, most studies have been confined to molecules of  $C_{2v}$  or  $D_{2h}$  point symmetry (e.g. Thulstrup et al., 1975; Hiratsuka et al., 1972; Yogev et al.,

---

\* only two of which are independent since  $K_{11} + K_{22} + K_{33} = 1$

FIG 1.3 SCHEMATIC REPRESENTATION OF A STRETCHED FILM DICHROISM MEASUREMENT



1974; Popov and Smirnov, 1971; Norden and Davidsson, 1976). The principal axes and the transition moment directions of such molecules are defined by symmetry and transitions of the same polarisation are segregated by virtue of having the same dichroism. In order to associate the transitions with the correct axes, it is necessary only to establish the relative magnitudes of the principal values,  $K_{11}$ ,  $K_{22}$  and  $K_{33}$ , which can usually be achieved on the basis of molecular shape (c.f. section 2.2). Alternatively, assignments may be made by comparison with SCF-LCAO calculations.

Little conclusive work has been published on molecules of lower symmetry. Gangakhedkar et al. (1974) have used the dichroism of infrared (IR) absorption to determine solute orientation. In some cases it is possible to identify IR bands with vibrations of a specific group of atoms within a molecule, for example a carbonyl group, and to assign the IR transition moment direction on the basis of the local symmetry of the group. The measured IR dichroism of the solute may then be used to provide information on orientation. This approach has not found wider use because of considerable experimental difficulties which will be discussed in Chapter Three. These are rather inadequately dealt with by Gangakhedkar et al. whose analysis of solute orientation is also faulty (c.f. section 2.2). Michl and collaborators (Michl, Thulstrup and Eggers, 1974; Thulstrup et al., 1976) have developed a correlation approach applicable to molecules which show a high degree of orientation and have a symmetric parent structure. In such cases the presence of an asymmetric substituent or a hetero-atom in the ring of the parent molecule represents a small "perturbation" whose effect on

orientation may be estimated with a fair degree of confidence.

This study of stretched films is in two parts. The first, contained in the next chapter, consists of an investigation of solute orientation mechanisms. Although the ready availability of orientation information for symmetric molecules expedites such investigations, there has been little effort expended in this direction, and the mechanism of solute orientation is completely unknown. Apart from its intrinsic interest, a theory of orientation could prove of great practical value by defining a relationship between orientation and other molecular properties easier to evaluate. If it could be shown that orientation resulted predominantly from repulsive interactions, one would expect to be able to deduce orientation properties from the shape of the molecule, if from dispersion interaction, from its polarisability properties, and if from polar interactions, from its dipole moment, or from the disposition of polar groups within the molecule. The other part of the work is concerned with the orientation and transition moments of derivatives of uracil, cytosine and xanthine in PVA films. These molecules form a difficult subject for study, because the degree of orientation is small, and there is no obvious correlation between molecular structure and orientation. Information on orientation was obtained from the IR dichroism of the carbonyl vibration bands. As will be discussed in Chapter Three only these IR bands of pyrimidines and purines are suitable for dichroism studies in PVA films. The assignment of the carbonyl vibrational modes, which is controversial for uracil and its derivatives, is discussed in Chapter Four. Chapter Five is concerned with evaluating the anisotropic polarisabilities

which are needed to assess the role of dispersion forces in orientation. In Chapters Six and Seven, the IR and ultraviolet (UV) dichroism measurements are used to determine the molecular orientation properties and the transition moment directions. The orientation information obtained from IR dichroism measurements is not sufficient to enable precise or unique solutions, but by making use of a generalised correlation approach, and by comparison of results with PSCS measurements, it is possible to assign orientation and transition moment directions within acceptable limits of accuracy.

## CHAPTER TWO

DICHROISM AND ORIENTATION2.1 Dichroism and Molecular Orientation

The dichroism  $R_Z$  is formally defined, for the purposes of this work, by the following ratios of integrated molar absorptivities:

$$R_Z = \int \epsilon_Z d\bar{\nu} / \int (\epsilon_Z + \epsilon_Y + \epsilon_X) d\bar{\nu}$$

From eqn 1.1

$$R_Z = \langle (e_Z \cdot \underline{m})^2 \rangle / \underline{m} \cdot \underline{m}$$

Angled brackets will be used to denote the average value of the enclosed quantity for all molecules in the sample. The direction of  $\underline{m}$  within the molecule can be defined by direction cosines  $(m_{1'}, m_{2'}, m_{3'})$  relative to a convenient set of molecule-fixed Cartesian axes  $(1', 2', 3')$ . For the pyrimidine and purine molecules studied the axes  $(1', 2')$  have been chosen as in fig 1.2. The orientation of a molecule relative to the film axes  $(X, Y, Z)$ , can be defined by direction cosines  $(l_{1'Z}, l_{1'Y}, \dots, l_{3'X})$ . Then since

$$e_Z \cdot \underline{m} = (l_{1'Z} m_{1'} + l_{2'Z} m_{2'} + l_{3'Z} m_{3'}) (\underline{m} \cdot \underline{m})^{1/2},$$

$$R_Z = \langle l_{jZ} l_{kZ} \rangle m_j m_k = K_{jk} m_j m_k; \quad j, k = 1', 2', 3'.$$

Summation over the indices  $j$  and  $k$  is assumed. The dichroism as defined above is thus related to the transition moment directions in a straightforward way. As mentioned in section 1.2, it is customary to approximate the ratio of integrated absorptivities by a ratio of absorbances at a particular wave-number, as follows:

$$R_Z = \frac{A_Z}{A_Z + A_Y + A_X}.$$

This expression is exact if  $A_Z$ ,  $A_Y$  and  $A_X$  are in the same ratio

throughout the spectral band observed. Since  $A_X$  is not measurable, a further approximation

$$A_X = A_Y$$

is made. This approximation will be shown, in section 2.3, to be quite accurate.  $R_Z$ , as evaluated from experimental measurements, is then given by

$$R_Z = \frac{A_Z}{A_Z + 2A_Y} \quad (2.1)$$

The orientation tensor  $K_{ij}$ , being symmetric, has principal axes (1,2,3) with associated principal values, abbreviated to  $K_1$ ,  $K_2$  and  $K_3$  (Temple, 1960), and when molecular properties are referred to the axes (1,2,3),

$$R_Z = K_1 m_1^2 + K_2 m_2^2 + K_3 m_3^2$$

with

$$K_1 + K_2 + K_3 = 1 \quad (2.2)$$

The axis labels may be made unique by specifying that

$$K_1 \geq K_2 \geq K_3$$

and it is not difficult to prove (see Appendix A.4) that

$$K_3 \leq R_Z \leq K_1$$

The principal values, or orientation parameters  $K_i$ , are a measure of the degree of correlation of molecular axis  $i$  with the stretching direction  $Z$ . If these axes are parallel for all molecules in the sample,  $K_i$  is equal to one, if perpendicular, to zero. For a randomly oriented sample, all  $K_i$ 's are equal to 1/3. Because axis 1 has the greatest correlation with  $Z$ , it is referred to as the orientation axis.

In the general case, the direction of the principal axes are unknown. Most molecules of interest, however, have either a plane or an axis of symmetry, and in these cases the principal axes, like the transition moments, are either parallel to or

perpendicular to the symmetry elements present. This is shown by writing an expression for the orientation parameter  $K_{ij}$  using Boltzmann statistics.

$$K_{ij} = N \int l_{iZ} l_{jZ} \Omega \exp(-U/kT) d\tau \quad (2.3)$$

where  $U$  is the energy associated with orientation  $(l_{iZ}, l_{jZ})$ ,  $\Omega$  is a distribution function such that  $\Omega dl_{iZ} dl_{jZ}$  is proportional to the number of states having energy  $U$ ,  $\tau$  is the domain of integration, and  $N$  is a normalising factor. It is clear that  $\Omega$  and  $U$  are invariant under symmetry operations of the molecular point group. Suppose that axis  $i$  is either parallel to a symmetry axis or perpendicular to a mirror plane. Then since  $l_{jZ}$  and  $l_{kZ}$  are associated with different irreducible representations of the molecular point group to  $l_{iZ}$ ,  $K_{ij}$  and  $K_{ik}$  vanish, making axis  $i$  a principal axis. In the case of a molecule having a plane of symmetry, in particular,

$$R_Z = K_3$$

for an out-of-plane transition and

$$R_Z = K_1 m_1^2 + K_2 m_2^2$$

for a  $(\pi^*, \pi)$  transition, since axis 3 is invariably observed (see next section) to be out-of-plane.

## 2.2 Orientation of Symmetric Molecules

Molecules having  $C_{2v}$  or  $D_{2h}$  point symmetry are ideal for the study of the orientation of solutes because the system of axes (1,2,3) is completely determined by symmetry and for an  $i$ -axis polarised transition

$$K_i = R_Z.$$

As discussed in the previous chapter, the identity of the axes  $i$  may be established by comparison of dichroic spectra with

calculations, thus enabling evaluation of the parameters  $K_1$ ,  $K_2$  and  $K_3$ .

The results presented here are for naphthalene, quinoline, anthracene and acridine which were studied in both PE and PVA films, and 9-aminoacridine, which was studied in PVA only. Quinoline, although strictly only of  $C_s$  symmetry, is similar to naphthalene in both its electronic and orientational characteristics, as will be seen. Shown in table 2.1 are the results of SCF-PPP-CI calculations of the  $(\pi^*, \pi)$  transitions in the range of interest; the method of calculation is described in the next chapter. The polarisation directions (1', 2', 3') correspond to the long, short, and out-of-plane molecular symmetry axes respectively; in the case of quinoline the calculated deviations of the transition moments from colinearity with these axes are shown in parentheses in the table. 9-aminoacridine has a  $pK_a$  of 10, the proton being attached at the ring nitrogen atom (Albert, 1966). The cationic form is discernible by an absorption band at  $31000 \text{ cm}^{-1}$  absent in the neutral species, and from this criterion is readily seen (fig 2.1) to be the predominant species in PVA films. The calculations for the neutral 9-aminoacridine molecule are included also in table 2.1: the intensity of band II is correctly predicted to be very low for this case. The calculations were in all cases consistent with photoselection and PSCS measurements of band polarisations, references to which are given in the table.

The dichroic spectrum of each compound showed distinct region of 1'- and 2'-axis polarisation, as follows:

- (i) naphthalene. Transition I was not observed owing to its low intensity, although highly sensitive linear dichroism

FIG 2.1 THE SPECTRUM OF 9-AMINOACRIDINE IN PVA RESOLVED INTO SYMMETRY-AXIS POLARISED COMPONENTS

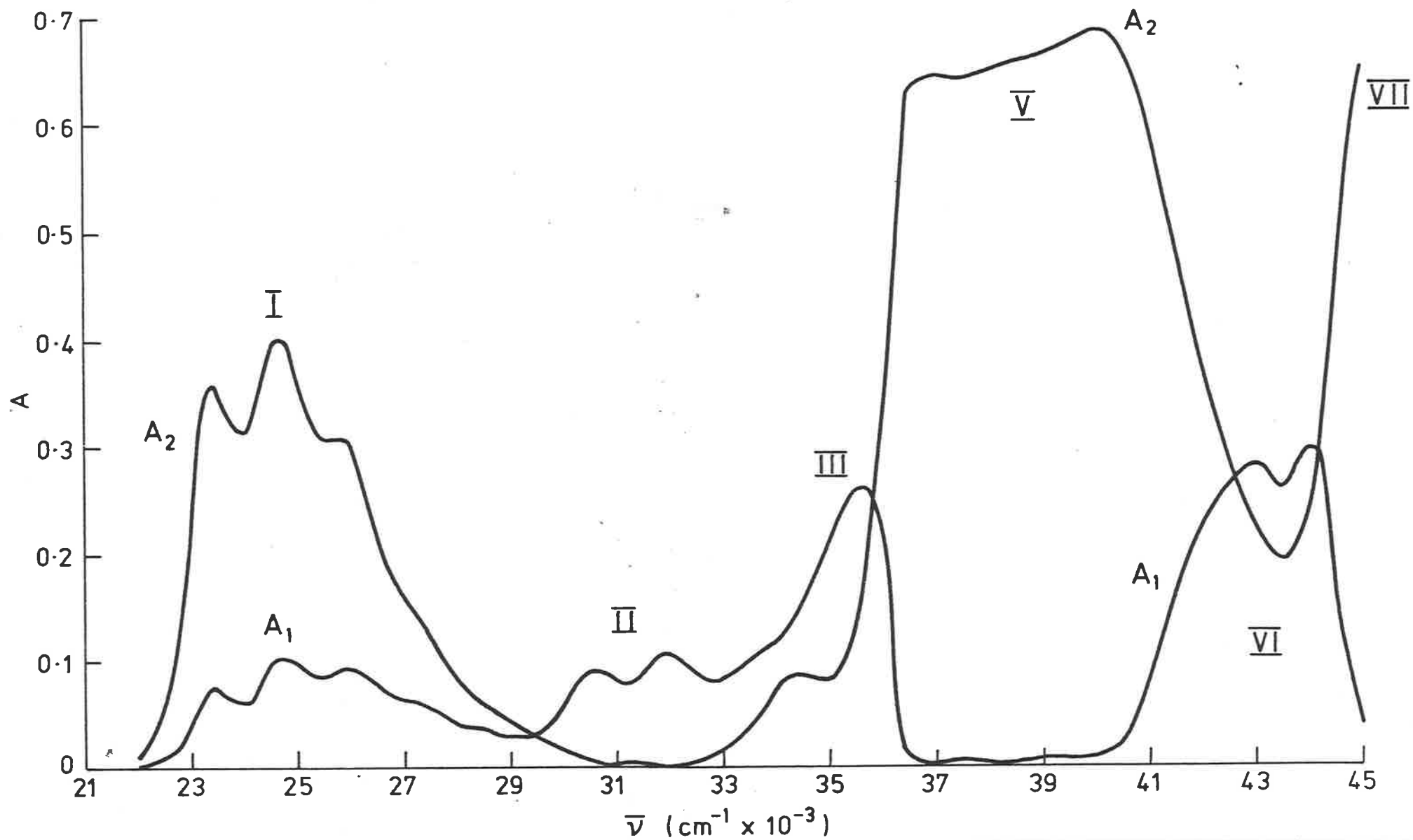


TABLE 2.1

CALCULATED ENERGIES, INTENSITIES AND POLARISATIONS OF ( $\pi^*$ ,  $\pi$ ) TRANSITIONS OF NAPHTHALENE, QUINOLINE,  
ANTHRACENE, ACRIDINE AND 9-AMINOACRIDINE

Compound	Energy of (0,0) Band in $\text{cm}^{-1}$	f	Polarisation Direction	Experimental Verification	
Naphthalene	I	32500	.002	1'	Davidsson and Norden (1974)
	II	35400	.08	2'	
	III	46100	.98	1'	
Quinoline	I	32900	.03	1' (3.8°)	Zimmerman and Joop (1961)
	II	35600	.07	2' (0.3°)	
	III	45200	.51	1' (1.5°)	
Anthracene	I ( ${}^1L_a$ )	26900	.05	2'	Michl, Thulstrup and Eggers (1974)
	II ( ${}^1L_b$ )	28800	.005	1'	
	III	36700	0		
	IV	37700	0		
	V	39700	0		
	VI ( ${}^1B_b$ )	40200	1.43	1'	
Acridine	I	27100	.05	2'	Wittwer and Zanker (1959)
	II	28800	.08	1'	
	III	34400	.01	1'	
	IV	40000	0	-	
	V	40400	1.10	1'	
	VI	41100	.20	1'	

(contd.)

TABLE 2.1 (contd.)

Compound	Energy of (0,0) Band in $\text{cm}^{-1}$	f	Polarisation	Experimental Verification
9-Aminoacridine Cation	I 26200 (26200)	.043 (.085)	2' (2')	Zanker and Wittwer (1960)
	II 28700 (29100)	.435 (.003)	1' (1')	
	III 30400 (36200)	.035 (.019)	1' (1')	
(9-Aminoacridine)	IV - (37000)	- (.001)	- (1')	
	V 37000 (38100)	.108 (.008)	2' (2')	
	VI 41900 (39100)	.058 (1.185)	1' (1')	
	VII 42600 (41100)	.015 (.003)	2' (2')	

techniques have shown it to be present (Davidsson and Norden, 1972; 1974). The dichroism of the low wavenumber edge of the spectrum was assigned entirely to transition II, and that of the high wavenumber limit to transition III.

- (ii) quinoline. Transitions I, II and III were sufficiently well separated to enable the assignment of a dichroism to all three transitions. As expected the 1'-axis polarised transitions I and III showed identical dichroisms
- (iii) anthracene and acridine. The dichroic spectrum of anthracene has been discussed in section 1.1. The dichroisms of transitions I and VI can be determined from the spectrum (fig 1.1). Both the calculated transitions, and the dichroic spectrum (Inoue et al., 1971) of acridine are similar to those of anthracene. The (0,0) component of transition I and the very intense transition V give the dichroism associated with axes 2' and 1', respectively.
- (iv) 9-aminoacridine. In fig 2.1 is shown the dichroic spectrum of 9-aminoacridine, resolved into 1'- and 2'-axis polarised components according to a procedure given in Appendix A.1. Although the spectrum is complex, bands II and V are well resolved and give regions of pure polarisation.

From the dichroisms of the 1'- and 2'- polarised regions of the spectra the values of the parameters  $K_1$ , and  $K_2$ , were found, the value of  $K_3$ , being derived from eqn 2.2. Depicted in figs 2.2 and 2.3 are the values of  $K_1$ , and  $K_2$ , of various films plotted as functions of the inverse polymer draw ratio,

$v^{-1}$ , defined as follows:

$$v^{-1} = \frac{\text{length of sample before stretching}}{\text{length after stretching}}$$

The data for naphthalene, quinoline and anthracene have been extracted from dichroic spectra reported in previous work (Bott, 1972). It is seen that for all the molecules studied

$$K_{1'} > K_{2'} > K_{3'}$$

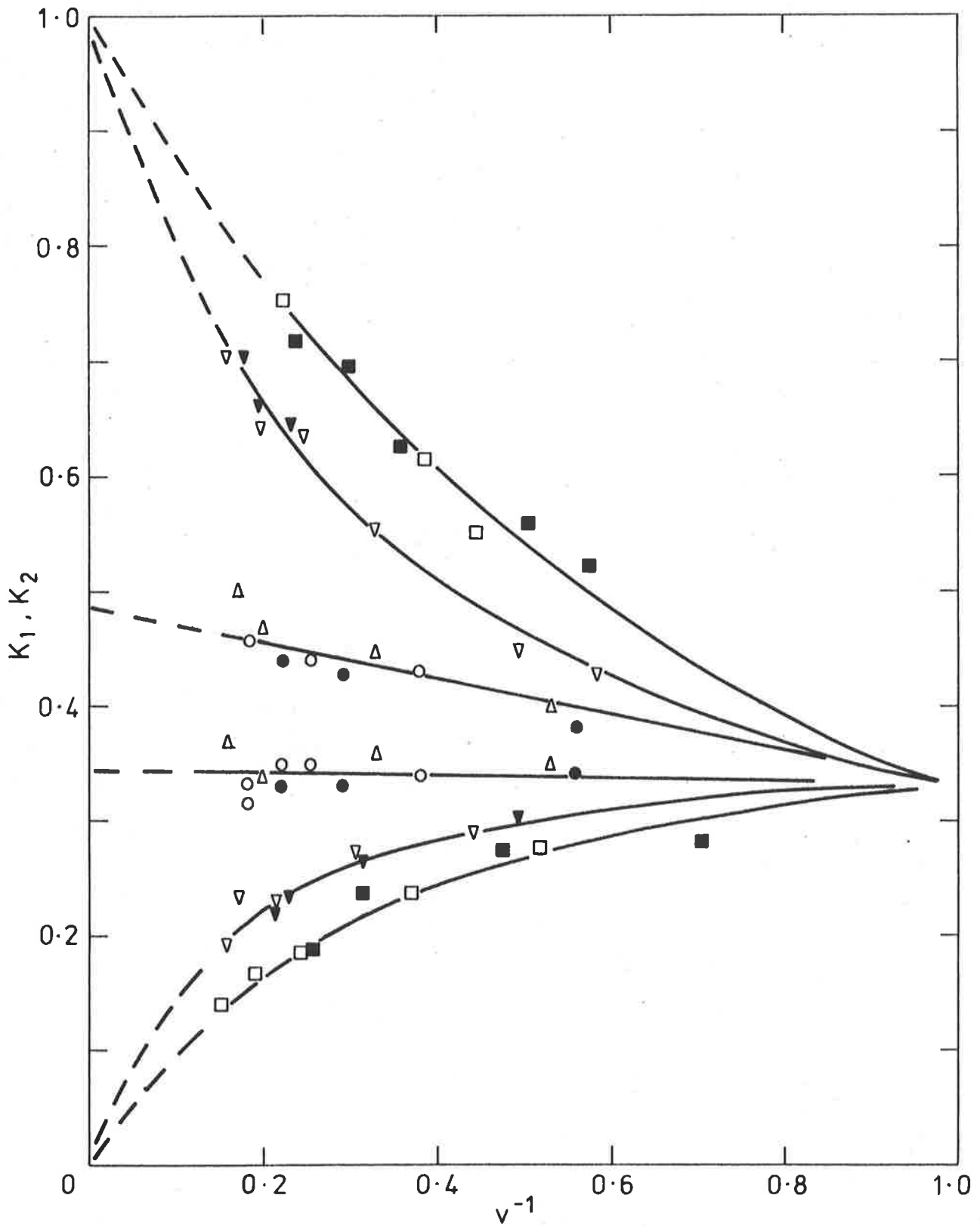
and therefore the axes (1',2',3') and (1,2,3) are identical in order. The long molecular axis is in each case the orientation axis, and the out-of-plane axis has the least correlation with the film Z-direction, a result which is almost universal for studies of orientation of symmetric molecules (e.g. Thulstrup, Vala and Eggers, 1970). In spite of the fact that  $K_2$  and  $K_3$  are significantly different in most cases, many authors (Tanizaki, 1965; Fucaloro and Forster, 1971; Yogev et al., 1971; Gangakhedkar et al., 1974) have used the assumption that the solute molecule behaves in orientation as though cylindrically symmetric about the orientation axis, axes 2 and 3 being equivalent. An example of the error which attends its use occurs in the work of Gangakhedkar et al., where the IR dichroism of naphthols was interpreted as showing the orientation axis was not parallel or perpendicular to the plane of the molecule.

A discussion of the other features of orientation is deferred until the orientation process has been analysed in more detail.

### 2.3 Polymer Orientation

Because the orientation of solute molecules in stretched

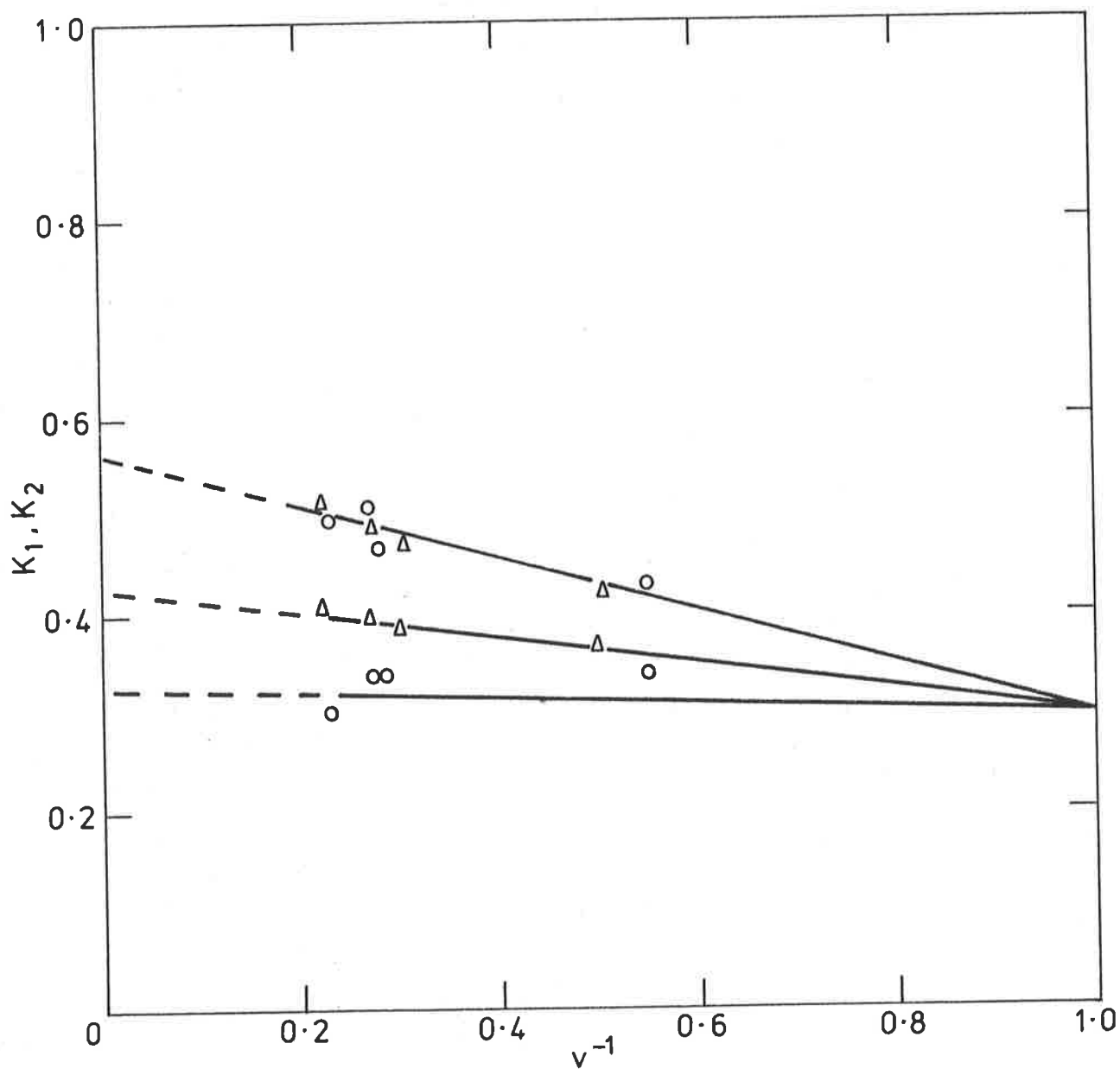
FIG 2.2 ORIENTATION PARAMETERS OF ANTHRACENE, ACRIDINE, NAPHTHALENE AND QUINOLINE AS FUNCTIONS OF INVERSE DRAW RATIO



○ NAPHTHALENE                      △ QUINOLINE  
 □ ANTHRACENE                      ▽ ACRIDINE

Filled and empty symbols refer to PVA and PE films, respectively

FIG 2.3 ORIENTATION PARAMETERS OF QUINOLINE AND 9-AMINOACRIDINE  
IN PVA FILMS



$\Delta$  QUINOLINE  
 $\circ$  9-AMINOACRIDINE

films depends on their interaction with the polymer molecules, investigation of solute orientation should begin with a study of the orientation properties of the polymer itself. In order to describe polymer orientation on a molecular scale, a Cartesian system (x,y,z) is attached to each monomer unit, with the z axis perpendicular to the plane of the CH<sub>2</sub> group. The average orientation of the axes z with respect to the film axis Z is described by means of a K parameter:

$$K_z = \langle l_{zZ}^2 \rangle.$$

A theoretical expression relating  $K_z$  to the draw ratio,  $v$ , of the film, can be obtained by assuming that the redistribution of the axes z resulting from stretching of the polymer film is governed by the geometric distortion of the film, that the density is unchanged by stretching, and that the deformation properties in directions X and Y are equivalent (Fraser, 1958; Tanizaki, 1965; Smirnov, 1952; Kratky, 1933; Kuhn and Gruen, 1942; Zbinden, 1964) as follows:

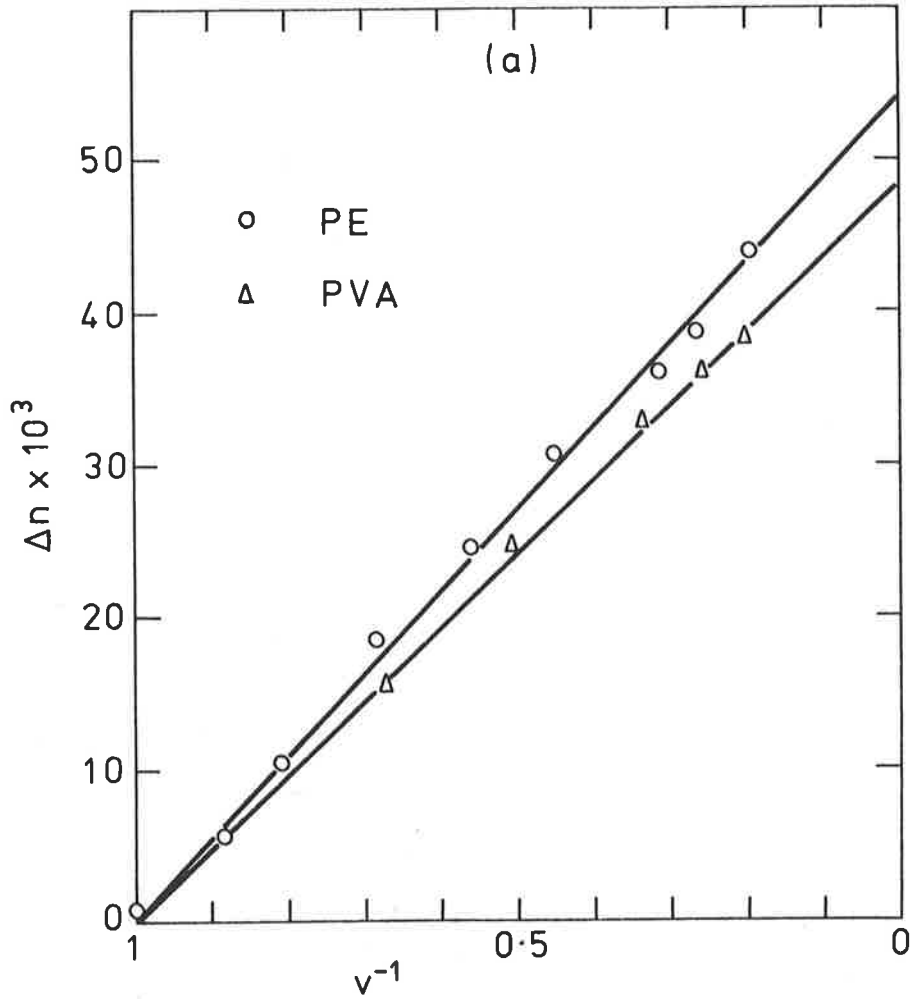
$$K_z = \frac{v^3}{v^3-1} \left[ 1 - \frac{\arctan(v^3-1)^{\frac{1}{2}}}{(v^3-1)^{\frac{1}{2}}} \right] \quad (2.4)$$

In fig 2.4(b) the value of  $K_z$ , calculated from this expression, is shown as a function of  $v^{-1}$ . It is seen that, to a good approximation, it can be replaced by the following:

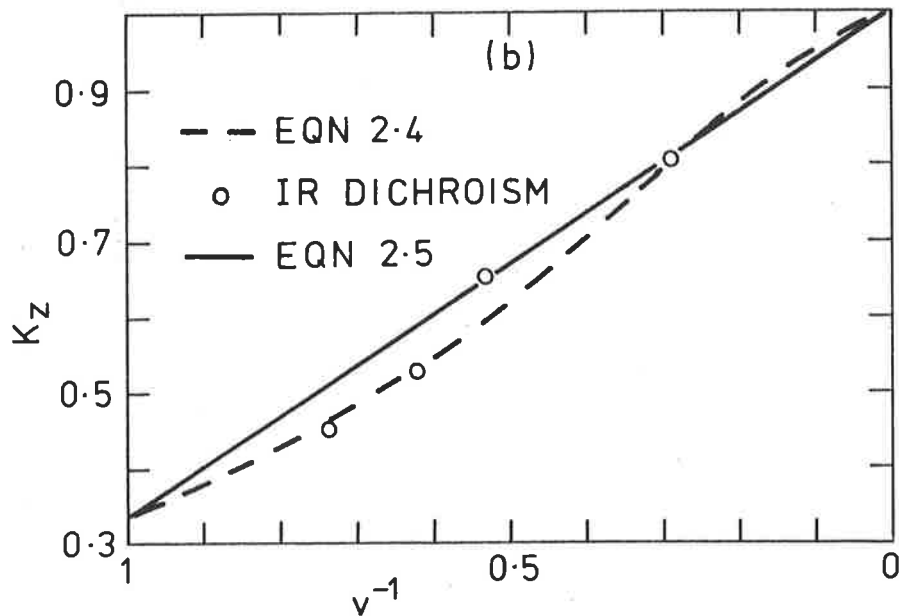
$$K_z = 1 - 2/3 v^{-1} \quad (2.5)$$

Experimental measurements of  $K_z$  as a function of  $v$  are in excellent agreement with eqn 2.5. In fig 2.4(a) the birefringences  $\Delta n (= n_z - n_y)$  of PVA (Gulrajani and Padhye, 1971) and PE (Schael, 1968) films are plotted as functions of  $v^{-1}$ . As  $\Delta n$  is a linear function of  $K_z$  (Stein and Read, 1969), the diagram demonstrates a precise linear relationship between  $K_z$

FIG 2.4(a) BIREFRINGENCE OF PVA AND PE AS A FUNCTION OF INVERSE DRAW RATIO



(b) THEORETICAL AND EXPERIMENTAL VALUES OF  $K_z$  AS A FUNCTION OF  $v^{-1}$



and  $\nu^{-1}$ . In fig 2.4(b) the dichroism of the  $1235 \text{ cm}^{-1}$  IR absorption band of PVA is plotted as a function of  $\nu^{-1}$ . This band has been assigned to the CH wagging mode of PVA, and is z-axis polarised (Krimm et al., 1956); therefore its dichroism ( $R_z$ ) is equal to  $K_z$ . This data, also, verifies the relationship 2.5.

It is commonly assumed that the properties of stretched polymer films are isotropic in the XY plane or equivalently, on a molecular scale, that the orientation distribution of polymer chains is axially symmetric about the Z direction (Michl et al., 1970; Tanizaki, 1959; Popov, 1975b; Yogev et al., 1971; Norden, 1971). As solute orientational characteristics are dependent on those of the polymer, the same symmetry would be present in the distribution of orientations of solute molecules in the film. There is considerable experimental support for these assumptions from X-ray diffraction measurements on PE, which fail to show any differences when the beams are directed down the film X and Y axes (Michl et al., 1970), from refractive index measurements on PE and poly(propylene) films, which show  $n_x$  and  $n_y$  to be identical (Schael, 1968), and considerations based on UV dichroism of solutes (Bott and Kurucsev, 1975). These results justify the assumption made in section 2.1 that  $A_z$  and  $A_y$  are equal. They do not however demonstrate cylindrical (Z-axis) symmetry in the local environment of each solute molecule, a hypothesis which will be discussed later in the chapter.

#### 2.4 Empirical Models of Solute Orientation

The obvious influence of molecular shape on orientation,

as for example the preferential orientation of the long axes and molecular planes observed of the compounds discussed in section 2.2, or the increase in orientation with molecular length (Lipasova and Nurmukhametov, 1976), has led a number of authors to propose empirical means of predicting orientation, where no attempt is made to discover the orientation mechanism involved. Indeed the first of these methods, which is due to Y. Tanizaki (1959; 1965), purports to interpret dichroism directly without the necessity of determining solute orientation. In this treatment, the solute is assumed to have the same orientation characteristics as the polymer, as given in eqn 2.4. The solute orientation parameters are given by

$$K_1 = K_z; K_2 = K_3 = \frac{1}{2}(1 - K_z),$$

$K_z$  being determined from the value of  $v$  according to eqn 2.4.

For  $(\pi^*, \pi)$  <sup>TRANSITIONS</sup>, the transition moment direction is related to the dichroism by the following variation of eqn 2.2:

$$R_z = K_z \cos^2 \theta + \frac{1}{2}(1 - K_z) \sin^2 \theta$$

where  $\theta$  is the angle between the transition moment direction and the orientation axis. This expression is, of course, quite contrary to experiment because it not only assumes incorrectly that  $K_2 = K_3$ , but predicts that all solutes should show identical orientation. To avert this difficulty, Tanizaki proposed that if  $\theta$  is regarded as a relative measure of angle, the correct relative angles of different transition moments are obtained by use of the expression. This assumption lacks any logical basis, and there is absolutely no reason to expect any correct prediction of transition moment direction by its use. In spite of this, Tanizaki's method of interpreting dichroism has had widespread use (Chae and Song, 1974; Tanizaki and Kubo-dera, 1967; Hiratsuka et al., 1972; Hoshi et al., 1972 and

references therein) being used, in particular, to interpret the dichroism of pyrimidines and purines in stretched PVA films (Fucaloro and Forster, 1971; 1974), and has received criticism in the literature only recently (Popov, 1975a). Tanizaki's justification of his treatment rests on the fact that it gives qualitatively correct results for symmetric molecules: table 2.2, for example, illustrates its application to the molecules studied in section 2.2. These correct predictions are fortuitous, and results for molecules lacking in symmetry axes cannot be expected to be of any value. For molecules of low dichroism, for example, such as the last three entries in table 2.2, the calculated value of  $\theta$  is always between  $40^\circ$  and  $55^\circ$ , and therefore the relative orientation of any two transitions is always calculated to be  $0^\circ \pm 15^\circ$  or  $95^\circ \pm 15^\circ$ , regardless of the true value. Therefore interpretation of dichroism based on Tanizaki's method, in particular the work on pyrimidines and purines of Fucaloro and Forster, must be regarded as unacceptable.

Recently Popov has proposed a method for finding the principal orientation axes and values, using correlations based on molecular shape (Popov, 1975b;c;d). A diagram of the solute molecule is drawn, with atomic radii, and circumscribed with a rectangle in such a way that the ratio of length to width of the rectangle is a maximum. From studies of some symmetric molecules in PVA films Popov has shown that the first orientation parameter increases with the ratio of length to width of the rectangle, whilst the second parameter is related in a less satisfactory manner to the length alone. As a test, the method was used to estimate the orientation parameters of naphthalene and acridine

TABLE 2.2

Y. TANIZAKI'S ORIENTATION MODEL

Molecule	Transition Polarisation	Transition Angle $\theta$ (degrees)	$\theta_1 - \theta_2$
Acridine	1	$\pm 32.7$	29.7 or 95.1
	2	$\pm 62.4$	
Anthracene	1	$\pm 22.4$	46 or 90.8
	2	$\pm 68.4$	
9-Aminoacridine	1	$\pm 41.8$	14 or 96.6
	2	$\pm 55.8$	
Quinoline (PE), Naphthalene	1	$\pm 44.9$	8.9 or 98.7
	2	$\pm 53.8$	
Quinoline (PVA)	1	$\pm 41.8$	7.5 or 91.3
	2	$\pm 49.5$	

Inverse Draw Ratio of Films: 0.25

cation, and the transition moment directions were then computed from the measured dichroisms. These were found to be  $0^\circ \pm 19^\circ$  and  $95^\circ \pm 10^\circ$  for naphthalene, and  $0^\circ \pm 27^\circ$  and  $90^\circ \pm 15^\circ$  for acridine cation (Popov, 1975a). Clearly, therefore, the method gives only qualitative results, even in cases where the principal orientation axis assignments may be taken for granted. The fact that it is not possible to find a correlation between orientation and molecular shape which is of general validity is illustrated by the difference in orientation of anthracene and acridine shown in fig 2.3, and by other instances (Michl and Eggers, 1974; Lipasova and Nurmukhametov, 1976) where molecules of identical shape have been found to have different orientation characteristics.

As was discussed in the Introduction, Michl, Thulstrup and

Eggers (1974) have been more successful in correlations applied in more restricted circumstances. For example, for a series of anthracenes with one or two methyl, amino or fluoro-substituents they found that the value of the  $K_1$  parameter increased in the same order as the ratio of length to width of the molecules. A similar, though less exact, correlation existed for  $K_2$ . By consideration of the  $K_1$  and  $K_2$  values of the symmetrically substituted molecules, the values for the unsymmetric molecules were conjectured. The orientation axes of the latter were assumed to be perpendicular to the smallest cross-section of the molecule, differing in these cases only by several degrees from the long axis directions of the symmetric parent structure. The agreement of transition moment directions derived by this method with later results of PSCS work (Bridge and Gianneschi, 1976) confirm its validity. Its scope, however, is limited to molecules of basic  $C_{2v}$  or  $D_{2h}$  symmetry, "perturbed" by small substituents, and having a high degree of orientation, and it cannot therefore be applied to the pyrimidines and purines of interest in this work.

## 2.5 Orientation Mechanisms

Although the connexion between molecular shape and orientation properties has long been recognised, interactions between solute and polymer molecules have not been adequately studied. Thulstrup, Michl and Eggers (1970) pointed out that the commonly observed long axis orientation of symmetric molecules could result from dispersion interactions as well as repulsive interactions, since the long axis of a molecule is normally its axis of greatest polarisability, and therefore both types of interaction

work to make this axis align parallel to the polymer molecules. From a study of diazonium and tetrazonium salts in PVA which showed the short axes of the solute molecules to orient preferentially in the stretching direction, it was concluded that polar interactions were of primary importance in determining orientation for such molecules (Tsunoda and Yamaoka, 1965), and other instances of short axis orientation have also been reported (Popov and Smirnov, 1962; Konev, 1967; Siodmiak and Frackowiak, 1972; Platonova et al., 1970) (however c.f. section 3.5). A theoretical treatment of the anisotropic interaction of naphthalene and alkane molecules is also of some interest as a model for interaction with PE molecules. The calculations predicted that dispersion interactions make the greatest contribution to the attractive potential, and determine the most stable relative configurations (Lamotte et al., 1974).

The only theoretical treatment of orientation of solutes in stretched films to appear (Lamotte, 1975) was largely derived from treatments dealing with nematic liquid crystals, in which dispersion interactions only were considered (Nehring and Saupe, 1969; Sackmann and Moehwald, 1972). These treatments are deficient in several ways. In particular, the magnitude of the solute orientation is not calculated explicitly, with the result that comparison of theory and experiment has been too indirect to enable any definite conclusion to be made as to the mechanism of orientation. In this section it will be shown that, if the interaction between each solute molecule and its nearest polymer molecule only is considered, a satisfactory treatment of orientation is possible. This serves as a basis for discussion, in a qualitative way, of more complete models

of orientation.

It is assumed that the portion of polymer molecule adjacent to the solute is in the all-trans configuration, in which case its orientation can be described by a single value of  $l_{zZ}$ . The solute orientations in the systems  $(X,Y,Z)$  and  $(x,y,z)$  are then related as follows:

$$l_{iZ}^2 = l_{iz}^2 l_{Zz}^2 + l_{iy}^2 l_{Zy}^2 + l_{ix}^2 l_{Zx}^2 + 2l_{iz} l_{iy} l_{Zz} l_{Zy} \\ + 2l_{iz} l_{ix} l_{Zz} l_{Zx} + 2l_{iy} l_{ix} l_{Zy} l_{Zx}; \quad i = 1', 2', 3'$$

where the symbol  $l_{\alpha\beta}$  denotes the direction cosine defining the relative directions of axes  $\alpha$  and  $\beta$ . As before,  $(X,Y,Z)$  are film-fixed Cartesian axes,  $(x,y,z)$  are the polymer axes and  $(1',2',3')$  are arbitrarily chosen solute-fixed axes.

One now considers the values of  $l_{iz}$ ,  $l_{iy}$  and  $l_{ix}$  (that is, the relative orientations of solute and polymer molecules) to be fixed, and averages over all values of  $l_{Zy}$ ,  $l_{Zx}$ , on the assumption that all orientations of the intermolecular vector  $\underline{r}$  (fig 2.5) perpendicular to  $z$  are equally probable. The averaging is done by writing

$$l_{Zz} = \cos\theta; \quad l_{Zy} = \sin\theta\cos\gamma; \quad l_{Zx} = \sin\theta\sin\gamma$$

and integrating over  $\gamma$ . The last three terms of the expression vanish, and

$$l_{iZ}^2 = \frac{1}{2}(1 - l_{Zz}^2) + \frac{1}{2}(3l_{Zz}^2 - 1)l_{iz}^2$$

Averaging over all solute molecules in the sample, one can write

$$\langle l_{Zz}^2 l_{iZ}^2 \rangle = \langle l_{Zz}^2 \rangle \langle l_{iZ}^2 \rangle$$

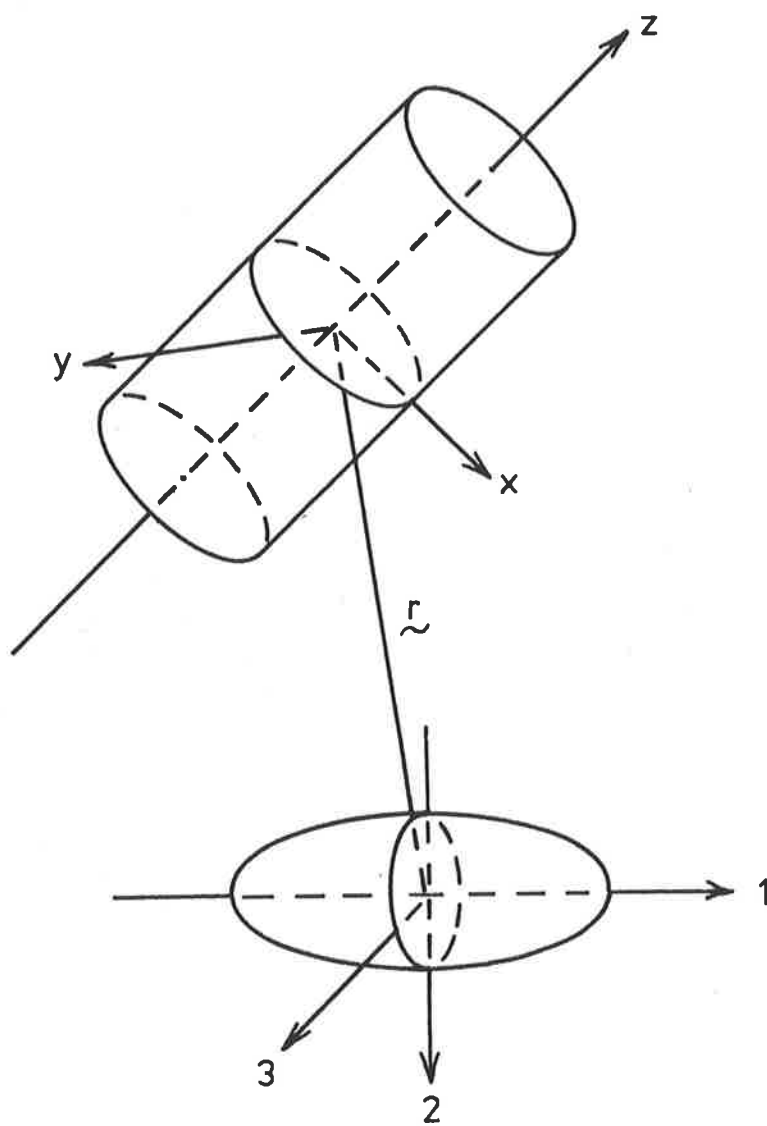
because, within the model used, the interaction of polymer and solute is independent of the polymer orientation. This gives

$$K_i = \langle l_{iZ}^2 \rangle = \frac{1}{2}(1 - K_z) + \frac{1}{2}(3K_z - 1)k_i \quad (2.6)$$

where

$$k_i = \langle l_{iz}^2 \rangle$$

FIG 2.5 RELATIONSHIP BETWEEN POLYMER-FIXED AND SOLUTE-FIXED COORDINATE AXES



Eqn 2.6 therefore predicts a linear relationship between  $K_z$  and the parameters  $K_i$ , because  $k_i$  is independent of  $K_z$ . If the contribution of dispersion forces only is considered, an analytic expression for  $k_i$  may be obtained. Using classical Boltzmann statistics, the expression for  $k_i$  is

$$k_i = N \int \int \int \Omega \exp(-U/kT) d\tau \quad (2.7)$$

which is analogous to eqn 2.3, the meaning of the symbols being the same. The following expression for  $U$  comes from the perturbation expression for the anisotropic dispersion potential (Mason, 1970) with London's approximations (London, 1937) inserted:

$$U = \sum_{\substack{i=1,2,3 \\ j=x,y,z}} U_{ij}$$

with

$$U_{ij} = -\frac{1}{4} \frac{\epsilon_i \epsilon_j}{\epsilon_i + \epsilon_j} \frac{b_i b_j}{r^6} \{ \underline{i} \cdot \underline{j} - 3(\underline{i} \cdot \underline{\lambda})(\underline{j} \cdot \underline{\lambda}) \}^2 \quad (2.8)$$

where  $\{i\}$  and  $\{j\}$  are the principal polarisability axes of the solute and polymer, respectively, the associated principal values being  $b_i$  and  $b_j$ .  $\epsilon_i$  and  $\epsilon_j$  are the ionisation potentials associated with axes  $i$  and  $j$ , and  $\underline{i}$ ,  $\underline{j}$  and  $\underline{\lambda}$  are unit vectors in the direction of the axes  $i$ ,  $j$ , and the intermolecular vector  $\underline{r}$  (fig 2.5) respectively,  $r$  being the length of  $\underline{r}$ .

In order to fit experimental data to eqn 2.8 it is necessary to assume that the  $\epsilon_i$  and  $\epsilon_j$  approximate isotropic potentials:

$$\epsilon_1 = \epsilon_2 = \epsilon_3 = \epsilon_s; \quad \epsilon_x = \epsilon_y = \epsilon_z = \epsilon_p$$

It is also necessary to make some assumption about the  $b_j$ 's as these cannot be equal to the polarisabilities of the whole polymer molecule. For this purpose, the polymer is divided into segments, each being equal in length to the solute molecule, and  $b_z$ ,  $b_y$  and  $b_x$  are put equal to the polarisabilities of one

segment, the interaction potential being summed over all segments. The geometry of interaction with the nearest segment, where  $\lambda.z = 0$ , is depicted in fig 2.5. It was found by calculation with typical values of the molecular constants that the contribution of the neighbouring terms were not significant, and it can be shown that in its properties of convergence the total sum of terms for a linear polymer molecule may be compared with  $\sum 1/n^6 = \zeta(6) = 1.017$ , showing that the remaining terms do not contribute significantly to the total energy. Finally, since it is not possible to determine experimentally  $b_x$  and  $b_y$ , but only the sum  $(b_x + b_y)$ , one writes

$$b_x = b_y.$$

It is shown in Appendix A.2 that, given these approximations, the part of the dispersion potential which is dependent on  $l_{1z}$  and  $l_{2z}$  may be written

$$U = U_0 \{ l_{1z}^2 (b_1 - b_3) + l_{2z}^2 (b_2 - b_3) \}$$

where

$$U_0 = -\frac{1}{4} \frac{\epsilon_s \epsilon_p}{\epsilon_s + \epsilon_p} \frac{b_z - b_y}{r^6} \quad (2.9)$$

Using arguments similar to those of section 2.1, it can be shown that for a potential of the type of eqn 2.9, the principal polarisability and orientation axes are identical.

In order to put eqn 2.9 into a form suitable for substitution into eqn 2.7, an average of  $r^{-6}$  needs to be found. Since any rigorous attempt in this direction would necessitate assuming a form for the repulsive potential, it is simply assumed that  $r$  has an average value, independent of  $l_{1z}$  and  $l_{2z}$ , which is equal to the distance of closest approach. This is in the spirit of the model assumed, which requires the solute to be closely bound to a single polymer unit. Writing

$$1_{1z}^2 = \cos^2 \beta; \quad 1_{2z}^2 = \sin^2 \beta \cos^2 \gamma; \quad \Omega = \sin \beta$$

one obtains

$$k_1 = B(a_1, a_2) / A(a_1, a_2)$$

with

$$B = \int_0^{\frac{\pi}{2}} \int_0^{\frac{\pi}{2}} \sin \beta \cos^2 \beta \exp(a_1 \cos^2 \beta + a_2 \sin^2 \beta \cos^2 \gamma) d\beta d\gamma$$

$$A = \int_0^{\frac{\pi}{2}} \int_0^{\frac{\pi}{2}} \sin \beta \exp(a_1 \cos^2 \beta + a_2 \sin^2 \beta \cos^2 \gamma) d\beta d\gamma$$

$$a_i = (b_i - b_3) U_0 / kT$$

It is shown in Appendix A.3 that the integrals may be expanded as rapidly converging series of powers of  $a_1$  and  $a_2$  as follows:

$$A = \frac{1}{4} \sum_{n=0}^{\infty} \frac{\Gamma(\frac{1}{2})}{\Gamma(n+\frac{3}{2})} I_n(a_1, a_2)$$

$$B = \frac{1}{4} \sum_{n=0}^{\infty} \frac{\Gamma(\frac{1}{2})}{\Gamma(n+\frac{3}{2})} \frac{1}{2n+3} (I_n + 2a_1 \frac{\partial}{\partial a_1} I_n)$$

the functions  $I_n$  being given by recursion formulae:

$$I_0 = \pi; \quad I_1 = \pi(a_1 + a_2) / 2$$

$$I_n = \frac{2n-1}{2n} (a_1 + a_2) I_{n-1} - \frac{n-1}{n} a_1 a_2 I_{n-2}$$

The other parameters are given by

$$k_2 = B(a_2, a_1) / A(a_1, a_2); \quad k_3 = 1 - k_1 - k_2$$

The ionisation potentials and polarisabilities used in the calculations are shown in table 2.3. The ionisation potentials used for PE and PVA are those of n-heptane and ethanol, respectively. The anisotropy of polarisability of PE and PVA were calculated from the anisotropic form of the Lorentz-Lorenz formula (Vuks, 1966)

$$\frac{n_i^2 - 1}{n_i^2 + 2} = \frac{4}{3} \pi N b_i; \quad i = x, y, z$$

$$n^2 = \frac{1}{3} (n_x^2 + n_y^2 + n_z^2)$$

where the axes  $i$  are the principal axes of the dielectric permeability tensor, and  $n_i$  and  $b_i$  are the associated refractive index and polarisability, respectively.  $N$  is the number of

TABLE 2.3

VALUES OF POLARISABILITY ANISOTROPIES AND IONISATION POTENTIALS  
OF NAPHTHALENE, QUINOLINE, ANTHRACENE, POLYETHYLENE AND PVA

Molecule	$\epsilon$ (ev)	$b_1 - b_3$ ( $\text{cm}^3 \times 10^{24}$ )	$b_2 - b_3$	Sources
Naphthalene	8.12	10.5	5.30	Kitagawa (1968); Cheng et al. (1971)
Quinoline	8.62	14.5	8.55	Dewar and Worley (1969); Lefevre and Lefevre (1955)
Anthracene	7.4	20.0	8.58	Kitagawa (1968); Gutman and Lyons (1967); Lefevre et al. (1968)
Polyethylene ( $-\text{CH}_2\text{CH}_2-$ )	10.1	0.46	0	Gutman and Lyons (1967)
Poly(vinylalcohol)	10.5	0.46	0	Gutman and Lyons (1967)

molecules per unit volume. The values of  $n_z$  and  $n_y$  were calculated from the isotropic refractive index

$$\bar{n} = \frac{1}{3}(n_z + 2n_y)$$

where it is assumed that  $n_x = n_y$ , and the limiting birefringence at infinite stretch (taken from fig 2.4(a)), which is equal to  $n_z - n_y$ . The value of  $N$  was calculated from the density. The relevant data are given in table 2.4. Measurement of flow birefringence has given a value of  $0.7 \times 10^{-24}$  for the anisotropic polarisability of PE (Brandrup and Immergut, 1966).

In table 2.5 are shown the values of  $k_1$ ,  $k_2$  and  $k_3$  calculated for naphthalene, quinoline and anthracene from the recursion formulae given above, and the data of table 2.3. Although the parameters of PE were used in the calculations, results for PVA

TABLE 2.4

ISOTROPIC REFRACTIVE INDEXES AND DENSITIES OF POLYETHYLENE AND

	$\bar{n}$	Density (gm cm <sup>-3</sup> )	<u>PVA</u> Sources
PE	1.515	.914	Schael (1968)
PVA	1.51	1.294	Brandrup and Immergut (1966), Pritchard (1970)

TABLE 2.5

CALCULATED AND EXPERIMENTAL LIMITING ORIENTATIONS DUE TO DIS-

	<u>PERSION INTERACTIONS</u>			
	$U_0/kT \times 10^{-24}$	$k_1$	$k_2$	$k_3$
<u>CALCULATED</u>				
Naphthalene	-.033	.36	.33	.31
	-.20	.48	.31	.21
Quinoline	-.033	.36	.34	.30
	-.20	.52	.31	.17
Anthracene	-.041	.39	.32	.28
	-.25	.68	.20	.12
<u>EXPERIMENTAL</u>				
Naphthalene and Quinoline in PE		.49	.33	.16
Quinoline in PVA		.55	.41	.04
Anthracene		.75	.20	.05

would be almost identical, because of the similarity in anisotropic polarisabilities and ionisation potentials. In the table there are two sets of calculated  $k_i$  parameters for each molecule. The values of  $U_0$  used to calculate the first set were obtained

using a value of  $r$  of 0.36 nm, which is the sum of the van der Waals radii of the two interacting molecules (Lamotte et al., 1974), and values of  $b_z$  and  $b_y$  for a length of (trans configuration) polymer chain equal to the length of the solute molecule with which it interacts. The second set of  $k_i$  parameters was calculated using six-fold larger values of  $U_0$ . Also shown in the table are the experimental values of  $k_i$ , derived from figs 2.2 and 2.3. Those for anthracene are rough estimates obtained by linear extrapolation from  $v^{-1} = 1$  through the first set of experimental points to  $v^{-1} = 0$ .

Diagrams 2.2 and 2.3 illustrate the relationship between  $K_1$ ,  $K_2$  and  $K_z$  for the compounds studied. Although the extrapolations to  $v^{-1} = 0$  for anthracene and acridine are rather arbitrary, the data clearly indicate different mechanisms of orientation for naphthalene, quinoline and 9-aminoacridine on the one hand, and anthracene and acridine on the other. In the former case, the data are in conformity with eqn 2.6. The experimental  $k_i$  values are much greater than the calculated values, as shown in table 2.5, but the values calculated using six-fold larger values of  $U_0$  are in good agreement with experiment. This indicates that the form of eqn 2.9 is correct, the enhanced value of  $U_0$  resulting either because interactions with more than one polymer molecule need to be taken into account, or because the approximations used in fitting molecular parameters to the dispersion potential are inadequate. As will be discussed later, it is believed that the latter is more likely to be the case. There are several reasons why the calculated value of  $U$  might be inexact: London's expression comes from the first term of the expansion of the exact dispersion potential in inverse,

even powers of  $r$ , which is asymptotic (Brooks, 1952), and therefore might be inadequate when  $r$  is of the same order of magnitude as the molecular dimensions. Also, polarisability is a frequency dependent property, and the values used in the calculation, which relate to the frequency of visible light, might be significantly less than those at molecular ionisation frequencies, which make the bulk of the contribution to the dispersion potential.

The fact that the orientation of naphthalene is not affected by a change from a non-polar (PE) to a polar (PVA) medium indicates that polar interactions are not important for this molecule. The orientation of quinoline in PVA, however, differs from that in PE. This is ascribed to the presence of hydrogen bonding between the hydroxyl group of PVA and the quinoline nitrogen atom. The value of  $k_3$  in PVA is equal to 0.04, demonstrating a high degree of correlation of the plane of the solute molecule with the direction of the polymer axis ( $z$ ). However with respect to directions in the plane of the molecule, the effect of the polar interactions is largely isotropic; this is shown by the fact that the values of  $k_1$  and  $k_2$  are changed relative to those in PE in roughly the same proportion. In spite of its charge, polar interactions do not seem to be of importance in the orientation of 9-aminoacridine. If they were of importance, one would expect a larger, rather than a smaller, degree of orientation than shown by acridine.

If naphthalene, quinoline and 9-aminoacridine do orient by interaction with one molecule of polymer only, the possibility that repulsive interactions contribute significantly to orientation can be ruled out, since such a mechanism would offer no scope for the preferred orientation of the long axis of the solute

in the Z direction, which is almost universally observed.

Anthracene and acridine are seen, from the non-linearity of the  $K_1$  and  $K_2$  parameters, to orient by a mechanism involving simultaneous interaction of each solute molecule with more than one molecule of polymer. The limiting behaviour of the K parameters indicates total correlation of solute and polymer orientation axes at high degrees of stretch; on the other hand there cannot be total correlation at low degrees of stretch, or the solute orientation would simply follow the polymer orientation, and be linear with  $K_z$ .

Because the molecular orientation is the same in PE and PVA, it is unlikely that polar interactions are of significance. Since the orientation of the two compounds is different, it is clear that repulsive interactions are not exclusively responsible for the orientation characteristics: repulsive interactions would be expected to be identical for molecules of the same shape. Thus dispersion interactions must be responsible for the differences observed between the two compounds. It is unlikely, however, that dispersion interactions alone would be capable of causing the large increase in orientation observed at large degrees of stretch. In order to construct a qualitative argument in this regard, it is necessary to consider firstly the way in which the polymer molecules are oriented about the solute, and then to formulate a solute potential which can be reasonably expected to describe the qualitative aspects of solute orientation.

Since it is not known whether the orientation distribution of the all-trans segments of polymer in the film is homogeneous, or whether adjacent segments tend to lie parallel as a result of their mutual interactions, two extreme cases are considered.

In the first, each solute molecule lies between parallel polymer segments, and in the second, the solute lies between segments whose orientations are mutually independent. If the first case were correct, all the assumptions underlying the derivation of eqn 2.6 would be satisfied, and  $K_1$  and  $K_2$  would vary linearly with  $K_z$ . Therefore the second case is assumed to describe the true situation with reasonable accuracy.

The simplest approach to formulating a dispersion potential is to follow treatments used in relation to nematic liquid crystals (Nehring and Saupe, 1969), which express the average potential, for a large number of solute molecules, in terms of powers of the direction cosines  $(l_{1Z}, l_{2Z}, l_{3Z})$ , relating solute orientation to the film axes  $(X, Y, Z)$ . (For nematic liquid crystals, the axis  $Z$  is the optic axis of the system.)

$$U = \sum_{i,k,l} C_{ikl} l_{1Z}^i l_{2Z}^k l_{3Z}^l$$

In Nehring and Saupe's treatment terms for which  $i + k + l \geq 4$  are neglected; and the expression for the anisotropic part of the potential becomes

$$U = -d_1 l_{1Z}^2 - d_2 l_{2Z}^2$$

The distribution of the orientations  $(l_{1Z}, l_{2Z})$  is regarded as being uniform, so that

$$K_i = \frac{1}{N} \int l_{iZ}^2 \exp(-U/kT) d\tau, \quad (2.10)$$

this expression being identical in form to eqn 2.7. It follows from eqn 2.8 that in the expression for the anisotropic potential  $U$  for a single solute molecule, the coefficient of  $l_{1Z}^2$  is linearly related to  $b_1 - b_3$  and the values of  $l_{2Z}^2$  of the surrounding polymer molecules, and that of  $l_{2Z}^2$  to  $b_2 - b_3$  and  $l_{3Z}^2$ . It is therefore reasonable to assume that the average potential has the form

$$U = -\left(K_z - \frac{1}{3}\right)\{f_1(b_1 - b_3)l_{1z}^2 + f_2(b_2 - b_3)l_{2z}^2\},$$

the factor  $K_z - \frac{1}{3}$  being necessary to make  $U$  vanish when polymer orientation is random. The linear dependence of  $U$  on  $K_z$  is exact if the solute molecules are in sites of axial symmetry with respect to the  $Z$  direction (Lamotte, 1975; Sackmann and Moehwald, 1972) but, as discussed in section 2.3, there are no grounds for such an assumption. The qualitative agreement of eqn 2.10 with experiment was tested by taking values of  $f_1$  and  $f_2$  suitable to give calculated  $K_1$  values of the same order of magnitude as found by experiment. This procedure as carried out for anthracene is illustrated in fig 2.6, and it is seen that, as expected, the predicted orientation at high degrees of orientation differs from that observed by experiment.

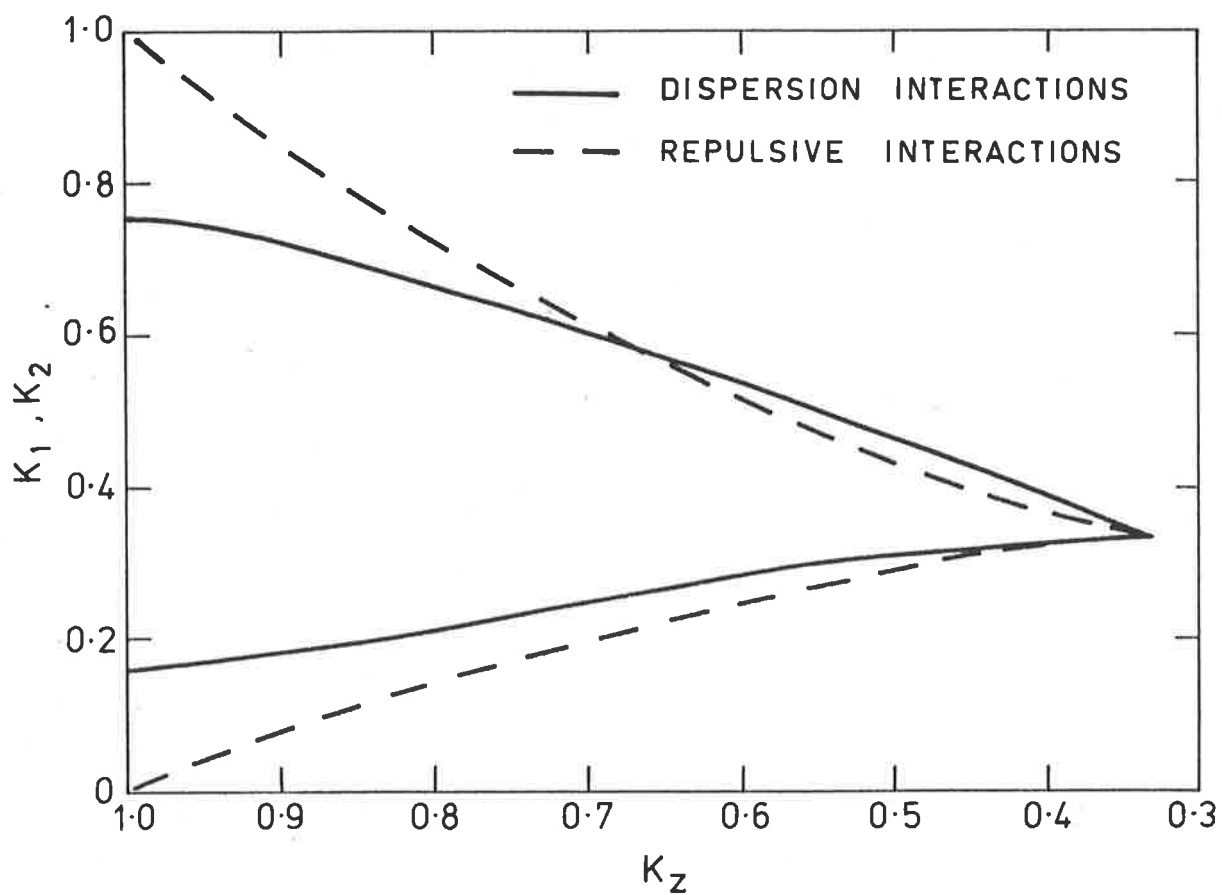
In order to model repulsive forces the following potential form, which was used by Luckhurst and Yeates (1976) in connexion with nematic liquid crystals, is used:

$$\begin{aligned} U(l_{1z}) &= 0 \text{ if } l_{1z} > l_{1z}^0 \\ &= \infty \text{ if } l_{1z} < l_{1z}^0 \end{aligned}$$

Such a potential would be experienced by a solute molecule restrained so that the angle between its orientation axis and the film  $Z$  axis did not exceed  $\arccos(l_{1z}^0)$ .  $l_{1z}^0$  is a function of  $K_z$ ; fig 2.6 depicts the predicted relationship between the solute orientation parameters and  $K_z$  for the simplest case, in which  $l_{1z}^0$  is a linear function of  $K_z$ . Predicted and observed behaviour are seen to be in qualitative agreement.

From these considerations, it is concluded that orientation in anthracene and acridine is dominated by repulsive interactions with the surrounding polymer molecules. The fact that similar behaviour is not shown by naphthalene, quinoline and 9-amino-

FIG 2.6 VARIATION OF  $K_1$  AND  $K_2$  OF ANTHRACENE WITH  $K_z$  ACCORDING TO HYPOTHETICAL POTENTIALS FOR SIMULTANEOUS INTERACTION OF SOLUTE WITH SEVERAL POLYMER MOLECULES



acridine, at least within the range of draw ratios used, is probably due to the smaller disparity between molecular length and width for these compounds, which does not engender such a large anisotropy in the repulsive potential. Their orientation characteristics are reasonably well described by the one-to-one interaction model, if it is assumed that the value of  $U_0$  has been underestimated by a factor of about six. It is unlikely that interaction with more than one polymer molecule could account for this discrepancy. Because  $U$  falls off rapidly with  $r$ , the only interactions of significance are those with nearest neighbours. For a six-fold increase in the anisotropic potential, it would be necessary for each solute molecule to be surrounded by six polymer segments, all at a distance of about 0.36 nm, if all the segments were parallel, or a greater number if, as has been seen, they were not. The pyrimidine and purine molecules to be studied are classified, by their shape, with those molecules for which repulsive interactions are not a dominant influence in orientation and in Chapters Six and Seven their orientation characteristics will be discussed in relation to the ideas expressed above on the orientation of such molecules.

CHAPTER THREEEXPERIMENTAL3.1 Materials

PE films were of commercial origin, about 0.1 mm thick, and were extracted with chloroform before use. PVA, 99.100% hydrolysed, was obtained from J.T. Baker Chemical Co., Phillipsberg, N.J., U.S.A. Acridine, L.R. grade (B.D.H. Chemicals Ltd., Poole, England) was purified by a method described by Jensen and Friedrich (1927). 9-Aminoacridine (Fluka) was recrystallised from ethanol. Caffeine, theophylline and theobromine were all L.R. grade (B.D.H.) and were recrystallised from water. Phthalimide (B.D.H., L.R. grade) was recrystallised from ethanol. The following were used without purification: uracil, thymine, cytosine, guanosine, cytidine, uridine, thymidine (Sigma Chemical Co., St. Louis, Mo., U.S.A.), 1-methylxanthine and 3-methylxanthine (Cyclo Chemicals, Los Angeles, Calif., U.S.A.), 1-methylthymine (Pfalz and Bauer Inc., Flushing, N.Y., U.S.A.), 9-methyladenine (Fox Chemical Co., Los Angeles, Calif., U.S.A.) and cytidine-5'-phosphate sodium salt (P-L Biochemicals Inc., Milwaukee, Wis., U.S.A.). Benzene, chloroform and cyclohexane, when used as spectroscopic solvents, were of Spectroscopic Grade, obtained from Merck and Co., Rahway, N.J., U.S.A. Dioxane was A.R. grade and showed no traces of acetal. It was distilled from sodium immediately before use.

3.2 Preparation of Films

PVA films were cast from solutions of PVA in water (5% w:v). Suitable quantities of solute (about 5 mg for the purine and pyrimidine bases) were dissolved in 12.5 ml of PVA solution,

which was poured into rectangular glass trays of about 100 cm<sup>2</sup> area floating on mercury. Clear films with a fairly uniform thickness of about .025 mm were obtained after 48 hr. The dissolved substance constituted about 1% of the dry weight of the film. PE films were doped by immersion in benzene or chloroform solutions of the required solute. PE films of the purine and pyrimidine compounds studied could not be prepared, owing to their low solubility both in organic solvents and in the film itself.

The doped films were clamped in a stretching device (Kelly, 1974), the portion of film undergoing stretching being a square of side 3 cm. PE films were found to be anisotropic in their mechanical properties, probably as a result of the rolling process which occurs during manufacture. The films stretched satisfactorily only when drawn in a direction perpendicular to the roller marks. However no optical anisotropy was observed in the unstretched films. The PVA films were stretched at a rate of about 1 cm/min, being in an enclosed area over a water bath at 50°C, to render them more ductile. The PE films were stretched rapidly at room temperature. The draw ratio  $v$  was measured by means of a pair of marks placed 1 cm apart in the centre of each film. The stretched films were washed with ethanol, to remove any solute present on the surface, and the tension was removed until the films were just taut. They were clamped directly into brass holders about the same size and shape as standard spectrophotometer cells (Kurucsev and Zdysiewicz, 1971). Gaskets of filter paper were used to prevent the films from slipping between the surfaces of the brass mount. PVA films thus mounted were heated at 100°C for 15 minutes in a

nitrogen atmosphere to eliminate infrared absorbance caused by residual water.

### 3.3 Spectroscopic Measurements

The UV dichroic spectra were determined by use of a Zeiss PMQII manual spectrophotometer equipped with an attachment that effectively eliminates light intensity losses caused by scattering (Kelly and Kurucsev, 1975). A Glan-Taylor calcite polariser (Archard and Taylor, 1948) was used: this imposed an upper limit of about  $45500 \text{ cm}^{-1}$  on the accessible spectral range. The instrument was operated at such slit widths as were necessary to give a resolution of  $250 \text{ cm}^{-1}$  or better.

Infrared spectra were recorded with a Perkin-Elmer Model 457 spectrophotometer, both beams of which were polarised (for film measurements) by matching grid polarisers (Cambridge Physical Sciences, Cambridge, England, IGP 225) mounted between source and sample. The largest slit setting was used in order to compensate for the attenuation of the beams caused by the polarisers. This had no effect on the accuracy of the measurements as the bands measured were very broad. In the areas of the spectrum used, nearly  $1800\text{-}1600 \text{ cm}^{-1}$  and  $1245\text{-}1225 \text{ cm}^{-1}$  (the latter for the data of fig 2.4(b) only) the response of the instrument was not greatly sensitive to the direction of polarisation of the beams, although in other regions it was very much so. The spectra in the region  $1800\text{-}1600 \text{ cm}^{-1}$  were the same whether or not the instrument was flushed with dry nitrogen to remove the effect of atmospheric absorption, and so this precaution was not taken with the majority of spectra.

In both the UV and IR regions the relative orientations of the film and the polarisation direction of the beam necessary

to measure  $A_Z$  and  $A_Y$  were achieved by rotating the polariser, rather than the film. The UV and IR absorbance due to the polymer itself was measured after removing the solute from the film by soaking in chloroform or benzene in the case of PE, or an ethanol/water mixture at 40°C in the case of PVA. The absorbance of the films used was between 0.05 and 0.15 in the region 25000  $\text{cm}^{-1}$  to 46000  $\text{cm}^{-1}$ . The absorbance of the PVA films in the region of carbonyl absorbance, 1800  $\text{cm}^{-1}$  to 1600  $\text{cm}^{-1}$ , was between 0.1 and 0.2; there was a "hump" at about 1200  $\text{cm}^{-1}$  owing to the presence of residual poly(vinyl-acetate). The reasons for confining IR measurements to this region are discussed in the next section. Spectra were measured at an ambient laboratory temperature of  $22.5 \pm 2.5^\circ\text{C}$ .

The IR solution spectra were measured by standard methods. The cell path lengths were calculated from measurements of interference fringes due to double reflection in the range 1100-800  $\text{cm}^{-1}$  by use of the formula

$$l = \frac{n}{2} \left( \frac{\lambda_1 \lambda_2}{\lambda_1 - \lambda_2} \right)$$

where  $n$  is the number of complete fringes between wavelengths  $\lambda_1$  and  $\lambda_2$ . The values of  $l$  measured in this way agreed to within 2% with direct measurements of the thickness of the cell spacers.

### 3.4 Experimental Errors and Difficulties

Neither of the spectrophotometers showed a significant amount of polarisation in the spectral regions used. The Glan-Taylor polarisers were assumed to be completely efficient and no correction was made to the measured UV/visible dichroisms. According to the manufacturer's specifications, the degree of

polarisation of the IR grid polarisers was better than 95% for wavelengths greater than 6  $\mu\text{m}$ , and therefore no correction was made for polariser inefficiency in the IR region, either. The alignment of the polarisers, and of the films in their holders, was estimated to be better than  $\pm 5^\circ$ .

As was mentioned in the Introduction, serious impediments exist to gaining information on molecular orientation from measurements of IR dichroism. This is particularly so in the case of pyrimidines and purines. In the first place, these molecules do not show a high degree of dichroism ( $K_1 - K_2 \approx 0.15$ ). Since the random variations in  $K_1$  and  $K_2$  from film to film are significant compared with this figure, it is necessary to perform both UV and IR dichroic measurements on the same sample. As a result, only those IR bands are available for study which are comparable in intensity with the UV bands. Secondly, most of the IR absorption of solutes in PVA films is masked by the high absorbance of PVA itself. The absorbance of films of the thickness used in this work is everywhere greater than 0.5, except in the region  $1500\text{ cm}^{-1}$  to  $2800\text{ cm}^{-1}$ . The only reasonably intense bands in this region are the carbonyl stretching bands, between  $1600$  and  $1800\text{ cm}^{-1}$ , and other double-bond stretching vibrations which, because they do not have determinable transition moments, are of no use for the purposes of this work. The absorbances of the carbonyl bands at the concentrations of solute used were in the range 0.1 to 0.3, that is, only slightly larger than that of the polymer itself. Since it was not possible to reproduce the polymer baseline consistently for IR absorbance, considerable variations in IR dichroism were observed for films prepared under similar conditions. In order to average out random errors arising

from this source, data were collected for several films of each compound, all stretched to approximately the same extent, and the spectra, corrected for polymer absorbance, were added to give the values of  $A_z$  and  $A_y$  used to calculate the dichroism.

To date, the only other work to make use of IR dichroism in determining the orientations of molecules of low symmetry has been that of Gangakhedkar et al. (1974), which was mentioned in the Introduction. Most of the IR bands studied in that work lay in regions where PVA absorbance was several times greater than that of the solute. In spite of the authors' claims, it seems impossible that such a high background absorbance could be adequately compensated by the use of techniques of differential spectroscopy in conjunction with a conventional spectrophotometer. In the present work, therefore, no attempt has been made to study any solute bands other than the carbonyl bands.

To judge the compatibility of IR and UV dichroism measurements, phthalimide was used as a model compound. The phthalimide molecule (fig 3.1) has  $C_{2v}$  point symmetry (Matzat, 1972). The carbonyl bands at 1767 and 1720  $\text{cm}^{-1}$  are long- and short-axis polarised respectively, the former having higher dichroism, indicating that the long-axis of the molecule is the orientation axis. The UV dichroic spectrum (fig 3.1) in PVA shows a weak, long-axis polarised transition (I) at 33000  $\text{cm}^{-1}$ , and an intense, short-axis polarised transition (III) beginning at 40000  $\text{cm}^{-1}$ , as predicted by PPP-CI calculations (table 3.1) and in agreement with measurements of polarised fluorescence (Sarzhevskii, 1963).

Shown in table 3.2 are the IR and UV dichroisms of phthalimide, being derived from results for six films. The observed long-axis dichroisms are in good agreement, but the UV

FIG 3.1 UV DICHOIC SPECTRUM OF PHTHALIMIDE

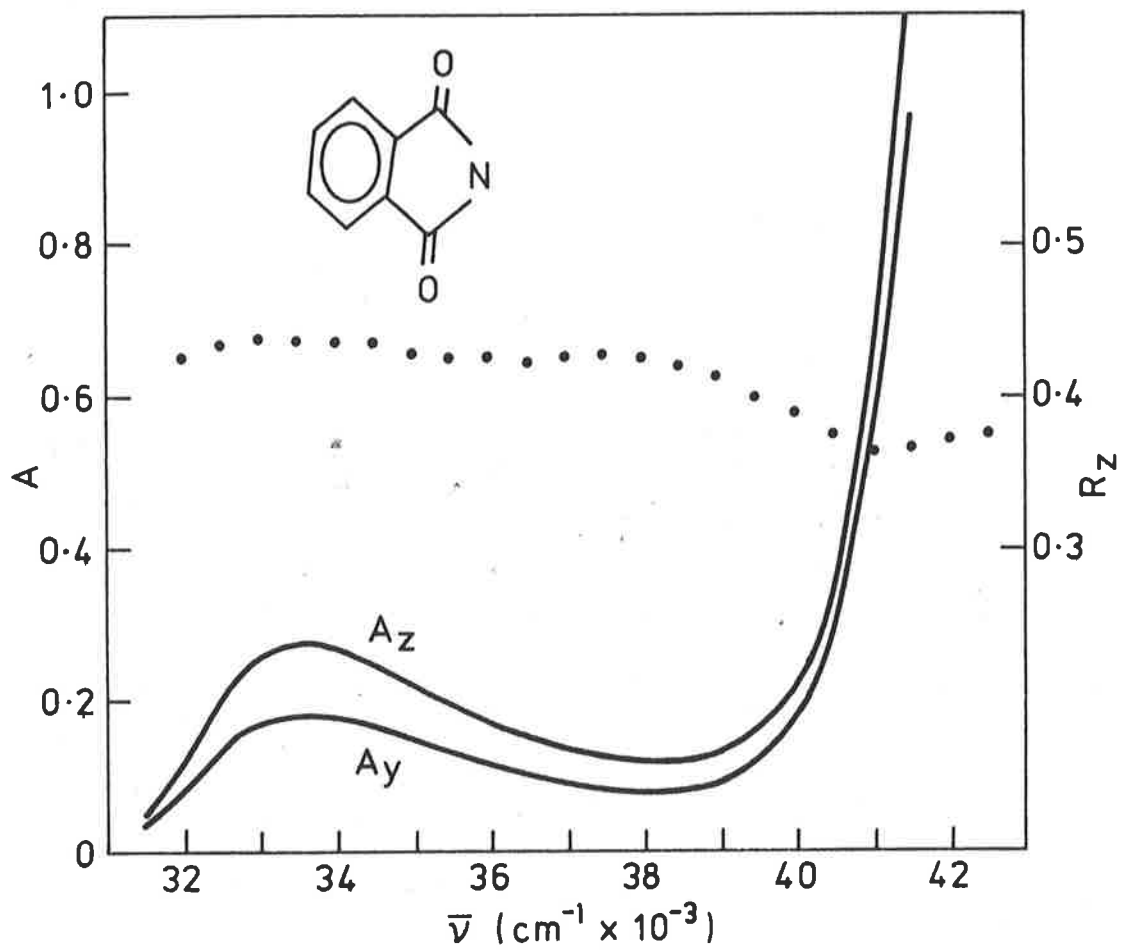


TABLE 3.1

PPP-CI CALCULATIONS FOR PHTHALIMIDE

(Atomic Coordinates from Matzat, 1972)

Transition	$\bar{\nu}$ ( $\text{cm}^{-1}$ )	f	Polarisation
I	35300	.045	1
II	37500	.006	2
III	42600	.316	2
IV	46800	.400	1

short-axis dichroism is considerably larger than that of its IR counterpart: it is seen that the calculations predict two fairly intense transitions of opposite polarisation in the region and it is likely that these transitions are closely situated in the observed spectrum, causing mixed polarisation. The fact that the dichroisms of the long-axis polarised transitions are in agreement indicates that the IR dichroisms may be considered reliable when calculated in the manner described, particularly as the intensity of the  $1767 \text{ cm}^{-1}$  band of phthalimide is much lower than the intensities of the carbonyl bands of the pyrimidine and purine compounds studied.

TABLE 3.2

IR AND UV DICHROISM OF PHTHALIMIDE

$\bar{\nu}$ ( $\text{cm}^{-1}$ )	$R_Z$	Polarisation
1767	.424	1
33500	.428	1
1720	.347	2
41000	.375	2

Several authors have pointed out the possibility of error due to non-uniform concentrations of solutes within films (Thulstrup, Michl and Eggers, 1970; Yogeve, Margulies, Sagiv and Mazur, 1974), although no estimate has been made of the extent to which such inhomogeneity occurs. Such errors would be observed mainly in experimental systems where Rochon polarisers are used, and it is necessary to rotate the sample rather than the polariser in order to achieve the necessary relative orientation of film and radiation polarisation. In the present measurements of UV-visible dichroism, owing to the slight degree of polarisation caused by the spectrophotometer, the slit width, at a given wavenumber, was slightly larger for measurements of  $A_z$  than for  $A_y$ . The difference was less than 15% and it is unlikely that concentration inhomogeneity would cause any error in this case. A similar source of error, which does not seem to have been discussed previously, is orientational inhomogeneity of the stretched film. This type of error, if present, would be more pervasive as it would result from the use of different slit widths at different wavenumbers and, for visible/UV measurements in the present case, these can vary by up to a factor of 3. The effect of changing slit width can be removed only by taking a series of spectra, moving the sample for each in such a way that a specific area of film is eventually covered (Thulstrup, Michl and Eggers, 1970). The degree of orientational inhomogeneity in films has, once again, never been determined, but the fact that parallel transitions in different regions of the spectrum as, for example, those of quinoline, are observed to have identical dichroisms, serves as evidence that it is not a significant source of error. In measurements of the IR and UV dichroisms

of a single sample, both types of error could occur if the spectrophotometer beam passed through different portions of the sample in each case, a possibility which was eliminated in the present work by siting the sample so that the beam passed through the same part of the film in both UV and IR measurements.

Brief mention must finally be made of techniques where the state of polarisation of the spectrophotometer beam is changed continuously during sampling of the spectrum (Jaffe et al., 1967; Norden and Davidsson, 1972). The second method, in particular, involving use of a modified CD spectrometer, enables direct measurement of the linear dichroic difference spectrum ( $A_Z - A_Y$ ) to a degree of accuracy two orders of magnitude better than that obtainable by conventional means. Such accuracy is invaluable in cases where molecular orientation is very small (Norden, 1975), either for qualitative interpretation of spectra or for the study of symmetric molecules where the problem of orientation is trivial. However the problem which is of central concern in this work, that of obtaining accurate transition moment direction of molecules of low symmetry, arises from the paucity of means available for establishing the average orientation of solutes in the films, rather than from spectrophotometric errors, at least in the visible/UV range. The errors of interpretation which result from inadequate knowledge of the orientation factors greatly exceed, as will be seen in Chapters Six and Seven, the limitations imposed by the sensitivity of the dichroism measurements.

### 3.5 Aggregation

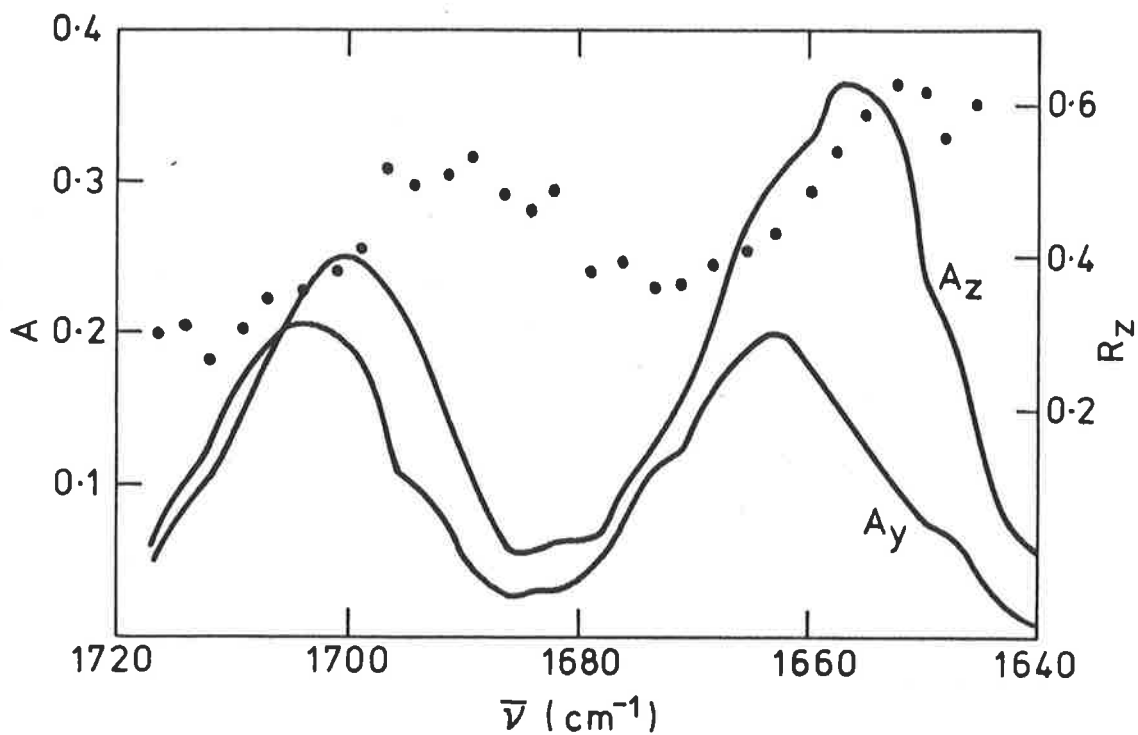
In PVA films prepared as described in section 3.2, using about 5 mg of a solute with a molecular weight of about 200, the concentration of solute in the film is about  $10^{-1}$  M, giving an average distance between solute molecules of about 25 Å, compared with about 5 Å in the crystal. It can be assumed that at such distances the effect of intermolecular interaction on molecular states is negligible. At such high concentrations of solute, however, it is necessary to ensure that the solute is in fact dispersed unimolecularly. In most of the published work, no attempt has been made to detect possible aggregation of the solute, and it is possible that reported instances of "short-axis" orientation (section 2.5) were, in fact, due to the presence of crystals in films: there have been no general criteria for the detection of aggregation; the formation of crystals is often not detectable by visual inspection and is difficult even with the aid of a polarising microscope, owing to the presence of small, birefringent inhomogeneities in the polymer itself. Furthermore in some cases non-crystalline aggregates appear to be present. It is desirable therefore to have criteria by means of which the presence of aggregated molecules of solute may be inferred from the spectra. Films of caffeine in PE provide an example of a system in which aggregation occurs and in terms of which the effects of aggregation on dichroic spectra may be discussed.

Films prepared by immersing PE strips in saturated solutions of caffeine in chloroform contained needle-like crystalline inclusions which could be seen with the aid of a polarising microscope. Spectra of the films showed dichroisms of less

than 1/3, indicating that the molecular planes were oriented perpendicular to the film Z axis, contrary to the usual experience of orientation of aromatic compounds. Furthermore, the carbonyl vibrational bands were each observed to be split into two components whose greatly different dichroisms showed them to be approximately orthogonal, indicating the presence of intermolecular coupling of excited (vibrational) states.

At lower concentrations of solute, the dichroisms increased, to eventually fall within the range normally observed, and the presence of crystals was no longer detectable. However, the splitting in the dichroisms of the carbonyl bands persisted (fig 3.2(a)), indicating the presence of a non-crystalline aggregated form of caffeine. The UV dichroism, even at very low concentrations (less than 0.25% w:w) showed a marked variation within the first band, as illustrated in fig 3.2(b). For isolated molecules, bands I and II each result from single electronic transitions of caffeine (see Chapter 7) whose transition moments are almost orthogonal. In fig 3.2(b) the dichroism of region I<sub>a</sub> is seen, however, to be almost the same as that of band II. In addition the intensity of absorption in this region is much greater than for isolated molecules (fig 3.3). It seems likely that these effects result, as do those in the vibrational spectrum, from coupling of molecular states induced by intermolecular interactions. It was proposed by Kikkert et al. (1973) that the absorption in region I<sub>a</sub> in PE is due to a ( $\pi^*$ ,n) transition which is of very low intensity in polar media. The data of fig 3.3, however, belie this hypothesis as they show that the spectra of caffeine in polar (H<sub>2</sub>O) and non-polar (cyclohexane) media are identical apart from a

FIG 3.2(a) IR DICHRISM OF CAFFEINE IN PE



(b) UV DICHRISM OF CAFFEINE IN PE

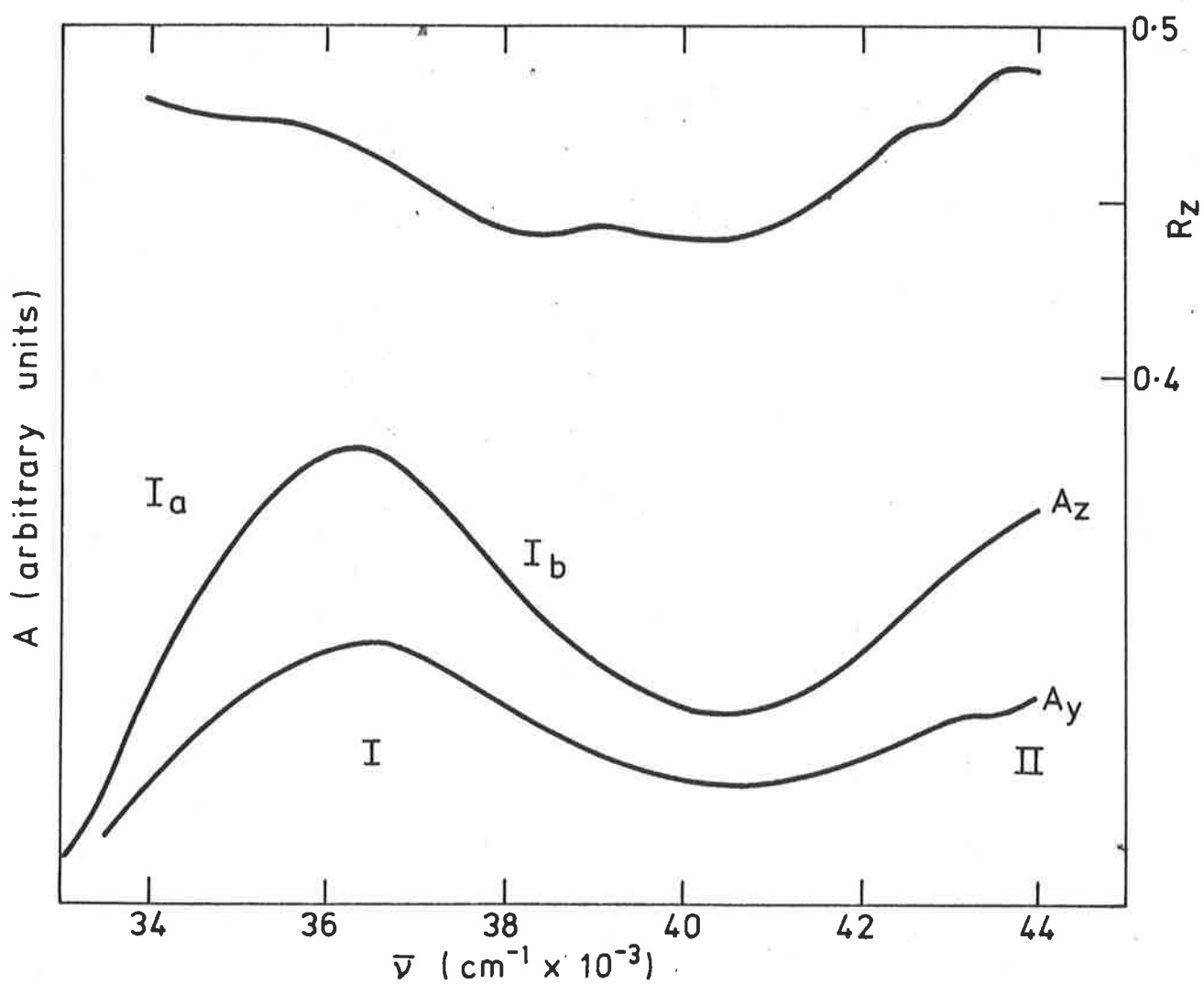
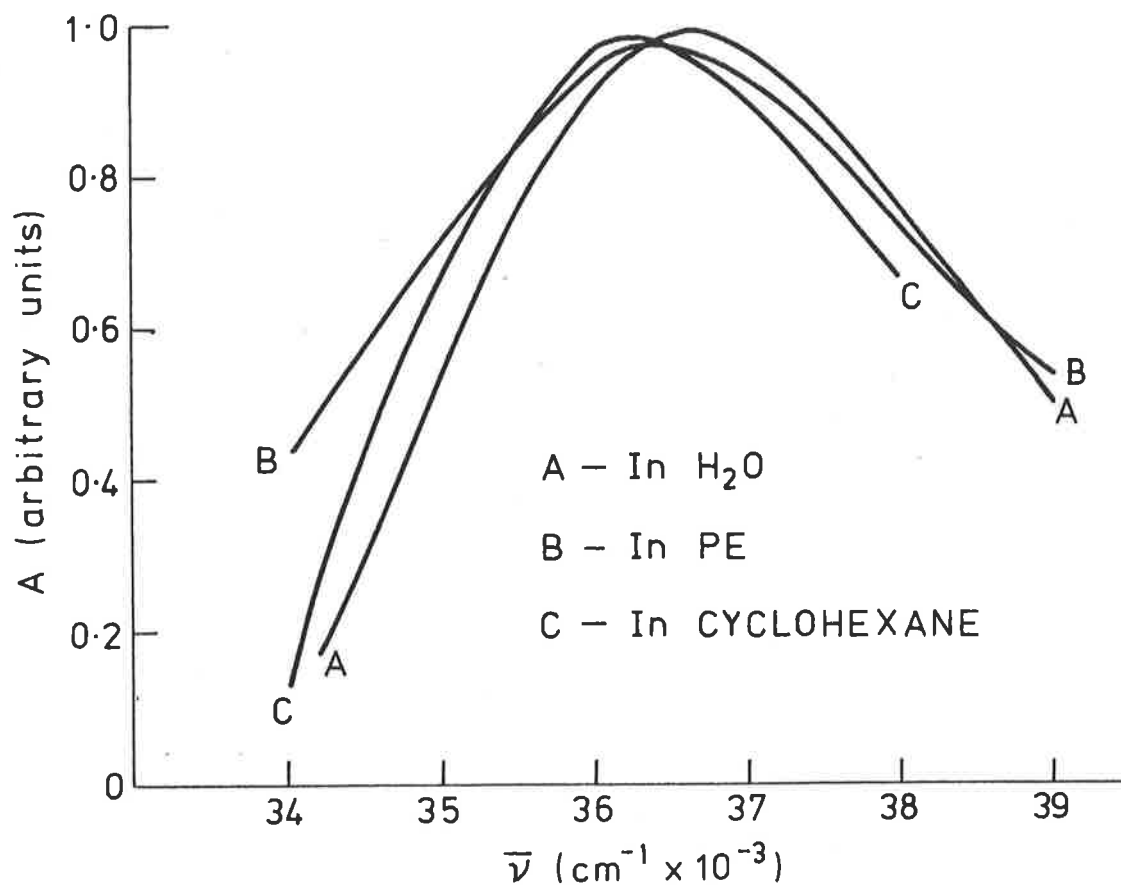


FIG 3.3 UV SPECTRA OF CAFFEINE IN VARIOUS SOLVENTS



slight red shift in the latter.

Large variation of dichroism within a single UV or IR band therefore, provides a criterion by which the presence of aggregation in solutes in stretched polymer films may be detected, and was used as a test for the presence of aggregation in the pyrimidine and purine films whose spectra are discussed in Chapters Six and Seven.

### 3.6 PPP-CI Calculations

The method of calculation used in this work is that of Bailey (1969, 1970). This method differs from others (eg. Pullmann and Pullmann, 1968; Michl, Thulstrup and Eggers, 1974) in two main respects. Firstly, the two centre core ( $\beta$ ) integrals are calculated through a rigorous (within the approximations of the PPP theory) relationship with the atomic overlap integrals, rather than being "semi-empirically" assigned, and secondly, in assigning the one-centre core and  $\gamma$  parameters a distinction is made between pyridine-, pyrrole-, amino- and lactam-type nitrogen atoms. Slater or Clementi basis functions are used: in the calculations done in this work results were found to be very similar and the basis used is not specified in the various tables. In the CI calculations all possible singly excited configurations are mixed; a mixed dipole-length/-dipole-velocity method (Hansen, 1967) is used in evaluating oscillator strengths and transition moment directions. In the calculations for the 9-aminoacridine cation, the one-centre core parameters were adjusted as described by Mataga and Mataga (1959) (model I); all other parameters were as for 9-aminoacridine. The molecular geometries used in the calculations were taken from X-ray crystallographic work, references

to which, in the case of the pyrimidine and purine compounds for which calculations were made, are given in Chapter 5.

CHAPTER FOURCARBONYL STRETCHING VIBRATIONS OF PYRIMIDINES AND PURINES

Use of the infrared dichroism of the carbonyl stretching bands of pyrimidines and purines in order to gain information on their orientation in stretched films necessitates a preliminary study aimed at determining the moment directions of the transitions associated with the bands. The problem of determining the molecular vibrational motion associated with each transition, and thereby determining the moment direction, forms the subject of this chapter.

4.1 Carbonyl Vibrational Modes

As cytosine and its derivatives contain only a single carbonyl group the assignments of the carbonyl vibrational mode and the transition moment direction are straightforward. The Raman spectra of cytosine, 1-methylcytosine, cytidine and 5'-CMP (sodium salt) in neutral D<sub>2</sub>O and H<sub>2</sub>O solutions show two bands in the double bond stretching region, at 1655 and 1610 cm<sup>-1</sup>, approximately (Lord and Thomas, 1967). The 1655 cm<sup>-1</sup> band was assigned in that work to the carbonyl vibration because of its high polarisation, and proximity to the carbonyl bands of uracil. A corresponding intense band at 1650 cm<sup>-1</sup> occurs in the IR spectra of cytidine (Hartman, 1967) and 5'-CMP (Tsuboi et al., 1973) in neutral D<sub>2</sub>O, with a band of medium intensity at about 1615 cm<sup>-1</sup>. In PVA films, cytidine and 5'-CMP showed intense bands at 1648 and 1643 cm<sup>-1</sup>, respectively, and these were ascribed to the carbonyl stretching vibration. Cytosine itself (fig 6.10b) showed bands at 1660 and 1630 cm<sup>-1</sup>, and the former was ascribed to carbonyl stretching. The origin of the 1630 cm<sup>-1</sup> band is not known. The carbonyl vibration

is assumed to involve motion of the atoms only along the bond axis, the transition moment, as a result, being in this direction also. Under this assumption, the transition moment direction for cytosine is as given in table 4.4; those of cytidine and 5'-CMP are assumed to have the same values.

Uracil, xanthine and their derivatives contain two carbonyl groups which usually give rise to two distinct bands of unequal intensity in the IR spectrum, which will be referred to as  $\nu_s$  and  $\nu_a$ , the former having the higher wavenumber. In the case of the xanthenes, there has been no attempt in the literature to interpret these bands; in the case of uracil and its derivatives the interpretation is controversial, two conflicting hypotheses having been put forward. In the first it is proposed that they arise from separate carbonyl vibrations, the difference in frequency resulting from differences in the chemical environment (one carbonyl group has a conjugated double bond). The alternative view is that the two carbonyl vibrations are essentially degenerate, the observed splitting arising from a second order effect which causes coupling. In the case of uracil and its derivatives, the view which has been expressed by most authors (Shimanouchi et al., 1964; Tsuboi et al., 1975; Lord and Thomas, 1967; Susi and Ard, 1971; Kyogoku et al., 1967; Tsuboi, 1974) is that the  $\nu_s$  band is due solely to  $C_2 - O$  stretching, whilst the  $\nu_a$  band results from  $C_4 - O$  stretching. The only experimental basis for this assignment appears to be a study by Miles (1964) of the isotopic shift in the carbonyl bands of uridine-4- $O^{18}$  relative to those of uridine in neutral  $D_2O$  solution: the  $\nu_s$  band had no shift whilst the  $\nu_a$  band had a shift of  $-5 \text{ cm}^{-1}$ . Two independent sets of normal mode

calculations (Tsuboi et al., 1973; Susi and Ard, 1971) also predicted that the wavenumber of the  $C_4 - O$  stretching is lowered by coupling with the  $C_5 - C_6$  stretching vibration. On the other hand, Horak and Gut (1961), who studied the solution spectra of a large number of derivatives of uracil and 6-aza-uracil in the region of carbonyl absorption, concluded that the separation of the carbonyl bands is due solely to a coupling effect. They pointed out that these compounds belong to the general class of cyclic imides, and that even those imides such as phthalimide, which have  $C_{2v}$  symmetry, and in which, therefore, the carbonyl groups have identical chemical environments, show a splitting of the carbonyl bands of the same magnitude as that observed in asymmetric molecules.

The infrared absorption associated with the carbonyl vibrations of cyclic imides with four-, five-, and six-membered rings has been studied in great detail by Fayat and Foucauld (1970). The compounds studied showed, in general, two bands of unequal intensity in the region  $1650$  to  $1900\text{ cm}^{-1}$ . In the malonimides the carbonyl bonds are almost coaxial. One would therefore expect a mode resulting from in-phase coupling of the carbonyl vibrations, being of approximate "g" symmetry, to give an intense Raman band and a weak IR band, and a mode resulting from out-of-phase coupling to give a weak Raman and an intense IR band. In fact the  $\nu_s$  and  $\nu_a$  bands, respectively, were observed by Fayat and Foucauld to have these properties. These authors also pointed out that in cases when the bonds are not coaxial the intensities of the in-phase and out-of-phase modes are related by

$$A_a/A_s = \tan^2\left(\frac{\alpha}{2}\right) \quad (4.1)$$

where  $A_a$  and  $A_s$  are the intensities of the in-phase and out-of-phase modes, respectively, and  $\alpha$  is the angle between the directions of the carbonyl bonds. This equation results from a simple vector addition model of the two separate carbonyl vibrations, assumed to be of equal intensity, and presupposes the absence of differential solvent effects on the two bands. It was found by Fayat and Foucauld to apply satisfactorily to the solution spectra of a variety of cyclic imides with substituents both on the ring carbon and imido nitrogen atoms. The intensities of the two bands in the Raman spectrum were also, as expected, roughly the reverse of those in the infrared.

The presence of splitting in other dicarbonyl systems has been discussed by Bellamy (1973) and Bellamy et al. (1960) and has been ascribed to mechanical coupling effects. Therefore, taking the view that uracils and xanthenes are typical representatives of the total class of cyclic imides, it must be concluded that their  $\nu_s$  and  $\nu_a$  carbonyl bands result from in-phase and out-of-phase coupled vibrations, respectively. The isotopic shift effect observed for uridine is not very strong evidence in favour of the alternative hypothesis. The carbonyl band of guanosine is shifted  $-14 \text{ cm}^{-1}$  by isotopic substitution (Howard and Miller, 1965), whilst in simple ketones shifts of about  $-30 \text{ cm}^{-1}$  are observed (Bellamy, 1973). The small shift observed for uridine can be taken as an indication that the effect of substitution is reduced as a result of the delocalisation of the carbonyl oscillation. The normal mode calculations, similarly, do not constitute very strong evidence: they are essentially least squares fitting procedures in which a set of force constants is adjusted to give a best fit to the

observed wavenumbers. For example in the calculations of Tsuboi et al., the potential used involved bond-stretching constants, angle deformation constants and repulsive force constants between nearest non-bonding atoms. The interaction between the carbonyl groups in this potential is zero and it is therefore not surprising that the carbonyl vibrations are predicted to contribute predominantly to different bands. On the other hand, whilst there is no compelling evidence in favour of the view that the carbonyl bands can be assigned to separate carbonyl vibrations, certain features can be observed in the spectra of uracil derivatives which tend to discredit this view, and yet which can be explained by, or at least are consistent with, the coupling hypothesis (xanthine will be discussed later in this section). The first of these is the relative intensities of the two bands in both the IR and Raman spectra. In 5'-UMP in neutral D<sub>2</sub>O solution, for example (Tsuboi et al., 1973) the  $\nu_a$  band is observed to be more intense than the  $\nu_s$  band in the IR, but less intense in the Raman spectrum. It was shown above that observations such as these can be explained in terms of the coupling hypothesis. One would expect the bands to be of equal intensity in both spectra if due to vibrations of separate carbonyl groups. The normal mode calculations predict that the  $\nu_a$  band is coupled with the C<sub>4</sub> - C<sub>5</sub> vibration, in which case it would have a lower intensity than  $\nu_s$ . The second feature involves the effect of substituents on the imido nitrogen atom on the splitting of the carbonyl frequencies, some data for which is shown in table 4.1, being taken from the work of Horak and Gut. It is seen that in dihydrouracil and dihydro-6-azauracil, and in 1-methyldihydrouracil, both  $\nu_s$  and  $\nu_a$

TABLE 4.1

WAVENUMBERS OF CARBONYL  $\nu_s$  AND  $\nu_a$  BANDS OF SOME URACILS  
IN DIOXANE SOLUTION (HORAK AND GUT, 1961)

Compound	$\bar{\nu}_s$ ( $\text{cm}^{-1}$ )	$\bar{\nu}_a$
Dihydrouracil		1709 (in pyridine)
1-Methyldihydrouracil		1712
3-Methyldihydrouracil	1727	1684
Dihydro-6-azauracil		1723
1-Methyldihydro-6-azauracil	1722	1709
3-Methyldihydro-6-azauracil	1730	1687
3-Ethyldihydro-6-azauracil	1728	1678

bands have the same wavenumber, and in 1-methyldihydro-6-azauracil the splitting is small. These observations are consistent with the normal mode calculations, which attribute the lowering in frequency of the  $\nu_a$  band to coupling with the  $C_5 - C_6$  double-bond vibration. However the fact that the presence of a methyl substituent on the imido nitrogen reintroduces the splitting, shows that this agreement is fortuitous. The coupling hypothesis can be used to explain some of the effects seen. Firstly, the key effect of the 3-substituent shows that the motions of the imido-nitrogen atom and its substituent are of importance in the splitting process. Motion of the nitrogen atom would be an essential factor in mechanical coupling of the carbonyl vibrations. Secondly, it is seen that the effect of splitting is to decrease  $\bar{\nu}_a$ , and that this decrease is greater the greater the mass of the substituent:  $\bar{\nu}_s$  remains virtually unchanged. This is consistent with the simple coupling model

shown in fig 4.1 where, it will be noted, the carbon and oxygen amplitudes have been drawn approximately equal, following Bellamy (1973). The  $\nu_s$  vibration is seen to involve motion of the carbonyl groups only, with no coupling to any other vibration in the molecule, in agreement with the observation that  $\bar{\nu}_s$  is approximately constant. On the other hand, the motion of the carbon atom in the  $\nu_a$  vibration is seen to be part of a concerted, in-phase rotational motion of all the groups attached to the imido-nitrogen atom, and in this way the mass of the substituent adds to the inertial mass of the carbon atoms and lowers the frequency of the  $\nu_a$  vibration.

The IR spectra of the xanthines in the carbonyl stretching region have not been the subject of a great deal of study, and no assignments have been made in the literature; however on the basis of the analysis above, interpretation of the spectra is quite straightforward. In fig 4.2 are shown the spectra of theobromine, theophylline and caffeine in dioxane solution. The values of  $\bar{\nu}_s$  and  $\bar{\nu}_a$ , shown in table 4.2, are seen to depend on the imido nitrogen substituent, as discussed.

TABLE 4.2

<u>WAVENUMBERS OF <math>\nu_s</math> AND <math>\nu_a</math> BANDS OF XANTHINES</u>			
Compound	Solvent	$\nu_s$ ( $\text{cm}^{-1}$ )	$\nu_a$
Xanthine	Pyridine	1700	(From Horak and Gut, 1961)
Theobromine	Dioxane	1700	
Caffeine	Dioxane	1706	1664
Theophylline	Dioxane	1705	1666

FIG 4.1 A MODEL FOR COUPLING OF CARBONYL VIBRATIONS IN CYCLIC IMIDES

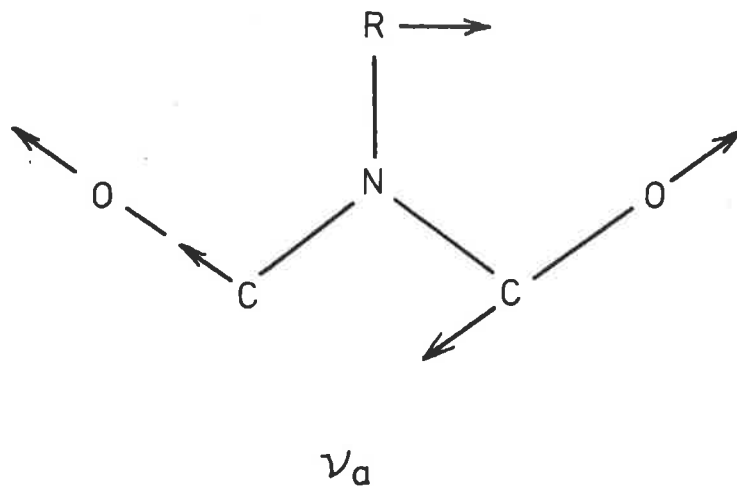
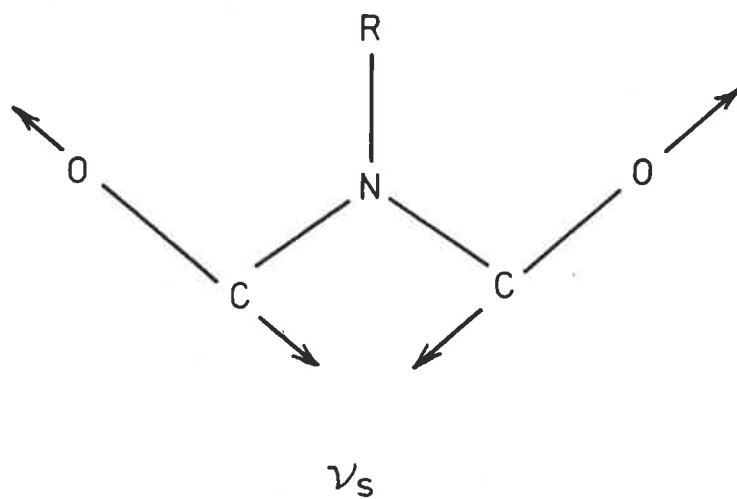
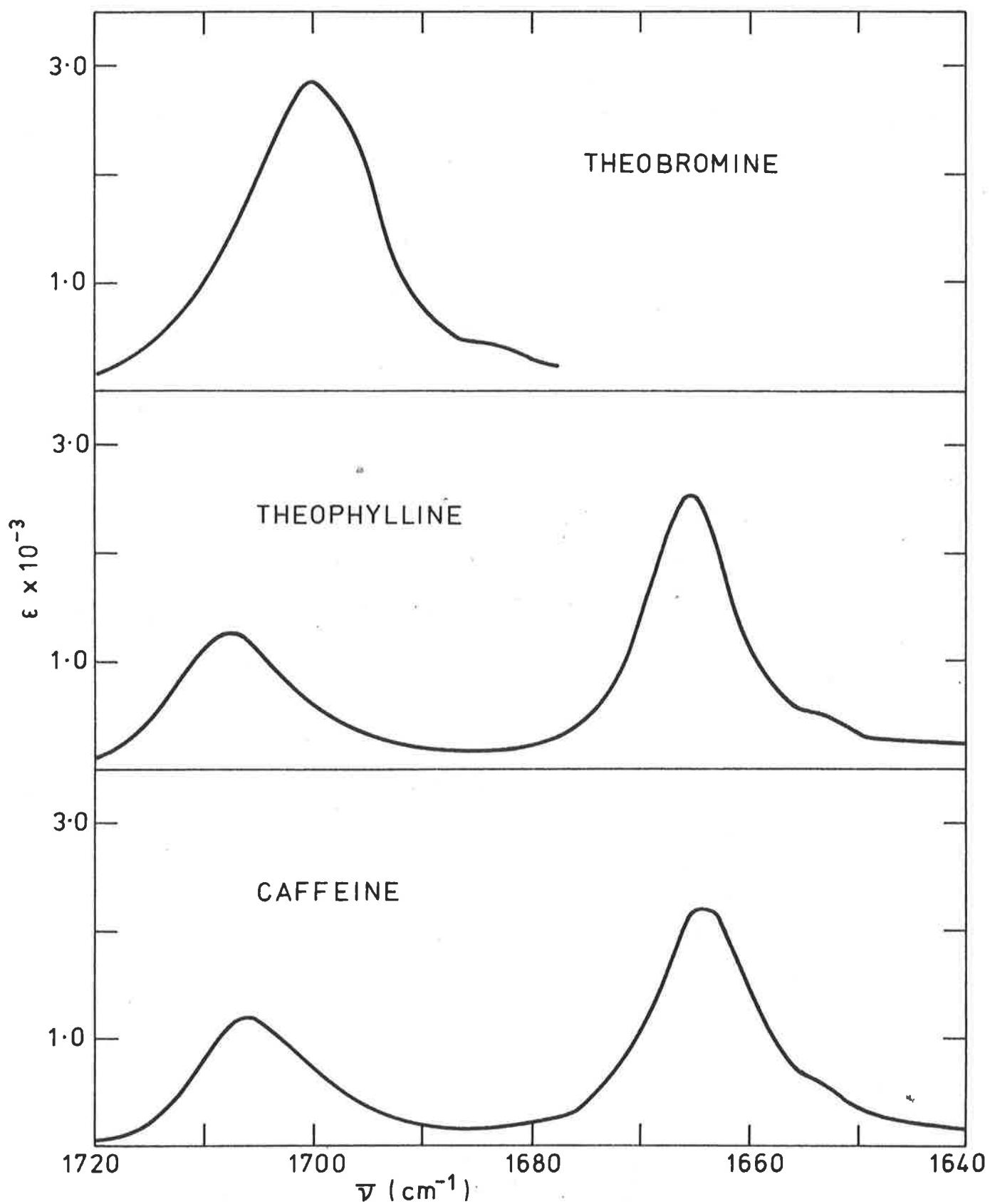


FIG 4.2 IR SPECTRA OF THEOBROMINE, THEOPHYLLINE AND CAFFEINE  
IN DIOXANE SOLUTION



The presence of only a single band in the spectrum of theobromine had been earlier put down to an enol tautomerism of one of the carbonyl groups (Blout and Fields, 1950), but later work on the UV (Pfleiderer and Nuebel, 1961; Cavalieri et al., 1954; Lichtenberg et al., 1971) and NMR (Lichtenberg et al.) spectra of xanthines showed that, at least in aqueous solutions, the diketo form was predominant. The fact that the total integrated carbonyl intensities of theobromine, theophylline and caffeine in dioxane (table 4.3) are all equal, within the limits of experimental error, shows conclusively that in this solvent the diketo tautomer only is present in significant quantities. Shown also in table 4.3 are the relative intensities of the  $\nu_s$  and  $\nu_a$  bands of theophylline and caffeine in dioxane. The angles of  $\alpha$  calculated from these values by means of eqn 4.1 are both  $107^\circ$ , which is in good agreement with the X-ray crystallographic values of  $115^\circ$  and  $113.5^\circ$  respectively (Sutor, 1958a;b), providing further evidence for the presence of coupling in this case.

TABLE 4.3

INTENSITIES OF  $\nu_s$  AND  $\nu_a$  BANDS OF XANTHINES

Compound	$A_s + A_a$ (relative)	$A_a/A_s$
Caffeine	1.00	1.89
Theophylline	1.06	1.75
Theobromine	0.98	-

The carbonyl modes of the uracils and xanthine, therefore, are assumed to consist of coupled in-phase and out-of-phase vibrations of the carbonyl bonds, as determined by the local

$C_{2v}$  symmetry of the imide group, the transition moment of the  $\nu_s$  vibration being parallel to the bisector of the angle  $\alpha$  between the carbonyl bonds, and the  $\nu_a$  vibration being perpendicular to it. The angles  $\theta'$  for the directions of the transition moments according to the convention of fig 1.2 are shown in table 4.4; the atomic coordinate data were taken from the references of table 5.1.

TABLE 4.4

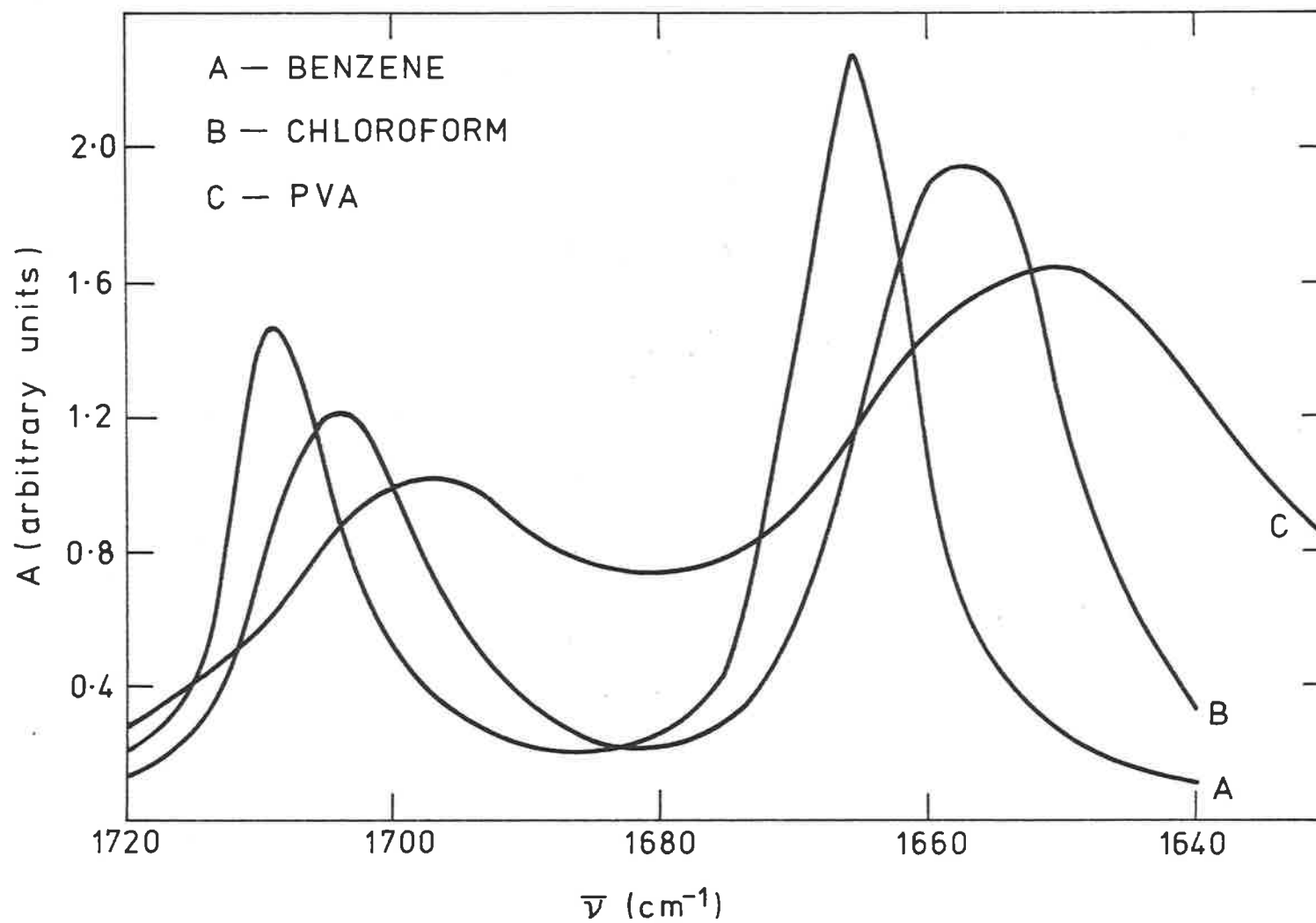
TRANSITION MOMENT DIRECTIONS OF CARBONYL TRANSITIONS

Compound	$\theta_s'$ (degrees)	$\theta_a'$
Cytosine		-59
Uracil	62	-28
Thymine	62	-28
1-Methylthymine	61	-29
Theophylline	61	-29
Caffeine	62.5	-27.5

4.2 Solvent Effects

From the spectra of the  $\nu_s$  and  $\nu_a$  bands of caffeine in benzene, chloroform and PVA solvents (fig 4.3), and from the data of table 4.5, it is seen that the type of solvent has a strong bearing on the spectral characteristics. The carbonyl band half-widths are drastically affected, the ratios  $A_a/A_s$  to a lesser extent. It is necessary therefore to seek some assurance that the IR transition moment directions are not affected by interaction with PVA. The fact that the amount of splitting ( $\bar{\nu}_s - \bar{\nu}_a$ ) is virtually independent of the solvent indicates that

FIG 4.3 SOLVENT EFFECTS ON CAFFEINE  $\nu_s$  AND  $\nu_a$  BANDS



the local symmetry of the imide group is not affected by the interaction, the carbonyl modes remaining resolved into in-phase and out-of-phase components according to this symmetry. Further evidence in support of this comes from the comparison of the IR and UV dichroisms of phthalimide, discussed in section 3.4. It was therefore assumed that the IR dichroisms observed are an accurate reflection of the transition moment directions of the unperturbed solute molecules, and that no corrections are necessary.

TABLE 4.5

SOLVENT EFFECTS ON $\nu_s$ AND $\nu_a$ BANDS OF CAFFEINE					
Solvent	$\epsilon^*$	$\bar{\nu}_s - \bar{\nu}_a$ ( $\text{cm}^{-1}$ )	$(\Delta\bar{\nu}_{\frac{1}{2}})_s$	$(\Delta\bar{\nu}_{\frac{1}{2}})_a$	$A_a/A_s$
Benzene	2.3	44	11	11	1.93
Dioxane	2.2	42	13	12	1.89
Chloroform	4.8	47	16	18	1.92
PVA	40	47	~37	~44	1.71

\* Dielectric constants from Weast (1971) and Pritchard (1970)

## CHAPTER FIVE

POLARISABILITY PROPERTIES OF PYRIMIDINES AND PURINES

The molecular polarisability is a second rank symmetric tensor which describes the magnitude of the dipole moment induced in the molecule by a weak electric field as follows:

$$\underline{m}_i = \sum_{j=1',2',3'} b_{ij} \underline{E}_j$$

Here (1',2',3') is an arbitrary molecular Cartesian system,  $\underline{E}_j$  are the components in it of the applied field  $\underline{E}$ , and  $\underline{m}_i$  is the component of the induced dipole moment  $\underline{m}$  in the direction of axis  $i$ . There is a set of principal polarisability axes in which the polarisability tensor  $b_{ij}$  is diagonal, the values  $b_{ii}$  in this basis being referred to as the principal polarisabilities. According to the theory of orientation developed in Chapter Two, the principal orientation and polarisability axes are identical for molecules such as pyrimidines and purines, and the orientation principal values  $K_1$ ,  $K_2$  and  $K_3$  are related to the principal polarisabilities. It is the purpose of this chapter to obtain the polarisabilities of the pyrimidines and purines whose orientation properties are to be determined in Chapters Six and Seven, so that the relationship of their polarisability and orientation properties may be discussed.

### 5.1 Lorentz-Lorenz Equations for Isotropic and Anisotropic Media

In isotropic materials,  $\underline{m}$  has the same direction as  $\underline{E}$ , and  $b$  is a constant. The Lorentz-Lorenz formula, which relates  $b$  to the dielectric permittivity of the medium, can be derived by use of a model in which each molecule is regarded as being sited in a spherical cavity, surrounded by material of isotropic

polarisability (Born and Wolf, 1970):

$$\frac{4\pi}{3}Nb = \frac{\epsilon - 1}{\epsilon + 2}$$

where N is the number of molecules per unit volume. The dielectric permittivity is related to the more readily measurable refractive index by means of Maxwell's formula:

$$\epsilon = n^2$$

The relationship of molecular (or unit cell) polarisabilities and refractive index properties of anisotropic crystals has been treated by Vuks (1966). In this case the principal polarisability axes are identical with the principal axes (g,m,p) of the dielectric permittivity tensor, whose directions, relative to the crystallographic axes, may be fairly readily determined by optical methods. The magnitudes of the principal polarisabilities are given by

$$\frac{4}{3}Nb_i = \frac{n_i^2 - 1}{n^2 + 2}; \quad i = g, m, p \quad (5.1)$$

with

$$n^2 = \frac{1}{3}(n_g^2 + n_m^2 + n_p^2)$$

The derivation of this equation relies upon the same spherical cavity model described above. However Vuks points out that both eqn 5.1 and the Lorentz-Lorenz equation for isotropic media are essentially empirical equations whose validity is substantiated by their agreement with other experimental measurements of polarisability properties, rather than by theoretical arguments. For most of the pyrimidines and purines studied, the necessary optical data are available to determine the unit cell polarisability properties, and it remains to show how the molecular properties may be obtained, in turn, from these.

## 5.2 Unit Cell and Molecular Polarisability Properties

The crystals of most of the pyrimidine and purine compounds studied belong to the space group  $P_{2_1/a}$  (or  $P_{2_1/c}$ ), whose symmetry elements are illustrated in fig 5.1(a). The direction of the screw axes, which are parallel to the *b* crystallographic axis, defines one of the principal dielectric axes, which will be called *g*. There are four molecules in the unit cell, which are designated *a, a', b, b'*. *a* is related to *a'*, and *b* to *b'*, by a centre of inversion, and therefore the molecular planes of each pair are parallel. *a* is related to *b*, and *a'* to *b'*, by the  $2_1$  operation. In addition to these interrelationships, it is found that the  $2_1$  axes are approximately parallel to the molecular planes (see table 5.1), and therefore all the molecules in the crystal are in parallel sheets or ribbons, a circumstance which does not generally occur with other classes of aromatic molecules crystallising in the same space group (e.g. benzene, naphthalene).

Assuming that the molecular polarisabilities are additive, they are related to those of the unit cell as follows:

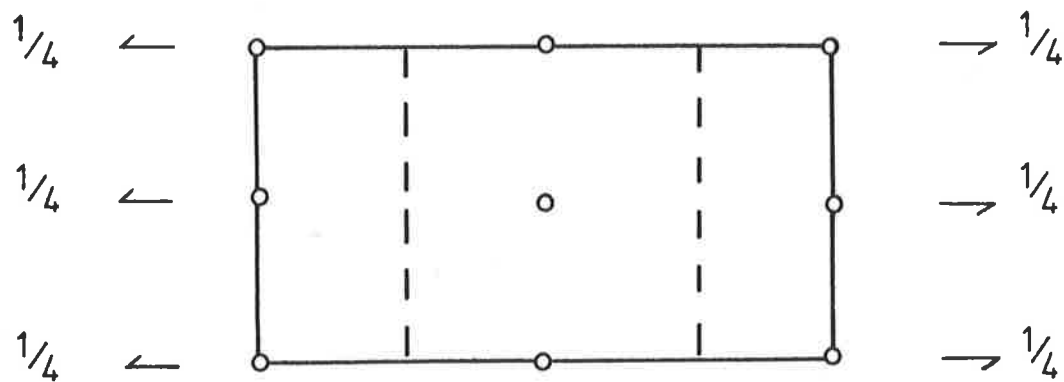
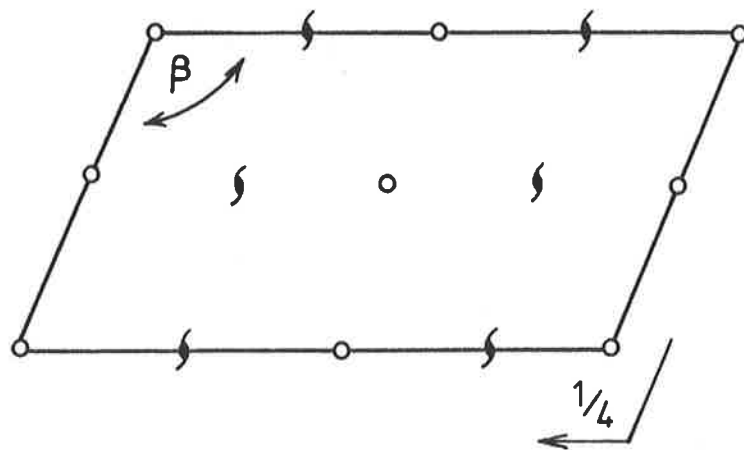
$$b_{ii} = \sum_{k,n,s} b_{kn}^{(s)} l_{ik}^{(s)} l_{in}^{(s)} \quad i,j = g,m,p;$$

$$s = a,a',b,b';$$

$$b_{ij} = \sum_{k,n,s} b_{kn}^{(s)} l_{ik}^{(s)} l_{jn}^{(s)} \quad k,n = 1',2',3'.$$

where (1',2',3') are molecular axes as in fig 5.1(b), in the present case to be considered identical with the Devoe-Tinoco axes of fig 1.2. Because the four molecules of the unit cell are related by the symmetry operations of the space group, the polarisability properties of the unit cell may be related to the orientation and polarisabilities of just one of these molecules, as follows:

FIG 5.1(a) SYMMETRY ELEMENTS OF SPACE GROUPS  $P_{2_1/a}$ ,  $P_{2_1/c}$



(b) UNIT CELL AND MOLECULAR AXES

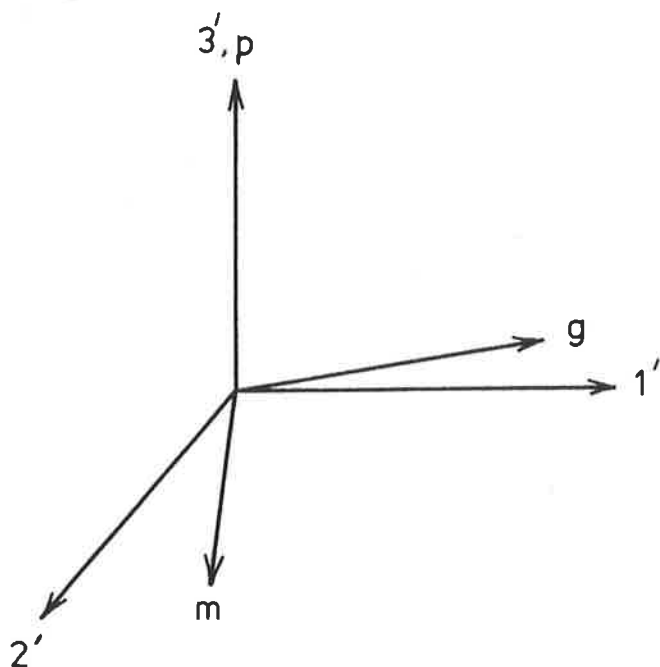


TABLE 5.1

CRYSTAL PACKING OF PYRIMIDINE AND PURINE MOLECULES

Compound	Space Group	Angle Between Screw Axis and Molecular Plane	Angle of Screw Axis with Molecular 1' Axis	Reference
Uracil	$P_{2_1}/a$	$1^\circ$	$-23^\circ$	Stewart and Jensen (1967)
Thymine	$P_{2_1}/c$	$4^\circ$	$31^\circ$	Ozeki et al. (1969)
Thymine. $H_2O$	$P_{2_1}/c$	$12.5^\circ$	$-62^\circ$	Gerdl (1961)
1-Methylthymine	$P_{2_1}/c$	$4^\circ$	$87^\circ$	Hoogsteen (1963)
Cytosine	$P_{2_1}^2 2_1^2 2_1$	$7.5^\circ$	$33^\circ$	Barker and Marsh (1964)
Cytosine. $H_2O$	$P_{2_1}/c$	$1^\circ$	$30^\circ$	Jeffrey and Kinoshita (1963)
Caffeine hydrate	$P_{2_1}/a$	$3^\circ$	$16^\circ$	Sutor (1958(b))
Theophylline. $H_2O$	$P_{2_1}/a$	$9^\circ$	$11^\circ$	Sutor (1958(b))

$$b_{ii} = 4 \sum_{k,n} b_{kn} l_{ik}^{(a)} l_{in}^{(a)} \quad i = g, m, p;$$

$$k, n = 1', 2', 3'$$

$$b_{mp} = 4b_{kn} l_{mk}^{(a)} l_{pn}^{(a)}$$

The equations for  $b_{gm}$  and  $b_{gp}$  become trivial as a result of the screw axis symmetry. Also, because only four components of the molecular polarisability tensor are non-vanishing, as a result of molecular symmetry, the equations reduce further to

$$b_{ii} = 4\{b_{1'1'} l_{1'i}^2 + 2b_{1'2'} l_{1'i} l_{2'i} + b_{2'2'} l_{2'i}^2 + b_{3'3'} l_{3'i}^2\} \quad i = g, m, p$$

$$b_{mp} = 4\{b_{1'1'} l_{1'm} l_{1'p} + b_{1'2'} (l_{1'm} l_{2'p} + l_{1'p} l_{2'm}) + b_{2'2'} l_{2'm} l_{2'p} + b_{3'3'} l_{3'm} l_{3'p}\} = 0$$

This provides a set of four linear equations which could, in general circumstances, be solved for the molecular polarisabilities  $b_{1'1'}$ ,  $b_{1'2'}$ ,  $b_{2'2'}$  and  $b_{3'3'}$ . Unfortunately, the fourth equation becomes trivial if the screw axis is parallel to the plane of molecular axes 1' and 2', and it has been seen that for pyrimidines and purines this is effectively the case. The equations are then:

$$b_{gg} = 4\{b_{1'1'} l_{1'g}^2 + 2b_{1'2'} l_{1'g} l_{2'g} + b_{2'2'} l_{2'g}^2\}$$

$$b_{mm} = 4\{b_{1'1'} l_{1'm}^2 + 2b_{1'2'} l_{1'm} l_{2'm} + b_{2'2'} l_{2'm}^2\}$$

$$b_{pp} = 4b_{3'3'}$$

the molecular and unit cell axes being related as in fig 5.1(b). There is no unique solution in this case for the in-plane polarisabilities and polarisability axes.

Whilst a rigorous approach to the problem fails to provide a means of deriving the in-plane molecular polarisability properties, an alternative approach is to assume that the molecular polarisabilities are simply equal to the projections

of the unit cell polarisabilities on the individual molecules. Some qualitative arguments can be advanced in favour of this assumption and as will be seen in the next section, it can also be justified a posteriori. To begin, the form of the dispersion interaction potential of two molecules, eqn 2.8, is recalled. The magnitude of the potential depends on the relative positions of the centres of electron oscillation of the two molecules, and the relative orientations of their polarisability axes. It has a minimum, if the two molecules are the same, when the relative orientations of their axes are identical. The features of molecular arrangement in pyrimidine and purine crystals indicate that such a potential does apply in the solid state. Firstly, the out-of-plane polarisability axes are certainly parallel, by virtue of the fact that all the molecules in the crystal are in parallel planes. Secondly, the fact that the hypothetical in-plane polarisability axes, being the screw axis direction and the direction perpendicular to it, maintain their identities in different molecular packing arrangements, is strong evidence that they do represent preferred orientational directions in the plane of the molecule. Thus in the two crystal forms of thymine and cytosine (table 5.1) the two sets of axes differ in both cases by only  $3^\circ$ ; the case of thymine is particularly convincing because the projections of the screw axis on the molecule in the two cases are orthogonal. Therefore, the fact that the screw axis is parallel to the molecular planes, which precludes a rigorous determination of the molecular polarisabilities from those of the unit cell, seems to arise from the presence of selective orientational axes within the molecules. This axis is therefore assumed to be one of the principal polarisability axes.

### 5.3 Molecular Polarisabilities

The direction of the hypothetical orientation axes for the molecules studied are shown in table 5.2. They are calculated as being either parallel to or perpendicular to the projection of the screw axes on the molecular planes, the direction selected being that associated with the largest value of the refractive index. The molecular polarisabilities, calculated by means of eqn 5.1, are shown also in the table. In calculating the polarisabilities of the hydrated crystals, no correction was made for the contribution of the water molecules to the unit cell polarisability. Although no experimental values are available for the polarisability of water, calculations show it to be virtually isotropic (Harrison, 1968) with  $b_1 = 1.2$ ,  $b_2 = 1.5$ ,  $b_3 = 1.7 \text{ \AA}^3$ . In all cases, the polarisabilities increase with the addition of alkyl substituents as one would expect, a result which supports the validity of the assumption made above concerning the molecular principal axis directions.

TABLE 5.2

MOLECULAR POLARISABILITIES OF PYRIMIDINE AND PURINE COMPOUNDS

Compound	Direction of Principal Axis 1 (deg)	$b_3$ ( $\text{\AA}^3$ )	$b_2$	$b_1$	Source of Optical Data
Uracil	-23	6.2	10.9	14.3	(Gilpin and McCrone, 1950 (
Thymine	31	7.3	14.4	14.7	(Biles et al., 1951
1-Methylthymine	-3	9.3	15.6	18.8	Stewart and Davidson, 1963
Cytosine.H <sub>2</sub> O	30	7.9	14.9	15.8	Winchell, 1954
Theophylline.H <sub>2</sub> O	-79	13.7	20.0	21.8	Lasheen and Ibrahim, 1975
	11	12.7	21.7	>23.2	Winchell, 1954
Caffeine hydrate	-74	13.1	22.5	23.7	Winchell, 1954

CHAPTER SIXORIENTATION AND TRANSITION MOMENTS OF URACIL AND CYTOSINEDERIVATIVES6.1 Observed and Calculated Transitions of Uracil and Cytosine Derivatives

Spectra of uracil, thymine, cytosine and their related nucleosides and nucleotides in aqueous solution and at various values of pH have been published by Beaven et al. (1955) and, in the far UV region, by Voet et al. (1963). The dichroic spectra in PVA of the derivatives studied are shown in figs 6.1 to 6.8. Similar spectra of some of these compounds have appeared previously (Fucaloro and Forster, 1971; 1974; Fucaloro, 1969).

The spectra and transitions of pyrimidines have been classified by means of correlations with those of benzene (Clark and Tinoco, 1965), whose lowest energy transitions are to states of  $B_{2u}$ ,  $B_{1u}$  and  $E_{1u}$  symmetry, at energies of 38000, 49000 and 55500  $\text{cm}^{-1}$  respectively. In view of the large differences in structure between benzene on the one hand, and cytosine and uracil on the other, it is doubtful whether such comparisons are meaningful, and the transitions of pyrimidine and purines will be referred to simply as I, II, etc, in increasing order of energy. Band I of uracil and cytosine derivatives, at 36500  $\text{cm}^{-1}$ , appears to arise from a single  $(\pi^*, \pi)$  transition. The absorption spectra of single crystals of 1-methyluracil and cytosine monohydrate (Eaton and Lewis, 1970; Lewis and Eaton, 1971) have vibrational structure in band I which was shown to arise from a single progression of a  $(\pi^*, \pi)$  transition in both cases. ORD, CD and MCD spectra (Miles et al., 1967; Voelter et al., 1968) confirmed this

FIG 6.1 UV DICHOIC SPECTRUM OF URACIL

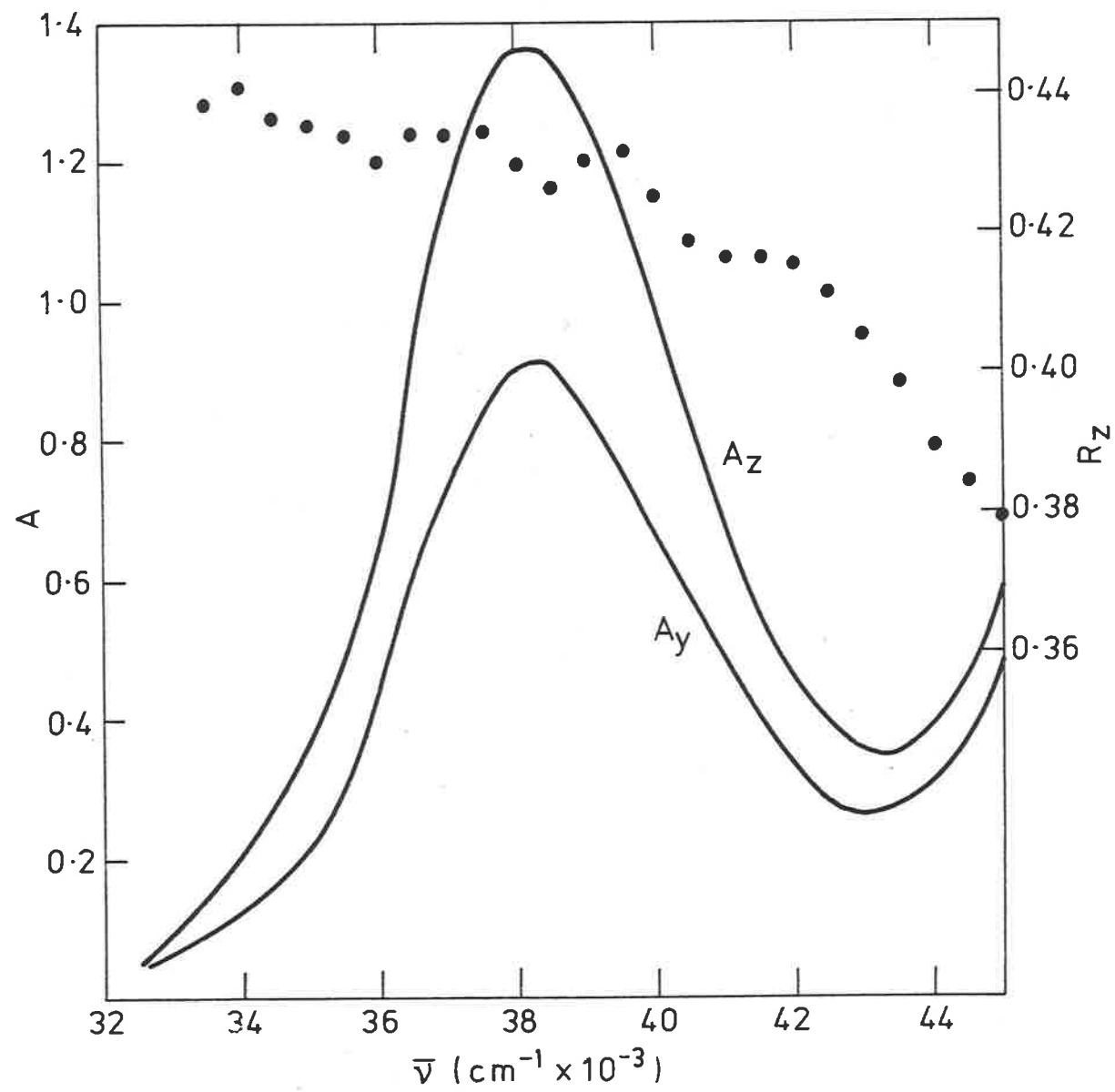


FIG 6.2 UV DICHOIC SPECTRUM OF URIDINE

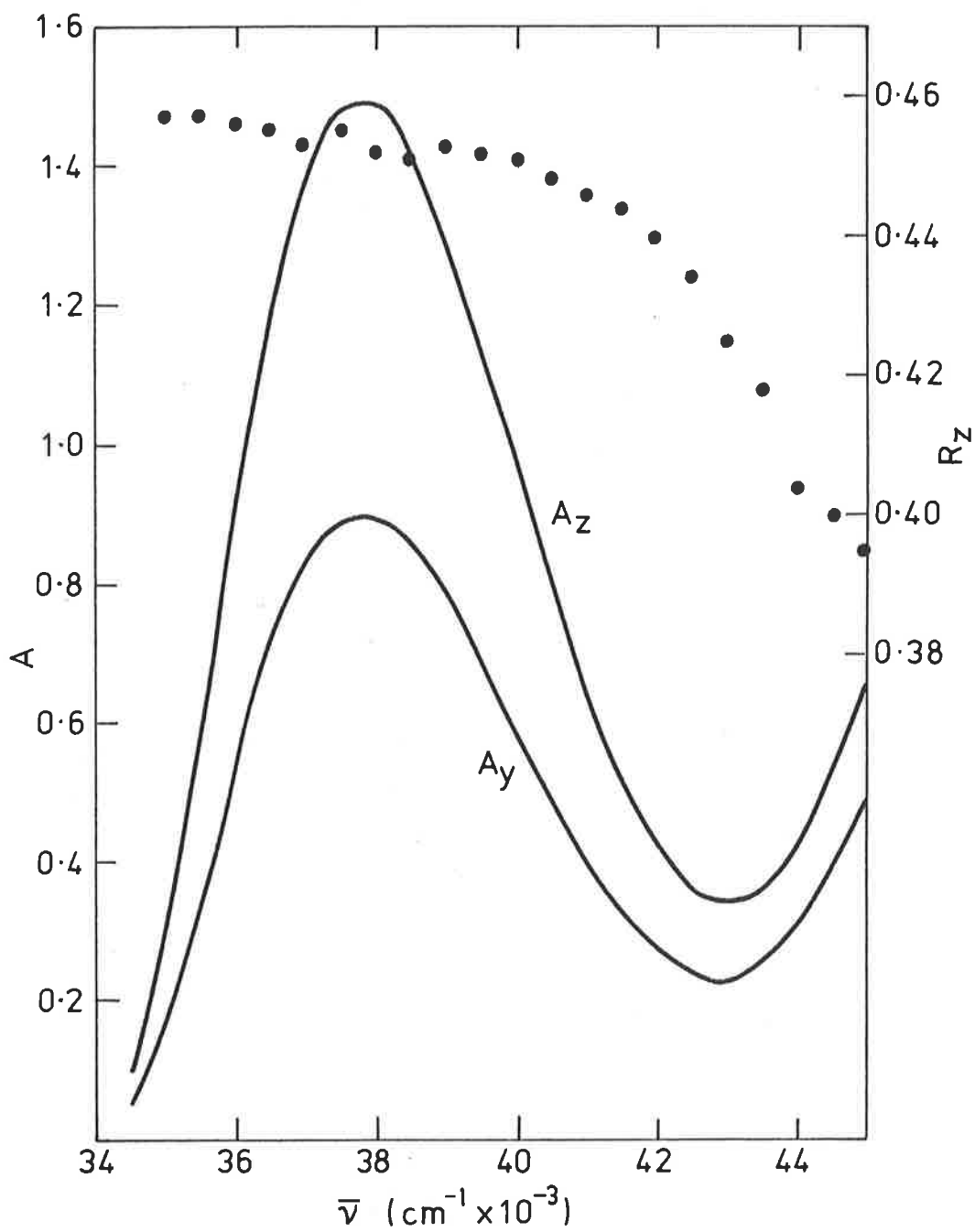


FIG 6.3 UV DICHOIC SPECTRUM OF THYMINE

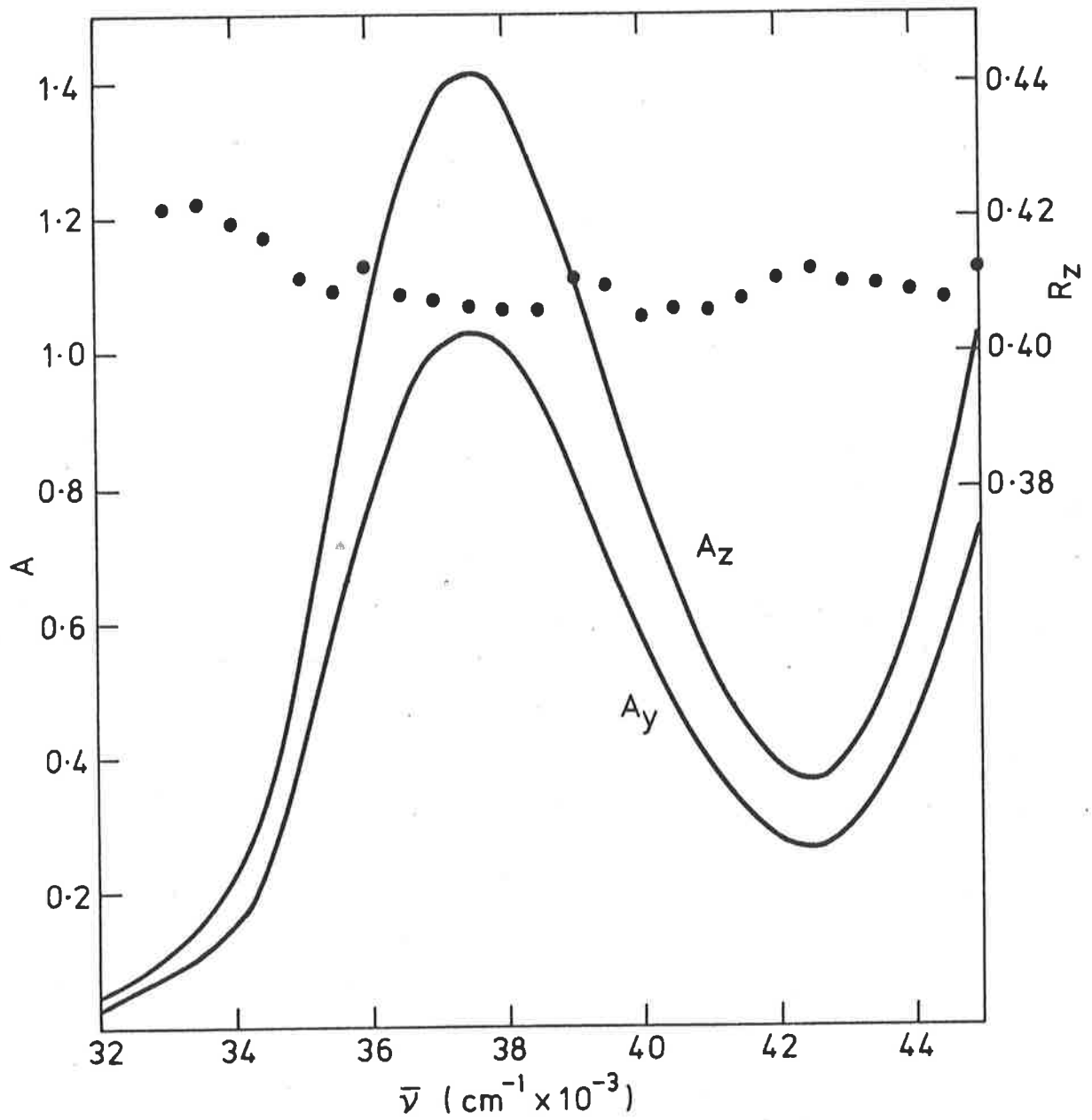


FIG 6.4 UV DICHOIC SPECTRUM OF THYMIDINE

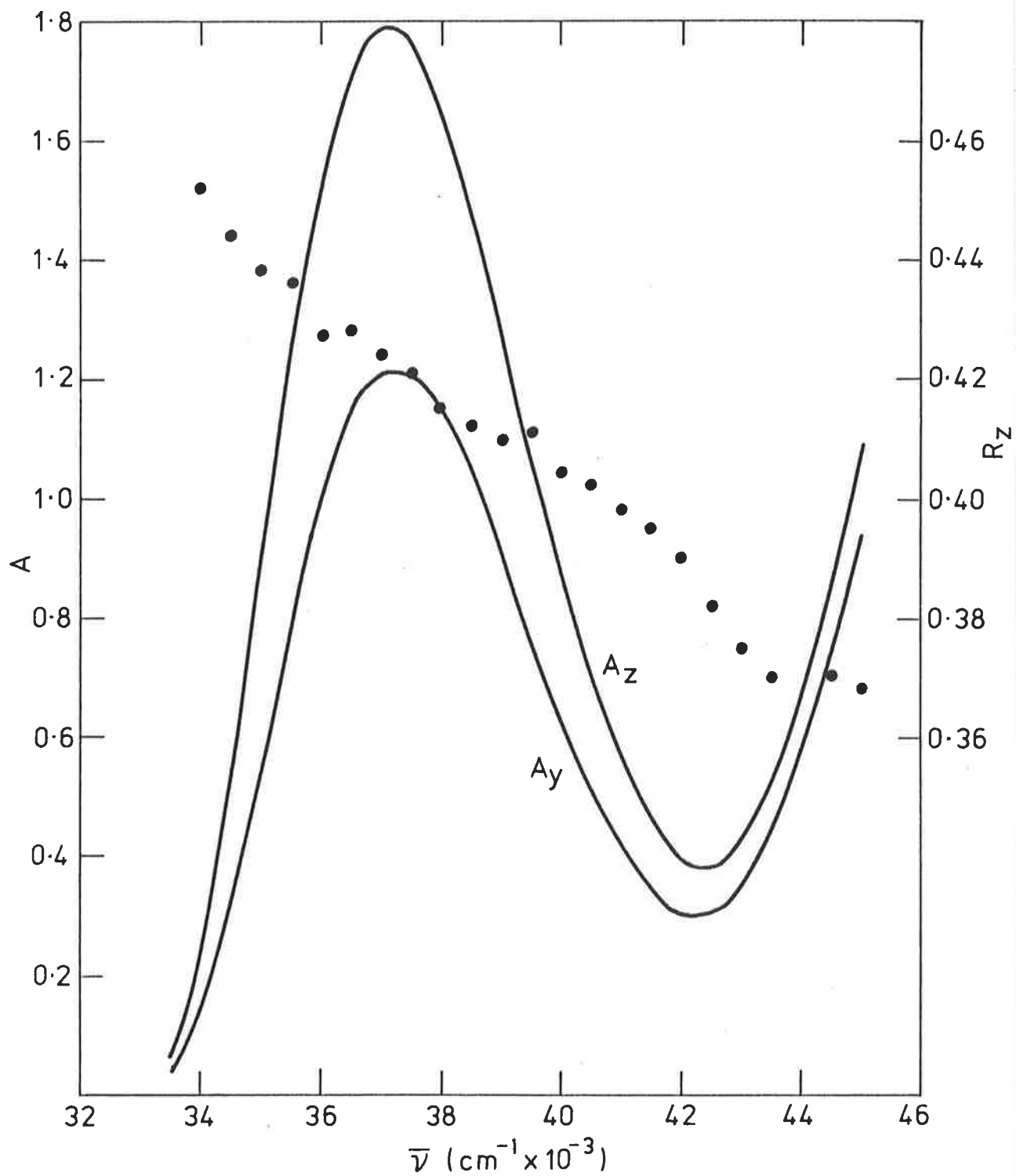


FIG 6.5 UV DICHOIC SPECTRUM OF 1-METHYLTHYMINE

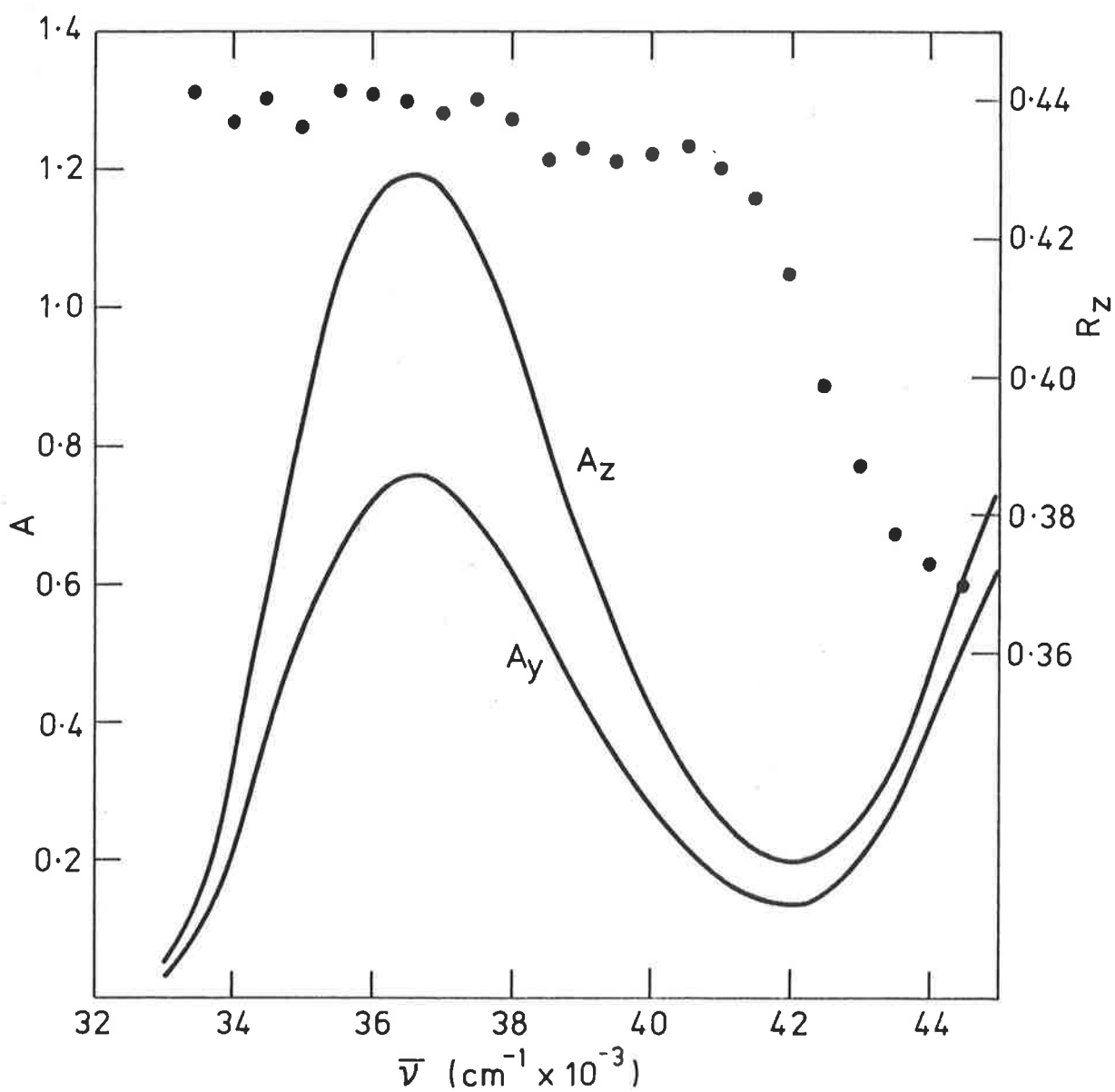


FIG 6.6 UV DICHOIC SPECTRUM OF CYTOSINE

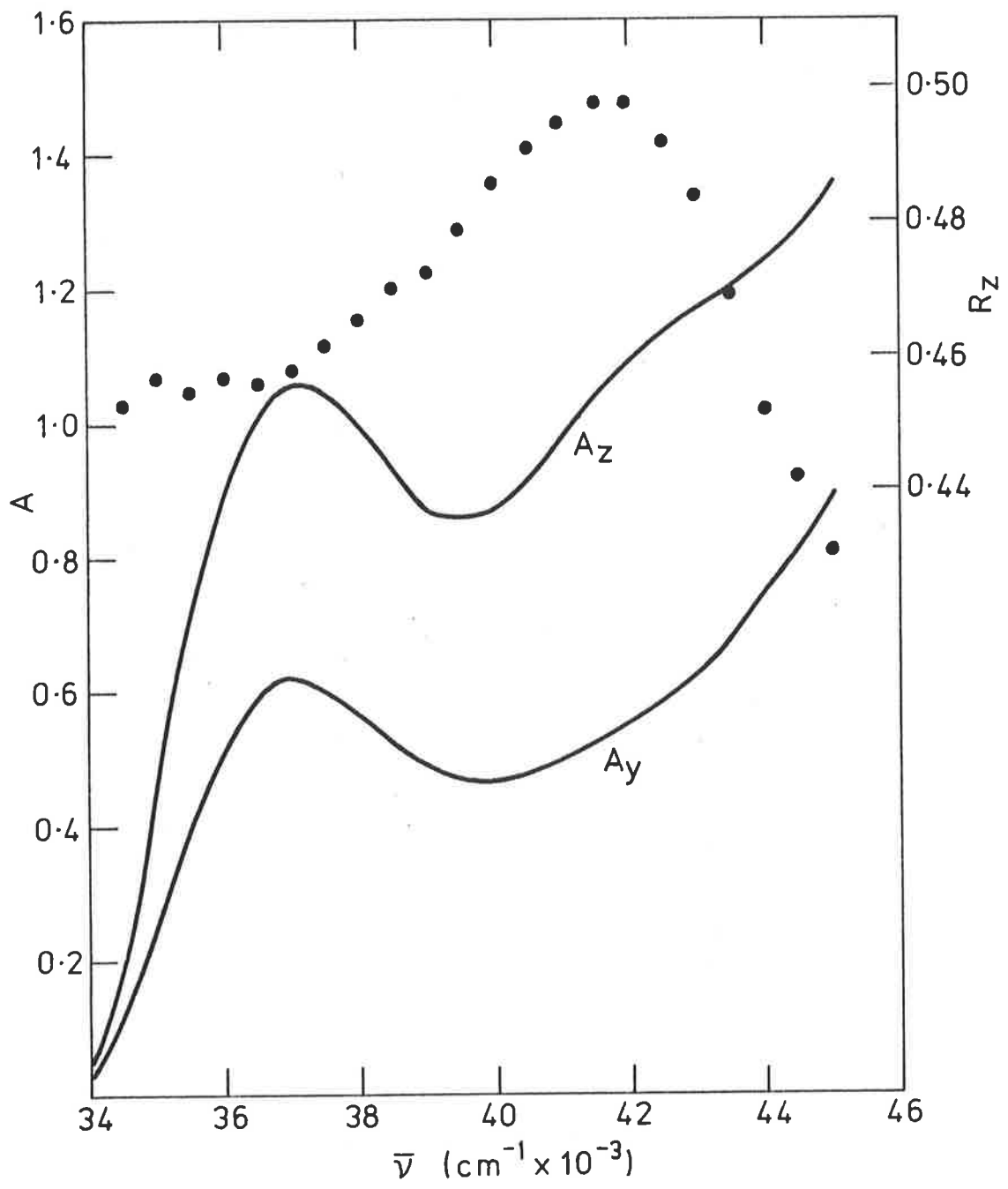


FIG 6.7 UV DICHROIC SPECTRUM OF CYTIDINE

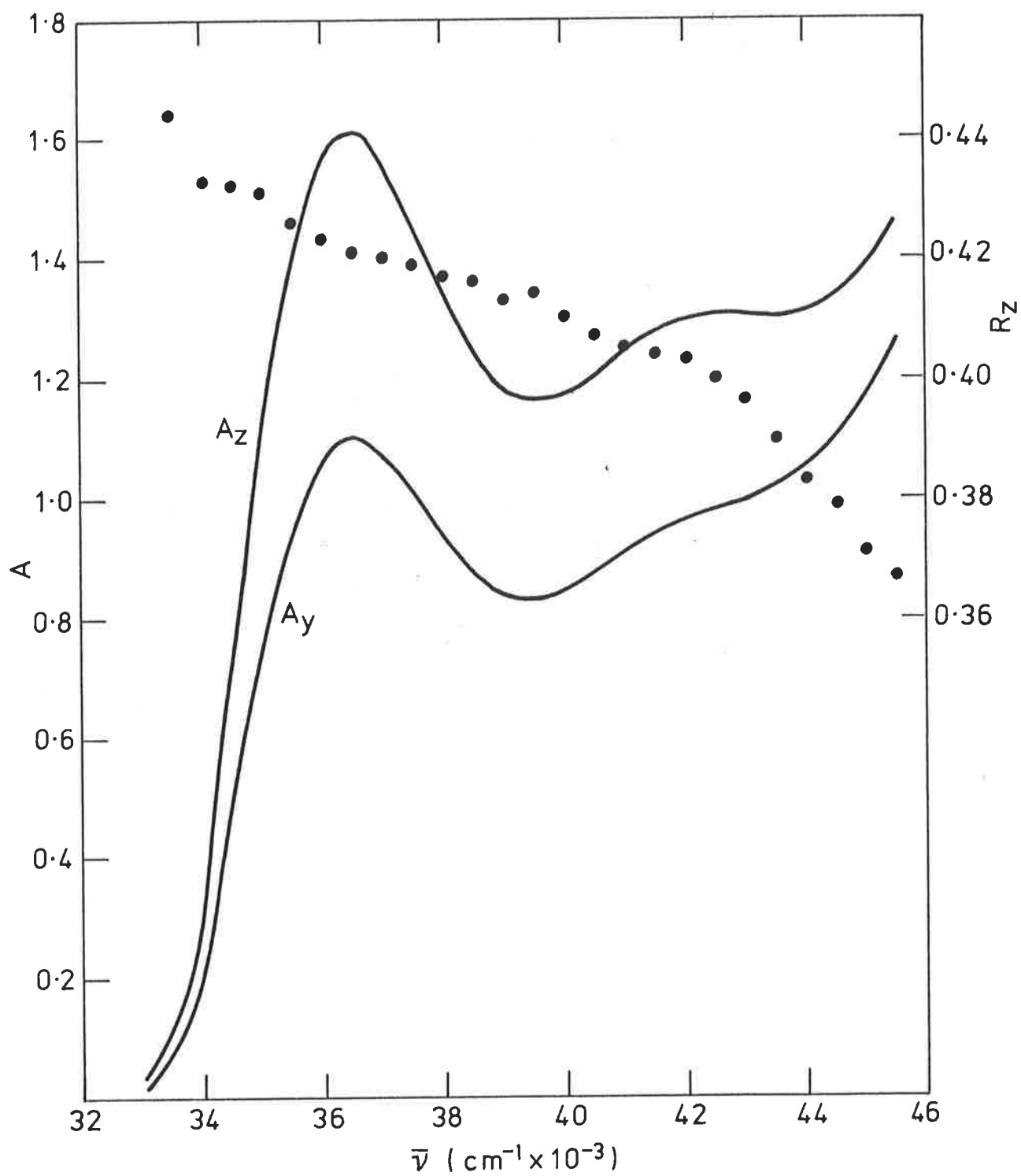
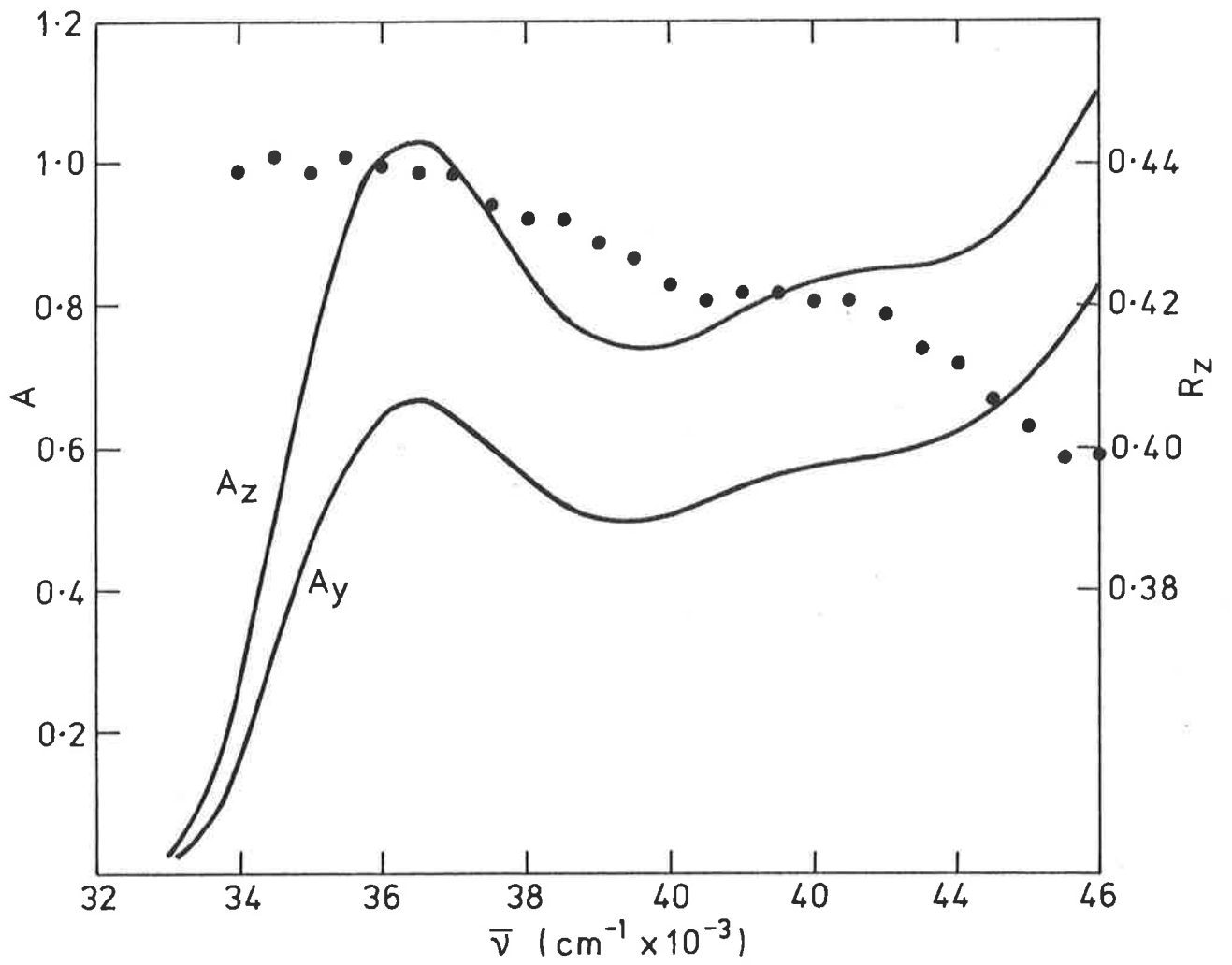


FIG 6.8 UV DICHOIC SPECTRUM OF 5'-CMP



result in the case of uracil derivatives, but the CD result for cytosine derivatives indicated the presence of two unresolved bands of slightly different rotational strengths. The correlation of CD effects with electric dipole transitions is not, however, well established (Inskeep et al., 1972), and photoselection and single crystal reflectance measurements (Callis and Simpson, 1970) support the interpretation of Lewis and Eaton. Transition II of cytosine derivatives is observed as a weak band at  $42000\text{ cm}^{-1}$ . A corresponding band is not observable in uracil derivatives, either in solution or in the crystal (Steward and Davidson, 1963; Eaton and Lewis, 1970), but was observed by Clark and Tinoco as a weak band at  $43,500\text{ cm}^{-1}$  in 6-azauracil, and measurements of CD (Miles et al., 1967) also revealed its presence in uridine and thymidine, at about the same energy. Although not of sufficient intensity to be observed directly or to have a noticeable effect on the linear dichroism either in film or crystal spectra, this transition in the uracils will be referred to as transition II for the sake of correlation with calculations. Only the very inception of the next absorption band is observed in the film spectra, and it can therefore be assumed to be associated with a single transition, transition III.

$(\pi^*, n)$  transitions can, theoretically, occur in both uracil and cytosine derivatives, either as out-of-plane polarised components, or as in-plane components induced by vibronic coupling with  $(\pi^*, \pi)$  transitions. Neither type of transition was observed in the single crystal absorption spectrum of cytosine monohydrate (Lewis and Eaton, 1971), and while both were observed in the 1-methyluracil crystal (Eaton and Lewis, 1970), their intensities were less than one percent of those of the  $(\pi^*, \pi)$  transitions.

TABLE 6.1

CALCULATED TRANSITION ENERGIES, INTENSITIES AND TRANSITION MOMENT DIRECTIONS FOR

LOWEST ( $\pi^*$ ,  $\pi$ ) TRANSITIONS OF URACIL

Transition		PPP-CI		CNDO-CI	
		Bailey (1970)	Pullman and Pullman (1968)	Hug and Tinoco (1973)	Zhel'tovskii and Danilov (1974)
I	$\bar{\nu}(\text{cm}^{-1})$	40000	38700	40000	40600
	f	0.14	0.3	.45	0.38
	$\theta(\text{deg})$	-5	-10	-8	-8
II	$\bar{\nu}(\text{cm}^{-1})$	47000	43600	51000	52500
	f	0.14	0.06	.04	0.12
	$\theta(\text{deg})$	-47	-10	12	60
III	$\bar{\nu}(\text{cm}^{-1})$	48100	46800	54000	55200
	f	0.22	0.2	.30	0.18
	$\theta(\text{deg})$	26	52	-67	-

TABLE 6.2

CALCULATED TRANSITION ENERGIES, INTENSITIES AND MOMENT DIRECTIONS FOR  
LOWEST ( $\pi^*$ ,  $\pi$ ) TRANSITIONS OF THYMINE

Transition		PPP-CI	CNDO-CI	ab initio
			Zhel'tovskii and Danilov (1974)	Snyder et al. (1970)
	$\bar{\nu}(\text{cm}^{-1})$	39600	40800	62700
I	f	0.12	0.39	-
	$\theta(\text{deg})$	-6	-8	-15
		46800	52300	73000
II		0.19	0.15	-
		-62	70	-
		48500	55700	84900
III		0.19	0.21	-
		41	-	-

TABLE 6.3

CALCULATED TRANSITION ENERGIES, INTENSITIES AND MOMENT DIRECTIONS FOR  
LOWEST ( $\pi^*$ ,  $\pi$ ) TRANSITIONS OF CYTOSINE

Transition	PPP-CI			CNDO-CI		
		Bailey (1970)	Pullman and Pullman (1968)	Hug and Tinoco (1973)	Zhel'tovskii and Danilov (1974)	
	$\bar{\nu}(\text{cm}^{-1})$	31900	34400	33100	38000	36900
I	f	.10	.05	.10	.18	.15
	$\theta(\text{deg})$	19	-	70	18	41
		45100	42600	41100	47000	46600
II		.28	.11	.10	.26	.14
		-4	-	-2	24	-11
		49200	47800	46000	53000	51600
III		.30	.54	.40	.46	.72
		-51	-	-35	-45	-

Therefore their contribution to PVA spectra may be considered negligible. All of the three classes of calculations described in section 1.2 have been performed for at least one pyrimidine or purine molecule, and the results of some of these, for the three lowest energy transitions, are shown in tables 6.1, 6.2 and 6.3. It is usual to correlate the second calculated transition of uracil with the hypothetical transition II discussed above. The calculations will be discussed in detail below; before proceeding, however, attention will be drawn to two points. Firstly, the *ab initio* calculations give values for the transition energy which are far too high: this was discussed in the Introduction. The *ab initio* calculations used CI involving four singly excited states only. Secondly, the first two sets of figures for PPP-CI calculations on cytosine both come from Bailey-type calculations. The differences arise because the first set were based on the atomic coordinates of the cytosine monohydrate crystal structure, whilst those published by Bailey (1970) made use of the cytosine anhydrate data (table 5.1).

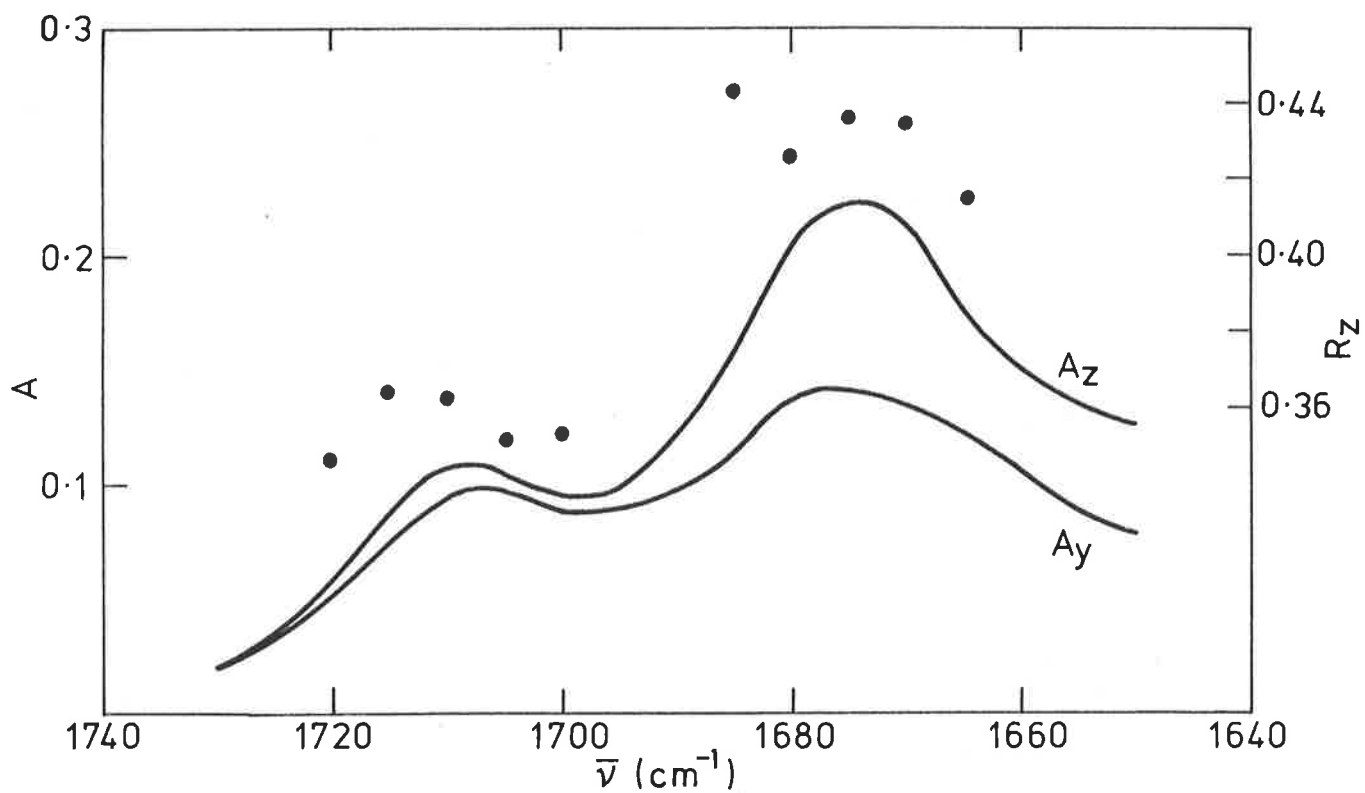
## 6.2 Dichroic Spectra

It is desirable firstly to ensure that none of the solutes studied is present in PVA films in an aggregated form, by applying to both the UV and IR dichroic spectra the criteria discussed in section 3.5. With regard to the UV spectra, the dichroism associated with the first absorption band is approximately constant for all compounds; however at the inception of the band the dichroism is observed to be, in most cases, slightly different to that of the remainder of the band. It is possible that absorption in this region is due to aggregated molecules,

as with caffeine in PE, and the dichroisms of the transitions were taken to be those observed in the main part of the band. The enhancement of dichroism is so much smaller than that observed in caffeine aggregates that, if the effect is in fact due to aggregation, it is unlikely that a significant proportion of the solute is not present in monomolecular form. The IR dichroic spectra of the uracil and cytosine derivatives studied, which are illustrated in figs 6.9 to 6.11, reinforce this conclusion. Whilst the dichroisms within each band tend to show a large random scattering compared with the UV, for reasons discussed in section 3.4, no splitting in dichroism of the type observed for caffeine in PE is seen in the spectra. The IR dichroic spectra of uridine and thymidine are not illustrated. The separation of the  $\nu_s$  and  $\nu_a$  bands of these compounds was not good enough to enable the dichroisms of the separate transitions to be observed, and therefore the spectra were of no value in determining the molecular orientation.

Shown in table 6.4 are the dichroism values subsequently used in this chapter to calculate molecular orientations and transition moment directions. The dichroic spectra from which these values are derived were accumulative spectra obtained by adding together  $A_z$  and  $A_y$  for three or four films of each compound, as discussed in section 3.4. Each of the spectra in figs 6.1 to 6.11, however, is that of a single film only. The values of dichroism quoted correspond to wavenumbers roughly at the centre of each band, except those for band III, which correspond to the largest wavenumber at which measurements were taken.

FIG 6.9(a) IR DICHROIC SPECTRUM OF URACIL



(b) IR DICHROIC SPECTRUM OF THYMINE

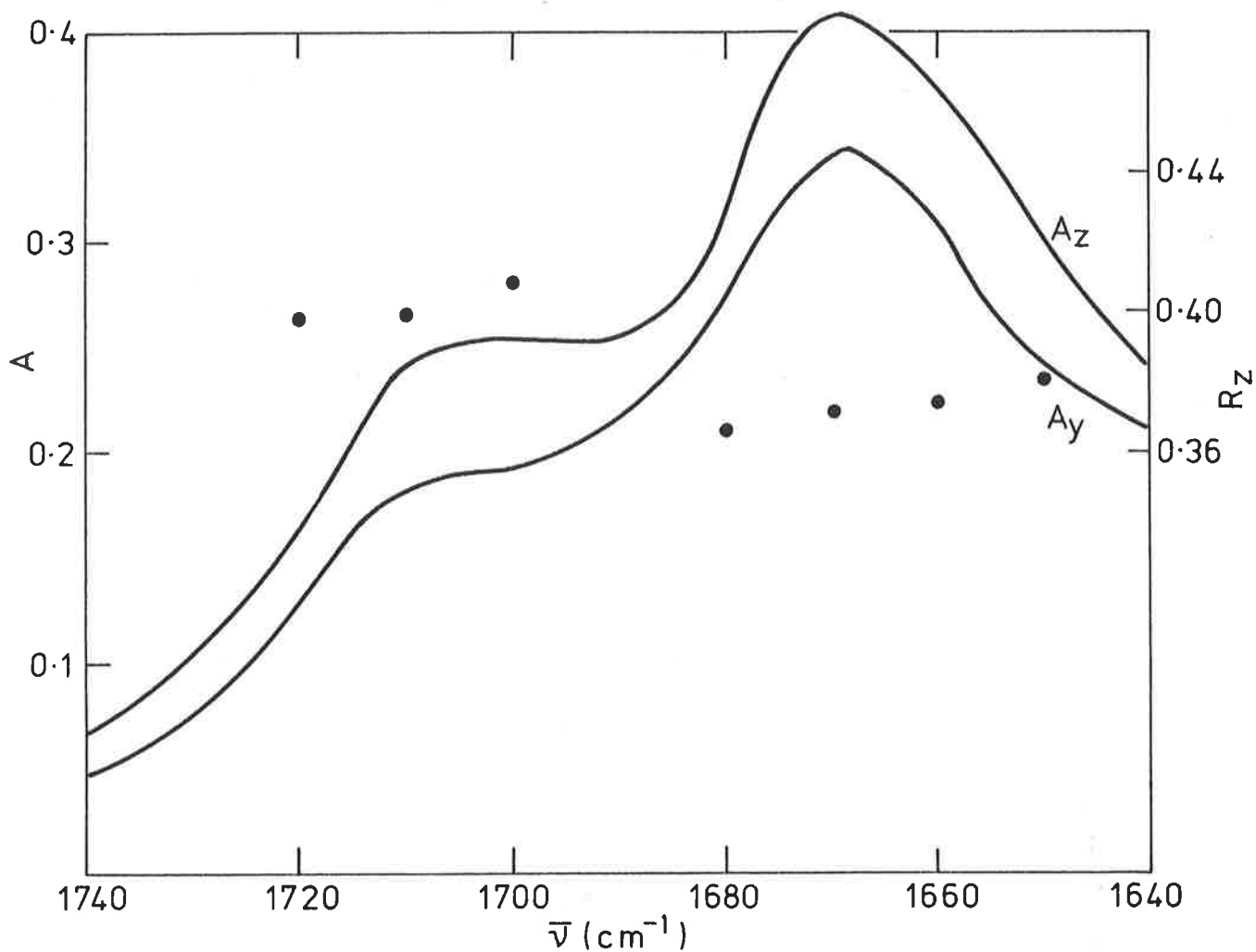
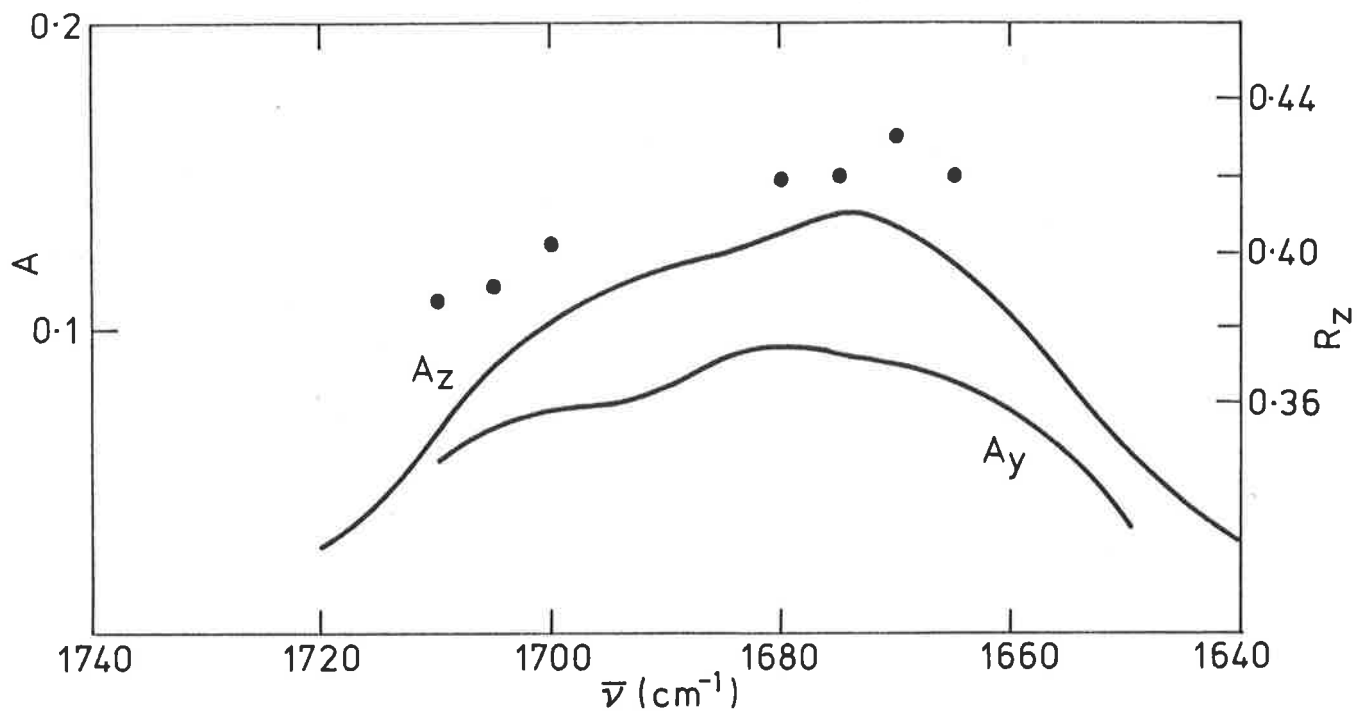


FIG 6.10(a) IR DICHROIC SPECTRUM OF 1-METHYLTHYMINE



(b) IR DICHROIC SPECTRUM OF CYTOSINE

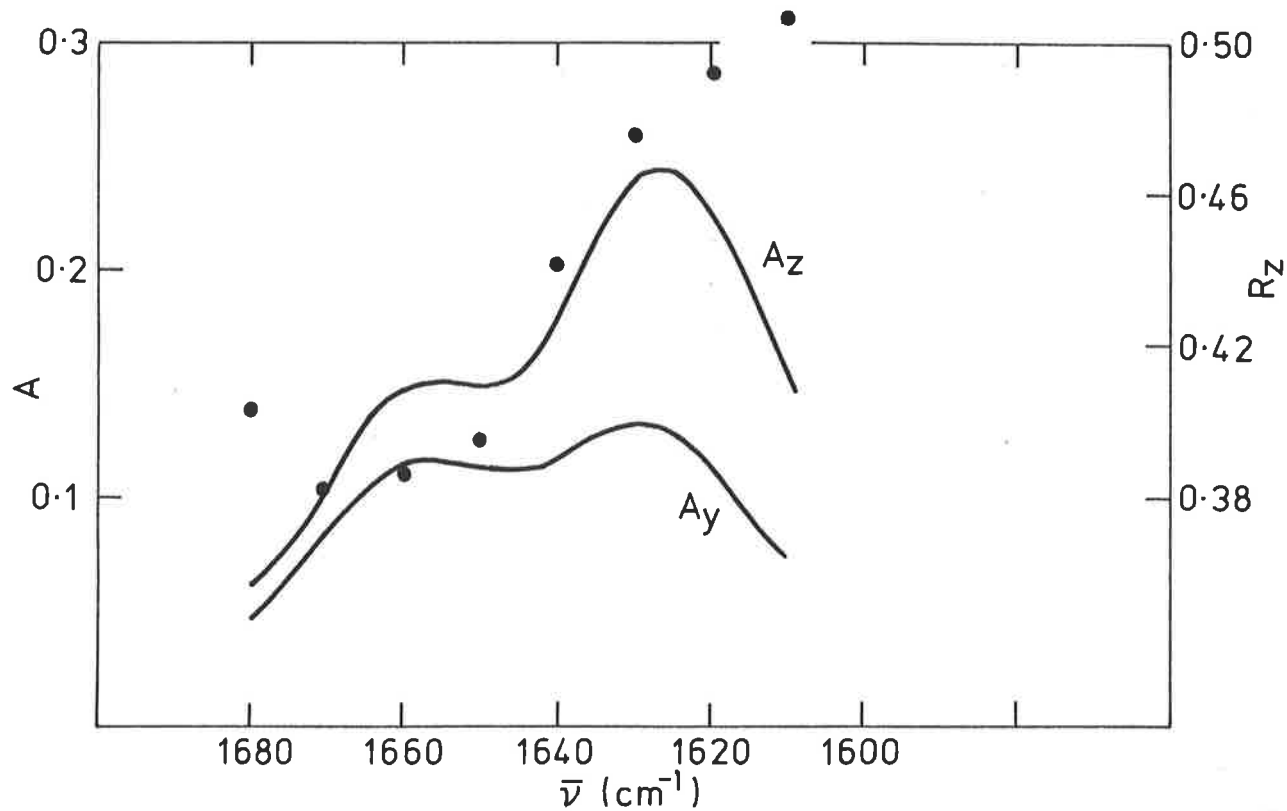
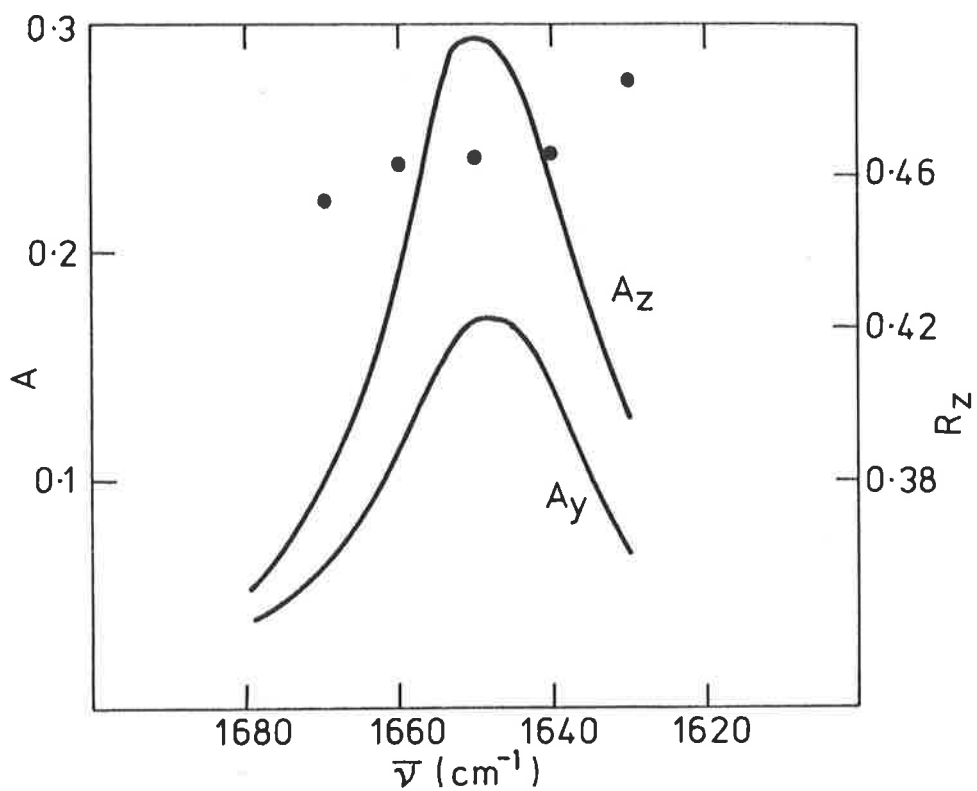


FIG 6.11(a) IR DICHROIC SPECTRUM OF CYTIDINE



(b) IR DICHROIC SPECTRUM OF 5'-CMP

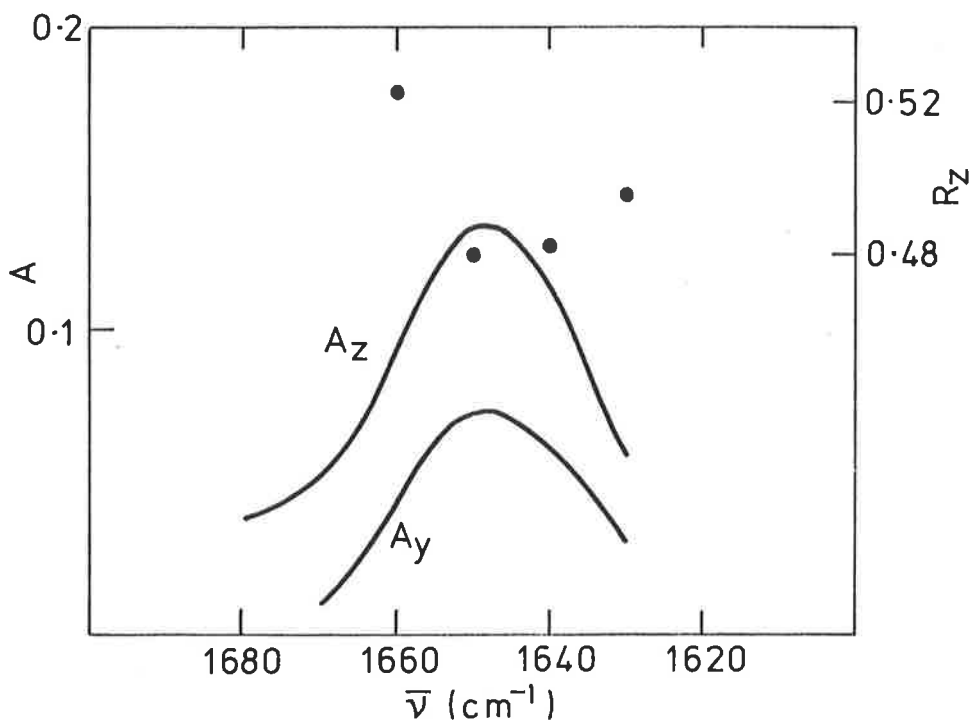


TABLE 6.4

IR AND UV DICHROISMS OF URACIL AND CYTOSINE DERIVATIVES

	$R_Z^s$	$R_Z^a$	$R_Z^I$	$R_Z^{II}$	$R_Z^{III}$
Uracil	.353	.401	.419	-	.381
Thymine	.420	.390	.405	-	.402
1-Methylthymine	.408	.408	.444	-	.363
Cytosine	.383		.452	.481	.418
Cytidine	.432		.434	.419	.374
5'-CMP	.441		.445	.426	.399

6.3 Orientation Axes and Orientation Parameters

There are three, independent parameters  $K_{ij}$  which specify the orientation of a planar molecule, and it is not possible to determine these precisely on the basis of data from just one or two IR transitions. The purpose of this section, therefore, is to provide the basis of a correlation approach for estimating the values of the orientation principal values, so that the directions of the orientation axes within the molecules may be derived from the carbonyl dichroisms.

As the UV and IR transitions of interest are polarised in the planes of the aromatic portions of the molecules, their dichroisms ( $R_Z^i$ ) and transition moment directions are related by the following version of eqn 2.2:

$$\begin{aligned}
 R_Z^i &= K_1 \cos^2 \theta_i + K_2 \sin^2 \theta_i & (6.1) \\
 &= K_1 \cos^2 (\theta_i' - \theta_1') + K_2 \sin^2 (\theta_i' - \theta_1')
 \end{aligned}$$

Here  $\theta_i$  is the angle which axis  $i$  makes with the orientation axis 1, whilst  $\theta_i'$  is the angle it makes with axis 1' of the conventional system of axes depicted in fig 1.2.  $\theta_1'$  is the

direction of the orientation axis in this system. In the molecules of planar geometry, this axis is in the plane of the molecule, whilst in uridine, thymidine etc., its direction is less certain; therefore treatment of the latter class of molecules will be deferred.

In this work, the correlation approach will consist of providing upper and lower bounds for the parameters  $K_1$  and  $K_2$ . The following inequality is derived from eqn 6.1 (see Appendix A.4):

$$K_2 \leq R_Z \leq K_1$$

It follows that if  $R_Z^{\max}$ ,  $R_Z^{\min}$  are the greatest and least values of dichroism observed for a particular film, then

$$R_Z^{\max} \leq K_1; K_2 \leq R_Z^{\min}$$

One observes in addition, from the data of table 6.4, that the values of  $R_Z$  of the planar pyrimidines studied lie within the range ( $1/3$ ,  $1/2$ ), and it is reasonable to assume therefore, that the limits of this range represent lower and upper bounds, respectively, of  $K_2$  and  $K_1$ , for the series of molecules. This assumption is supported by the fact that for almost all of the mono- and bi-cyclic aromatic compounds whose dichroisms in PVA have been reported, the  $R_Z$  values lie within the same range (eg. Tanizaki and Kubodera, 1967; Hoshi and Tanizaki, 1970; Tanizaki, Kobayashi and Hoshi, 1972; Tanizaki, Hiratsuka and Hoshi, 1972). Therefore  $K_1$  and  $K_2$  are assumed to obey the following inequalities for the planar pyrimidines studied:

$$\begin{aligned} R_Z^{\max} &\leq K_1 \leq .500 \\ .333 &\leq K_2 \leq R_Z^{\min} \end{aligned} \quad (6.2)$$

For the uracil derivatives, the values of  $K_1$  and  $K_2$  are further restricted by the following interrelationship, which follows

from eqn 6.1:

$$R_Z^a + R_Z^s = K_1 + K_2 \quad (6.3)$$

The IR dichroism data, together with any pair of values of  $K_1$  and  $K_2$  within the ranges defined by eqn 6.2, gives possible values of the orientation axis direction,  $\theta_1'$ , as is evident when eqn 6.1 is rewritten in the form

$$\cos 2\theta_i = \cos 2(\theta_i' - \theta_1') = \frac{2R_Z^i - (K_1 + K_2)}{K_1 - K_2} \quad (6.4)$$

The angles  $\theta_i'$  are known quantities, being the carbonyl transition moment angles as given in table 4.4. Therefore the range of values of  $\theta_1'$  may be found by allowing  $K_1$  and  $K_2$  to vary over all values given by the inequalities 6.2. This task of computation is made less onerous by the fact, proved in Appendix A.4, that the extrema of  $\theta_1'$ ,  $K_1$  and  $K_2$  occur together. Therefore the calculations need be done only for the values of  $K_1$  and  $K_2$  at the extremes of their range of values. The results of the calculations are shown in table 6.5. No calculations have been made for thymine for reasons which will be discussed in section 6.5. The two values of  $\theta_1'$  for each molecule result from the inability of the stretched film method (and alternative methods) to give more than the absolute value of a transition moment angle  $\theta_i$ , as discussed in the Introduction. The theoretical values of  $\theta_1'$ , which have been carried over from table 4.4, are placed adjacent to what is considered to be the correct choice of  $\theta_1'$ . The reason for the choice will become apparent later.

The values in the first entry for cytosine have been calculated using the principles described above, and lead to an excessive uncertainty in the value of  $\theta_1'$ , because eqn 6.3 cannot be applied. Therefore a further correlation was sought

TABLE 6.5

ORIENTATION PARAMETERS AND ORIENTATION AXES OF SIMPLE PYRIMIDINES

Molecule	$K_1+K_2$	$K_1$ $K_2$	$\theta_s$ (deg)	$\theta_1'$ (exp)	$\theta_1'$ (theory)
Uracil	.754	(.419, .421)	$\pm(62\pm1)$	-56 $\pm$ 1	
		(.333, .335)		0 $\pm$ 1	-23
Thymine	.800	$\approx$ .400	-	-	-
		$\approx$ .400			
1-Methylthymine	.816	(.453, .483)	$\pm(45\pm7)$	-74 $\pm$ 7	
		(.333, .363)		16 $\pm$ 7	-3
Cytosine	(.814, .850)	(.333, .383)	$\pm(72\pm18)$	49 $\pm$ 18	
		(.481, .500)		13 $\pm$ 18	30
		(.481, .500)		3 $\pm$ 9	
		(.333, .369)		59 $\pm$ 9	

to further restrict the values of  $K_1$  and  $K_2$  in this case. It was obtained by considering the value of  $K_1 + K_2$  (table 6.5), which is a measure of the alignment of the plane of the molecule with the stretch axis Z. It was assumed that the value for cytosine would not be greatly in excess of those for uracil and its derivatives, and an upper limit of 0.850 was applied. The second entry for cytosine shows the results calculated on this basis, and these were used in subsequent calculations of transition moment directions.

The non-planar pyrimidine derivatives are devoid of symmetry, and it is therefore not possible to assume a priori that the preferred orientation axis is parallel to the plane of the pyrimidine portion of the molecule. However the qualitative features of their orientation, as revealed in the UV and IR dichroisms, strongly suggest that this is the case: the IR and UV dichroisms of uridine, thymidine, cytidine and 5'-CMP are in excess of 1/3 for the whole region of spectrum studied; the same is true of the UV dichroism of guanosine (Fucaloro and Forster, 1971), showing that the plane of the pyrimidine portion tends in all cases to orient parallel to the axis Z. It therefore seems reasonable to assume that the orientation axis is in this plane. The upper and lower limits of  $K_1$  and  $K_2$  respectively, are taken to be .455 and .368 respectively, these being the greatest and least values of dichroism observed for the UV spectra of uridine, thymidine, cytidine and 5'-CMP. The results of calculations for cytidine and 5'-CMP are shown in table 6.7. As was mentioned previously the IR dichroism of uridine and thymidine did not give satisfactory information on the molecular orientation, and these molecules will not be discussed further.

#### 6.4 Transition Moment Directions

The electronic transition moment directions were calculated from eqn 6.4, using the values of  $\theta_1'$  as determined in the previous section, and the values of  $R_Z^i$  in table 6.4. There are now a total of four possible solutions, since there are two solutions for each value of  $\theta_1'$ . These are displayed in full in tables 6.6 and 6.7. Once more it is necessary to do the computations only for the cases when  $K_1$  and  $K_2$  have their maximum or minimum values, as the extrema of  $\theta_1'$  occur in these cases.

In order to choose the correct angles from those in tables 6.6 and 6.7, two criteria were applied. Firstly, it was assumed that the transition moment directions given by PSCS measurements approximate those in isolated molecules. Secondly, it was assumed that molecules differing only in the alkyl substituents on the pyrimidine ring have essentially the same electronic structure. Some indication that this is true can be seen in the similarity of the electronic spectra of uracil, thymine, and 1-methylthymine, and of cytosine, cytidine and 5'-CMP. The angles believed to be correct are shown at the bottom of each set of four entries in tables 6.6 and 6.7. For 1-methylthymine, 1-methyluracil and 6-azauracil, transition I is given by PSCS as being almost parallel to the 1'-axis; the calculations (tables 6.1, 6.2) are also in agreement in this regard. Therefore the correct values of  $\theta_1'$  and  $\theta_I'$  for uracil are seen to be  $0^\circ$  and  $0 \pm 10^\circ$ , respectively, and for 1-methylthymine,  $16^\circ$  and  $-9 \pm 7^\circ$  respectively. The PSCS work gives no precise statement concerning the direction of transition III. For 1-methylthymine, it is stated to be approximately perpendicular to transition I, and this would indicate  $-88 \pm 14^\circ$  as being the

TABLE 6.6

POSSIBLE ORIENTATION AXIS AND TRANSITION MOMENT DIRECTIONS

Molecule	<u>FOR SIMPLE PYRIMIDINES</u>			
	$\theta_1'$ (deg)	$\theta_I'$	$\theta_{II}'$	$\theta_{III}'$
Uracil	-56	-51±5	-	-14
		-60±5	-	82
	0	5±5)	-	42
		-5±5)	-	-42
1-Methylthymine	-74	-50±7	-	3±14
		82±7	-	30±14
	16	41±7	-	-88±14
		-9±7	-	-61±14
Cytosine	59±9	90±7	68±16	-76±4
		27±4	48±20	12±14
	4±9	-28±7	-6±16)	-43±4
		+35±14	15±20)	50±14

correct value. On the basis of the second criterion above, however,  $-42^\circ$  and  $-61 \pm 14^\circ$  must be considered more likely values for uracil and 1-methylthymine respectively.

Turning to cytosine, one finds that the fact that the PSCS results show  $\theta_I'$  and  $\theta_{II}'$  to be  $+14^\circ$  and  $-6^\circ$  respectively, enables the correct value of  $\theta_1'$  for cytosine, cytosine and 5'-CMP, and the correct values of  $\theta_I'$  and  $\theta_{II}'$  for the latter two molecules, to be selected. The two values of  $\theta_{II}'$  for

TABLE 6.7

POSSIBLE ORIENTATION AXES AND TRANSITION MOMENT DIRECTIONS FOR

	$\theta_1'$ (deg)	$\theta_I'$	$\theta_{II}'$	$\theta_{III}'$
Cytidine	80±11	-65±5	-45±5	3±17
		85±27	65±18	19±20
	-38±11	-53±5	-73±5	60±17)
		-23±27	-3±18	43±20)
5'-CMP	-80±9	-70±6	-42±6	-8±22
		87±21	62±17	29±28
	-38±9	-49±6	-76±6	70±28)
		-25±21	0±17	33±28)

cytosine overlap. There is a conflict in the choice of  $\theta_I'$  for cytosine, as the value  $35\pm 14^\circ$  is closer to the crystal value, whilst the value  $-28\pm 7^\circ$  is close to those of the other two compounds, and is therefore considered more likely to be correct. The value of  $\theta_{III}'$  for cytosine is clearly  $50\pm 14^\circ$ , but the results for the other two compounds are uninformative, save to say that  $\theta_{III}'$  is positive, and presumably close to the value for cytosine.

### 6.5 Discussion

#### Orientation Characteristics

No attempt will be made to calculate the  $k_i$  parameters of the pyrimidines, and compare them with the experimental values,

because of the uncertainties in the latter. Instead the orientation and polarisability properties of the pyrimidines will be qualitatively compared.

It has been seen, firstly, that  $R_Z^s$ ,  $R_Z^a$  and  $R_Z^I$  of thymine are all approximately equal. As the corresponding transition moments all have different directions,  $\theta'$  being  $60^\circ$ ,  $-30^\circ$  and  $0^\circ$  respectively, this shows that the values of  $K_1$  and  $K_2$  are approximately equal, a result which is in good agreement with the approximate equality of the polarisabilities  $b_1$  and  $b_2$  of thymine (table 5.2). Secondly, it is seen that the experimental values of  $\theta_1'$  for the other planar molecules are in good agreement with the theoretical values, within about  $20^\circ$  (table 6.5). Both results support the idea expressed in Chapter Two, that for molecules whose dimensions are not exaggerated along a single axis, dispersion forces play the primary role in orientation.

The results for the nucleosides and for 5'-CMP also indicate the predominance of dispersion interactions. It was seen above that the orientation behaviour of these molecules is dominated by their pyrimidine moieties. Because the pyrimidine molecule is bonded to the ribose ring approximately at right angles to the plane of the ring (Saenger, 1973; Furberg et al., 1965; Young et al., 1969) this cannot be a result of repulsive interactions: the molecule is not elongated along an axis in the plane of the pyrimidine molecule. Furthermore, because of the relative orientations of the pyrimidine and ribose ring, dispersion interactions with the polymer cannot occur in a cooperative manner: if one ring lies flat against a polymer molecule, so that dispersion interactions are maximised, the glycosidic bond will be pointing away at right angles to the

polymer z axis, thus minimising interaction with the other ring. The preferential binding of the pyrimidine ring with the polymer can be readily rationalised on the basis of dispersion interactions: the pyrimidine ring can approach much closer to the polymer than the ribose ring, which is puckered, and has hydroxyl and methyl groups protruding at right angles to the plane of the molecule..

A final interesting feature is the comparative orientation behaviour of cytidine and 5'-CMP as revealed by the  $R_z$  values in table 6.4. These are very similar, the values for 5'-CMP being uniformly larger than those for cytidine. This indicates that the presence of the charged phosphate group does not have a strong effect on orientation. It simply causes an increase in the correlation of the pyrimidine plane and polymer chain axis, an effect which is reminiscent of that of the polar bonding between quinoline and PVA, discussed in section 2.5.

#### SCF-MO Calculations

The remainder of this chapter is concerned with comparing the predictions of the various calculations, summarised in tables 6.1 to 6.3, with the results discussed in section 6.4, in order to assess their reliability in predicting the transition properties of pyrimidines and, to some extent, with identifying the reasons for their shortcomings. Hug and Tinoco (1973) pointed out that calculation of the transition monopoles at the atomic centres provides a convenient means of dissecting SCF-MO calculations. The transition monopoles give a measure of the transfer of electron density which occurs during the transition, and therefore provide a good representation of the nodal properties of excited states, where there is no natural

classification by symmetry. In addition, the extent to which excitation is confined to a particular portion of the molecule is revealed. Figures 6.12 and 6.13 show the calculated monopoles for transitions I, II and III of uracil and cytosine, respectively. The numerical values come from PPP-CI calculations, whilst the circles represent the values from the CNDO-CI calculations of Hug and Tinoco, the diameter of the circle being proportional to the magnitude of the monopole, and open and hatched circles referring to contributions of opposite sign.

Both sets of calculations agree in predicting transition I of uracil to be an internal charge transfer localised in the bond joining atoms 5 and 6, a prediction which is also made by the ab initio calculations. The fact that the observed transition moment is approximately parallel to the  $C_5 - C_6$  bond axis is consistent with this prediction. Of transition II nothing need be said, except that none of the calculations predict it to be of low intensity. The two sets of calculations disagree on transition III: the CNDO calculations predict a transfer of charge from  $O_7$  into the ring, whilst the PPP-CI calculations predict a transfer from  $O_8$ . The observed transition moment, of  $-42^\circ$ , is consistent with the former point of view. Both sets of calculations agree in predicting the 0 orbitals to be involved in both transitions II and III but do not seem to be capable of predicting the correct mixing of orbitals.

Turning to fig 6.13, one sees that for transition I both sets of calculations are, once more, in qualitative agreement, predicting positive monopoles at atoms 1 and 6, negative monopoles at atoms 3 and 5, and, as in uracil, little contribution from atoms 7 and 8. The CNDO-CI calculations show the main contributions to be from atoms 5 and 6, in a similar manner

FIG 6.12 CALCULATED TRANSITION MONOPOLES FOR URACIL

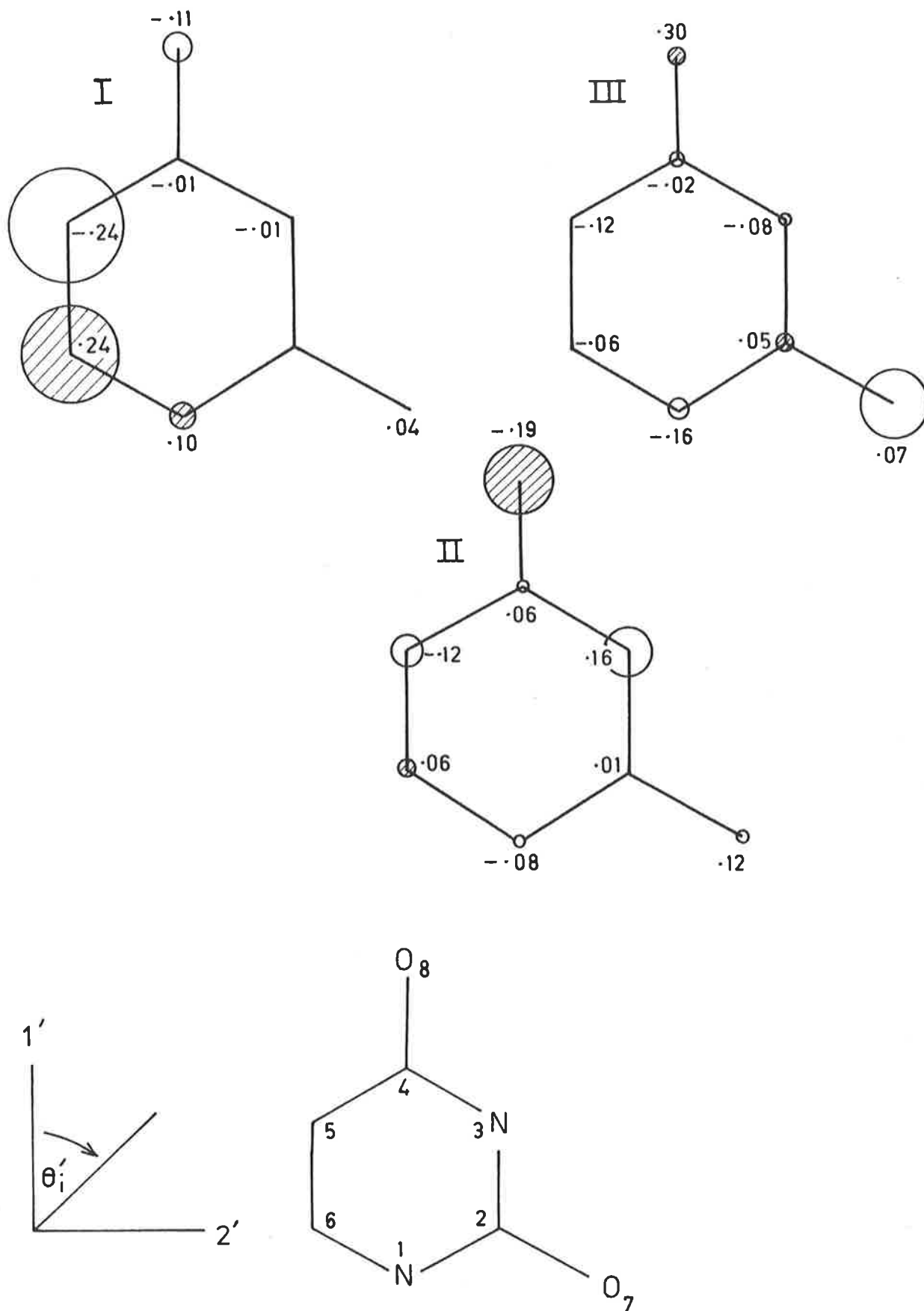
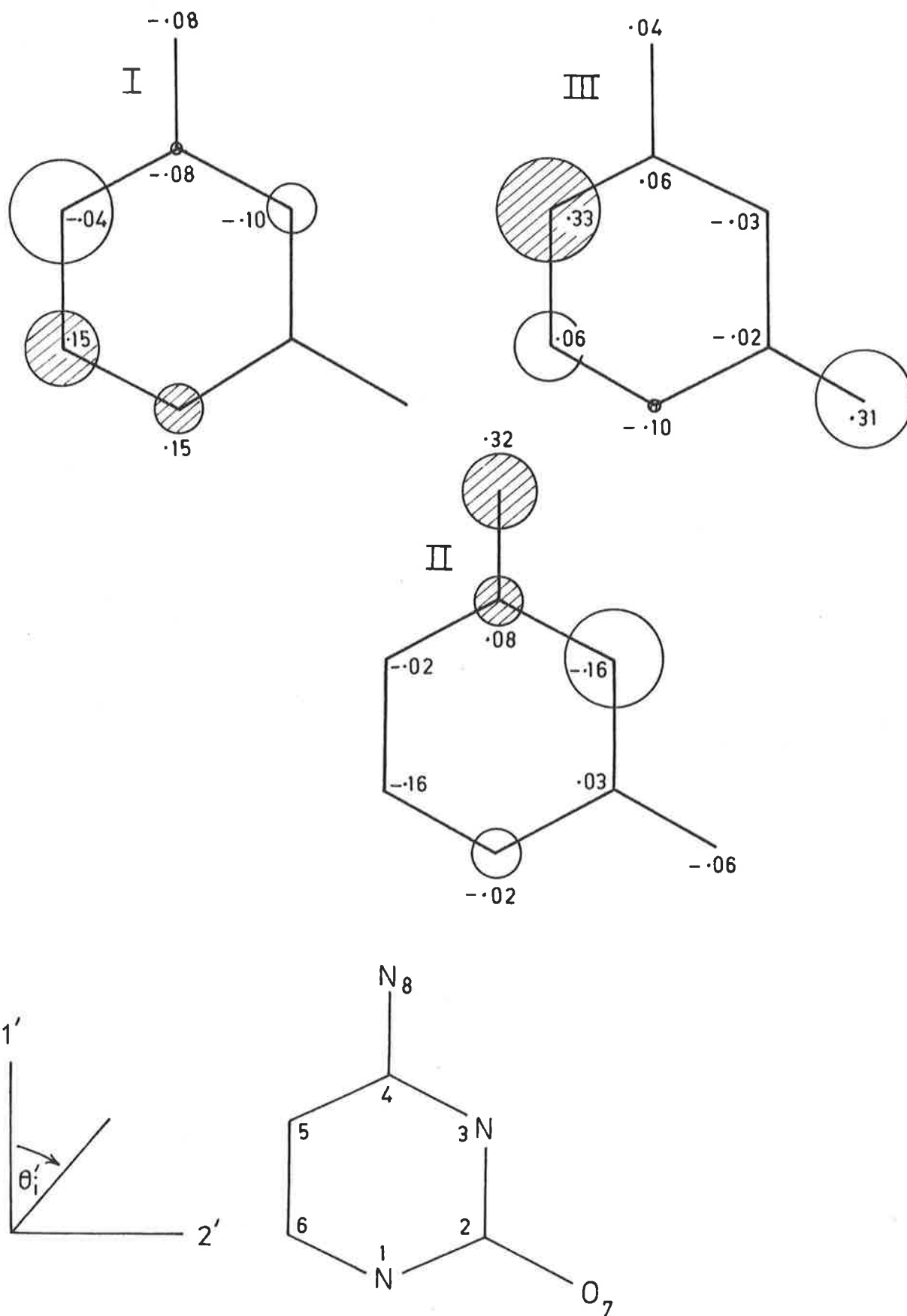


FIG 6.13 CALCULATED TRANSITION MONOPOLES FOR CYTOSINE



to transition I of uracil. This agrees with the experimental values of  $\theta_I'$  for cytidine, 5'-CMP and cytosine.

Both sets of calculations agree, once more, that atoms 7 and 8 are involved in transitions II and III and agree also that atom 8 contributes chiefly to transition II, and atom 7 to transition III. The first prediction is consistent with the observed transition moment direction, but the second definitely conflicts with the fact that the observed transition moment angle is positive.

A glance at tables 6.1 and 6.3 shows that there is disparity of results within each type of calculation, as well as between them. Pullman and Pullman, and, to some extent, Hug and Tinoco, adjusted parameters in their calculations in order to improve agreement with observed transition intensities and wavenumbers. Both sets of CNDO-CI calculations employed the same molecular geometries, and the results show that the calculated transition moment directions and intensities depend significantly on the choice of parameters assumed. Such comments apply equally to the PPP-CI calculations. As was mentioned in section 1.2, Ross et al. (1966) have reported results of CNDO-CI calculations in which vibronic coupling was taken into account. Their results indicated that the calculations were greatly improved thereby; however it has been commonly assumed that small changes in molecular geometry have no effect on calculated transition properties (Muller et al., 1974). Comparison of the PPP-CI (Bailey parametrisation) calculations for uracil and thymine, where the only differences are those of molecular geometry, show significant differences in the intensities and transition moment directions of transitions I and III, although the results are qualitatively the same. More

significant are the results for cytosine which, as explained above, differ in the molecular geometry assumed. The calculated energies and intensities are significantly different, although the maximum variation in bond length is  $.026 \text{ \AA}$ , and the maximum variation in bond angle  $2^\circ$  (Barker and Marsh, 1964). This gives a clear indication that for PPP-CI calculations at least, nuclear motion can be expected to lead to a significant mixing of the zeroth order molecular orbitals.

CHAPTER SEVENORIENTATION AND TRANSITION MOMENTS OF XANTHINE DERIVATIVES7.1 Observed and Calculated Transitions of Xanthine Derivatives

UV spectra of xanthine and its derivatives at various values of pH have been the subject of a good deal of attention, directed particularly to the problem of determining the predominant tautomers in the various ionic forms. Lawley (1971) surveyed the literature of the UV spectra of the purines in general and of their mono-anions and -cations. UV spectra of xanthines have been measured and discussed by Beaven et al. (1955), Cavalieri et al. (1954), Pfleiderer and Nuebel (1961), Lichtenberg et al. (1971), and Bergmann et al. (1972), and the PVA film spectrum of caffeine has been studied by Kikkert et al. (1973). The PVA film spectra of 1-methylxanthine, theophylline and caffeine are shown in figs 7.1, 7.2 and 7.3. The spectra of xanthines fall into two categories, depending on whether the hydrogen atom or other substituent on the imidazole ring is attached to nitrogen atom 7 or 9 (c.f. fig 1.2). In the first case band II is of low intensity and occurs as a shoulder of band III, whilst in the second case it is enhanced in intensity and shifted to the red. Whilst the biologically important purines, such as adenine, guanine and xanthosine, are substituted at position 9, purine in the solid state (Watson et al., 1965) and xanthine and its derivatives in aqueous solution (Pfleiderer and Nuebel, 1961; Lichtenberg et al., 1971; Bergmann et al., 1972) have the proton attached at atom 7. In the mono-anions of xanthines, however, the 9-tautomer is more stable. Caffeine has a methyl substituent at atom 7, and the spectrum of theophylline in PVA is so similar to that of caffeine that it can be assumed that the 7-H tautomer predominates. The spectrum of 1-methylxanthine in PVA, however,

FIG 7.1 UV DICHOIC SPECTRUM OF 1-METHYLYXANTHINE

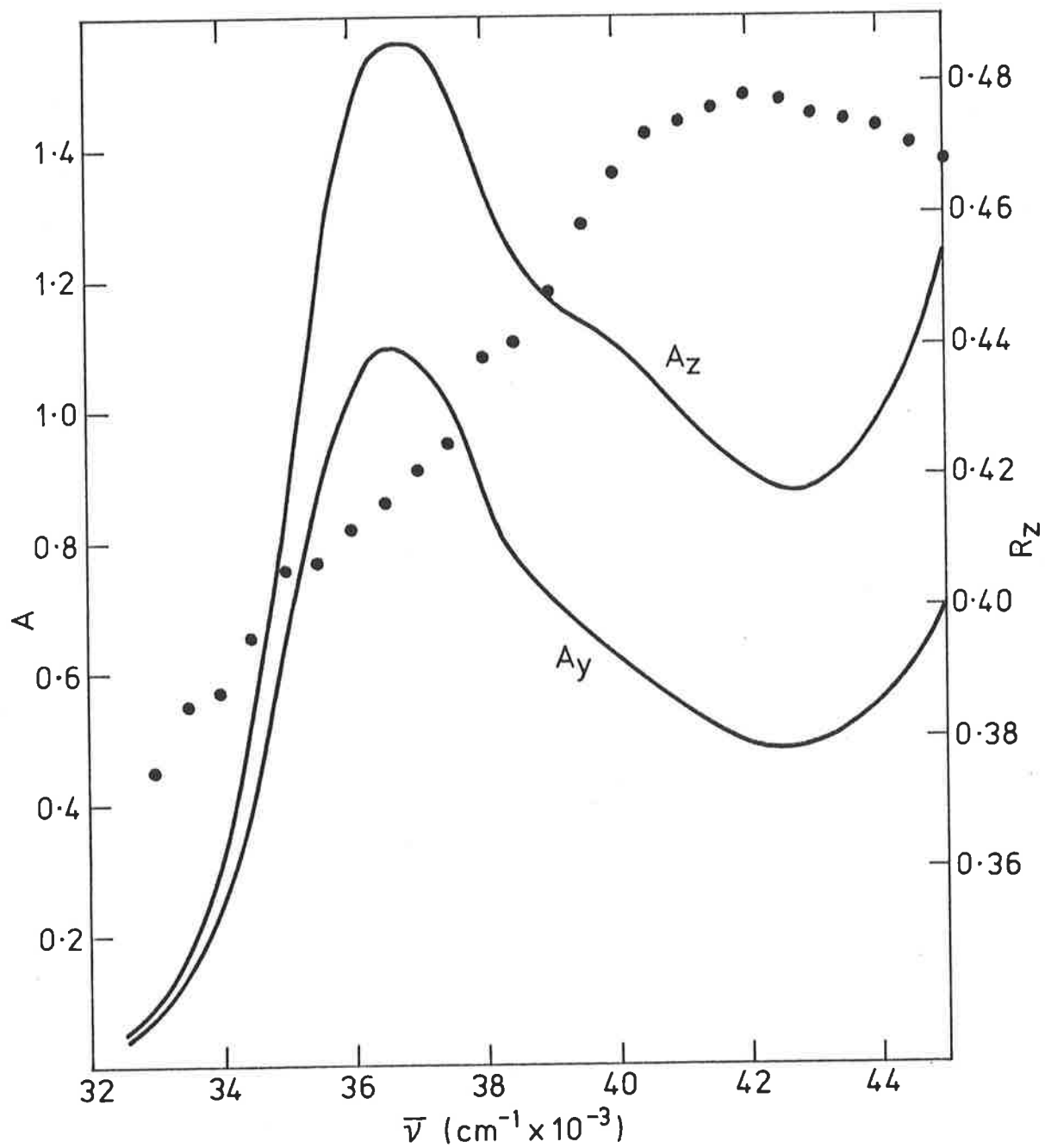


FIG 7.2 UV DICHOIC SPECTRUM OF THEOPHYLLINE

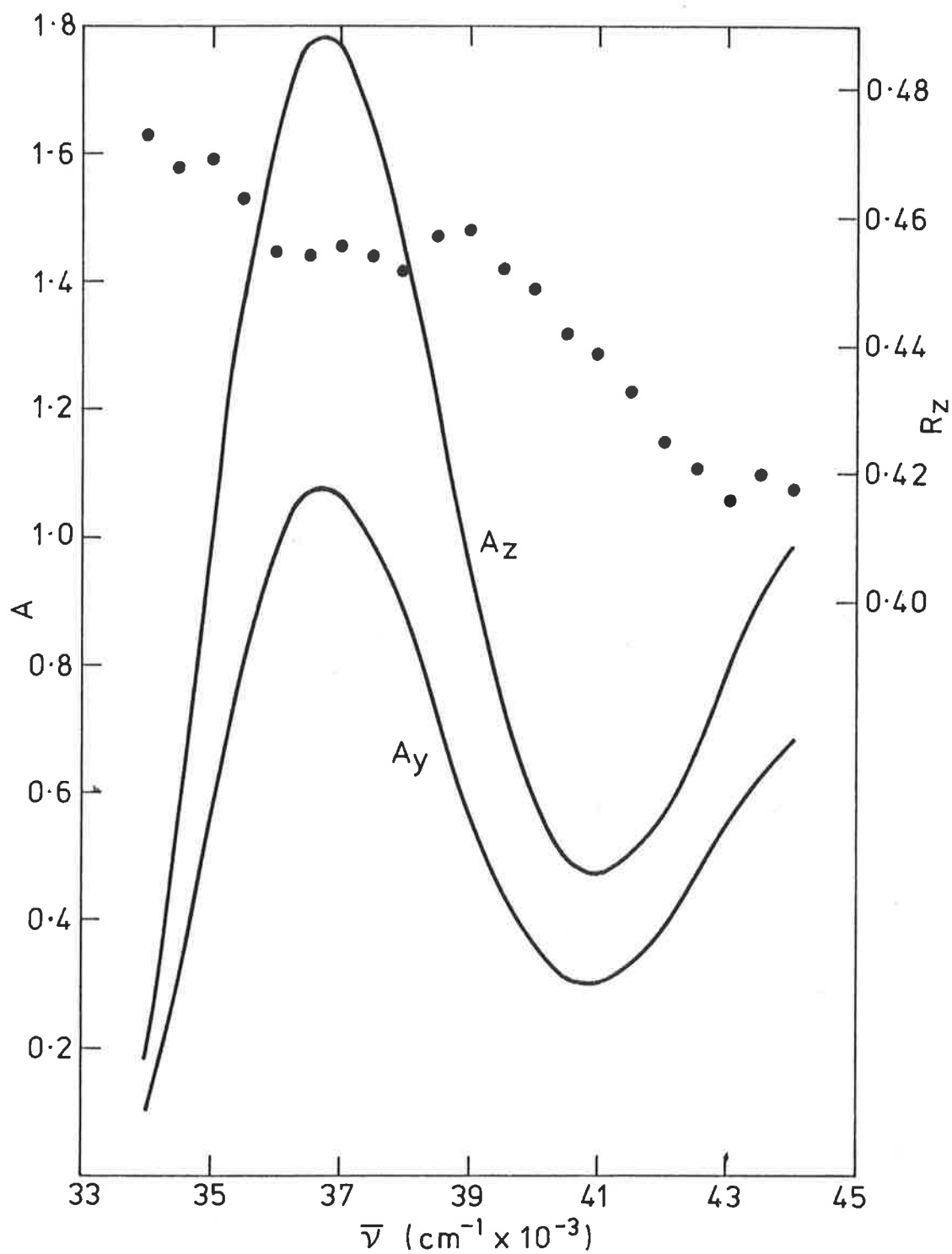
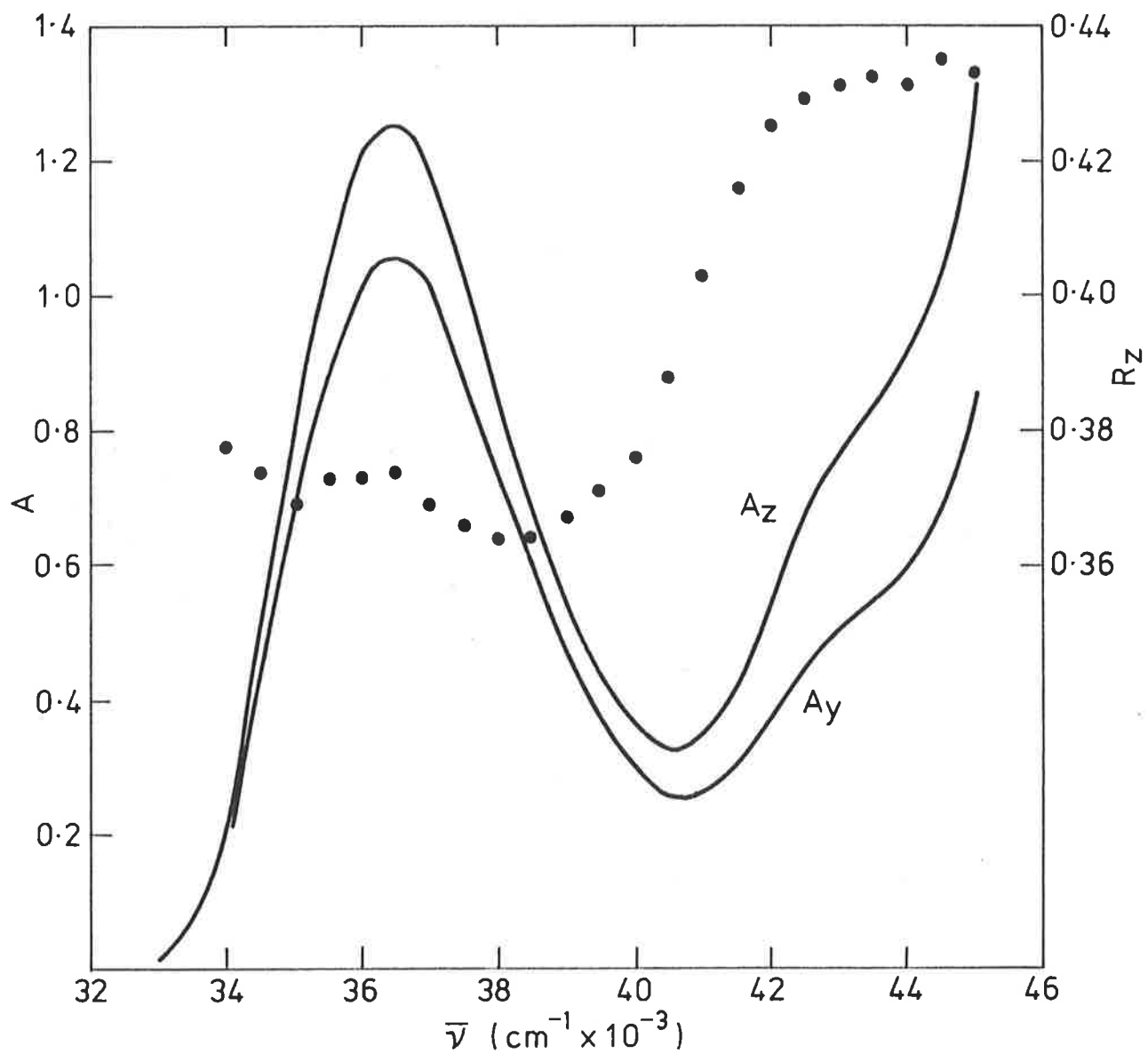


FIG 7.3 UV DICHOIC SPECTRUM OF CAFFEINE



is different from the aqueous spectrum, and from the spectra of caffeine and theophylline in PVA: band II is distinctly enhanced in intensity and shifted to the red, and this indicates that the 9-H tautomer predominates in PVA films. It is unlikely that the effect is due to ionisation, since the PVA spectrum does not resemble that of the mono-anion (Pfleiderer and Nuebel, 1961).

The results of PPP-CI calculations for theophylline, caffeine and 1-methylxanthine are shown in table 7.1. Atomic coordinates were as in the references of table 5.1. Since atomic coordinate data for 1-methylxanthine were not available, the coordinates of caffeine were used instead.

TABLE 7.1  
CALCULATED TRANSITION ENERGIES, INTENSITIES AND  
POLARISATIONS FOR LOWEST ( $\pi^*$ ,  $\pi$ ) TRANSITIONS OF XANTHINE DERIVATIVE

Transition		Theophylline	Caffeine	9-H Xanthine
	$\bar{\nu}$ ( $\text{cm}^{-1}$ )	39100	39700	41900
I	f	.12	.14	.10
	$\theta'$ (deg)	23	36	23
		45400	46300	46100
II		.06	.01	.12
		77	-36	70
		48600	47800	48800
III		.24	.19	.20
		67	49	-6

## 7.2 Dichroic Spectra

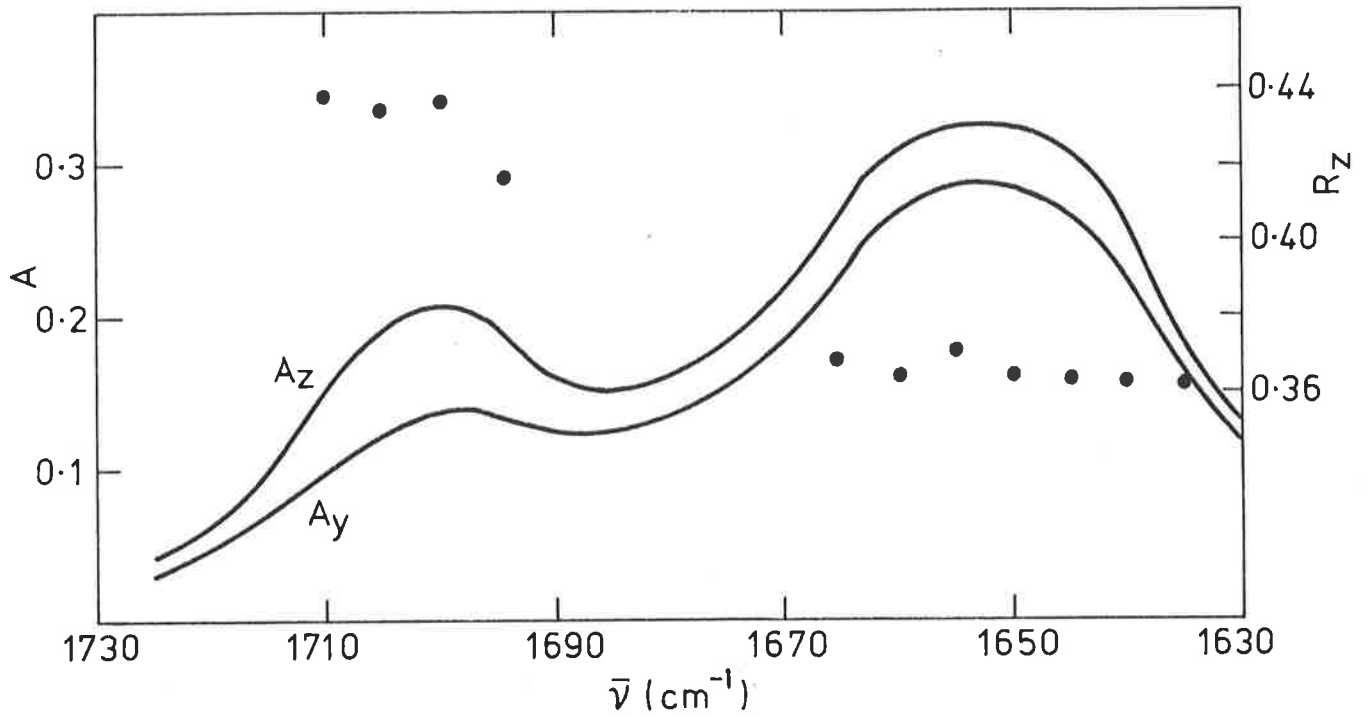
There is no evidence of aggregation in the UV dichroic

spectra of the xanthenes studied. There is no splitting of dichroism in band I of caffeine or theophylline; the first band of 1-methylxanthine shows a large variation in dichroism, but this arises from the fact that two overlapping transitions are present. The variation in dichroism at the inception of the first band which was observed in the spectra studied in the last chapter, is present also in the spectra of the xanthenes, and is ascribed to the same cause.

The IR dichroic spectra of theophylline, caffeine and 1-methylxanthine are shown in figs 7.4 and 7.5. Once again, there is no evidence of aggregation. The dichroism values for the various UV and IR transitions are shown in table 7.2. These were obtained by summing the dichroic absorbances  $A_Z$  and  $A_Y$  of several films, and calculating the dichroism on the totals, as before. The values for caffeine are derived from measurements on four different films, those for the other two compounds on three. The spectra illustrated in figs 7.1 to 7.5 pertain to a single film of each compound. The values of dichroism quoted correspond to wavenumbers at the centre of each band, except those for transitions I and II of 1-methylxanthine, which were evaluated at wavenumbers  $35000\text{ cm}^{-1}$  and  $41000\text{ cm}^{-1}$  respectively, and the dichroisms of the highest wavenumber band, which correspond to the highest wavenumber at which measurements were taken.

In interpreting the dichroism values, the same procedure was followed as was used in the previous chapter: the results are shown in table 7.3. Since there are no PSCS results for comparison, selection of the correct transition moment angles must rely on comparison with the calculations, where these can be considered reliable, from the discussion of the previous

FIG 7.4(a) IR DICHOIC SPECTRUM OF THEOPHYLLINE



(b) IR DICHOIC SPECTRUM OF CAFFEINE

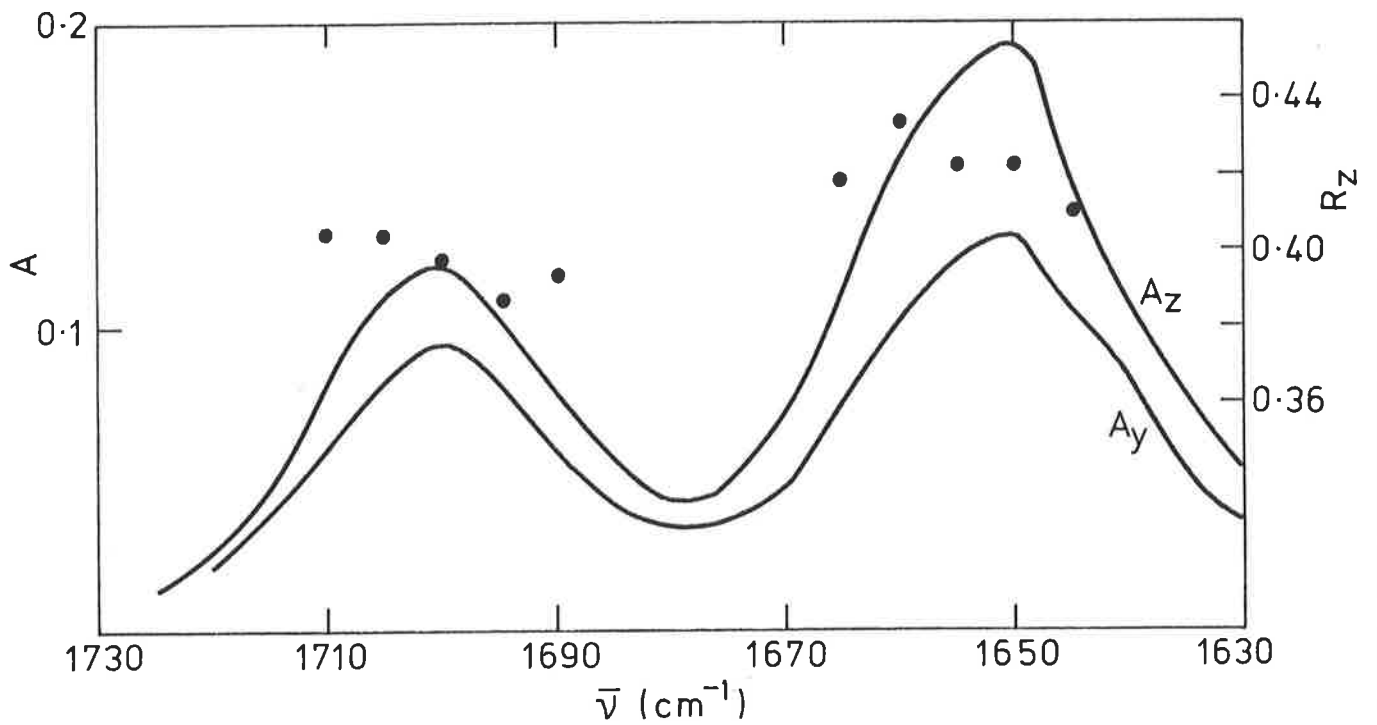
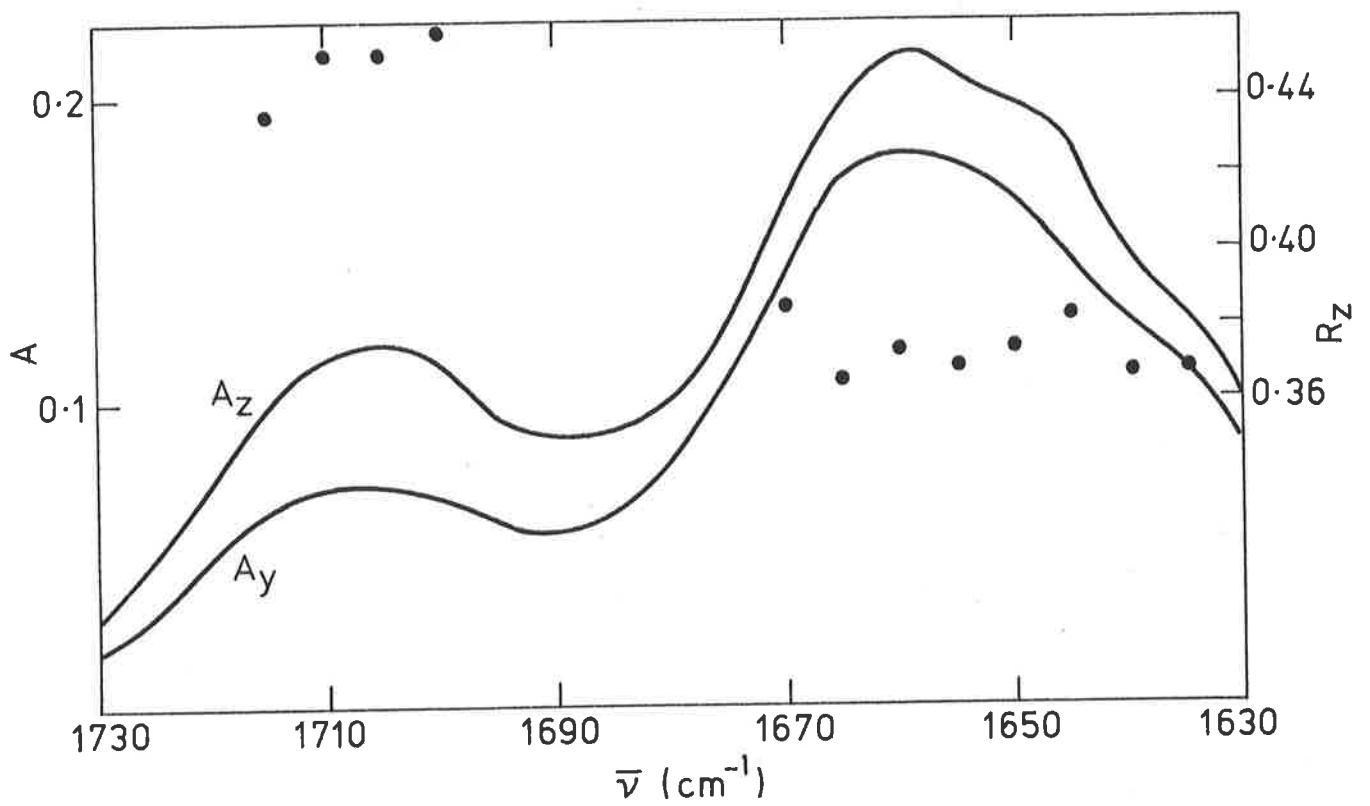


FIG 7.5 IR DICHOIC SPECTRUM OF 1-METHYLYXANTHINE



chapter. Once again, the value considered most likely to be correct is at the bottom of each set, in the tables.

TABLE 7.2

IR AND UV DICHROISMS OF XANTHINE DERIVATIVES

	$R_Z^s$	$R_Z^a$	$R_Z^I$	$R_Z^{II}$	$R_Z^{III}$
Theophylline	.422	.375	.449	.429	-
Caffeine	.378	.386	.378	.430	.421
1-Methylxanthine	.438	.366	.402	.461	.455

7.3 Orientation and Transition Moments

The transition monopoles for caffeine and 9-H-xanthine as given by PPP-CI calculations are shown in figs 7.6 and 7.7. There are no CNDO-CI calculations available for xanthines. It is very probable that transition I is located in the pyrimidine portion of the molecules, and is essentially the same as transition I of uracil and its derivatives: it has the same energy and intensity, and the calculations show it to be localised mainly in the  $C_4 - C_5$  region, and to be, at least qualitatively, short axis polarised. Therefore the correct values of  $\theta_I'$  for theophylline, caffeine and 1-methylxanthine are taken to be  $19 \pm 12^\circ$ ,  $-22 \pm 1^\circ$ , and  $-9 \pm 3^\circ$  respectively. Because of the photoselection result for caffeine (table 1.1), the value of  $\theta_{II}'$  is taken to be  $-73 \pm 4^\circ$ , and that of theophylline  $57 \pm 1^\circ$ , as this is the value closest to that for caffeine. The difference  $\theta_I' - \theta_{II}'$  for caffeine has a maximum of  $56^\circ$  as compared with the photoselection value of  $71^\circ$ . However as discussed in section 1.2 photoselection results are not of high accuracy, and therefore the discrepancy is not serious. It is not possible to make a

FIG 7.6 CALCULATED TRANSITION MONOPOLES FOR CAFFEINE

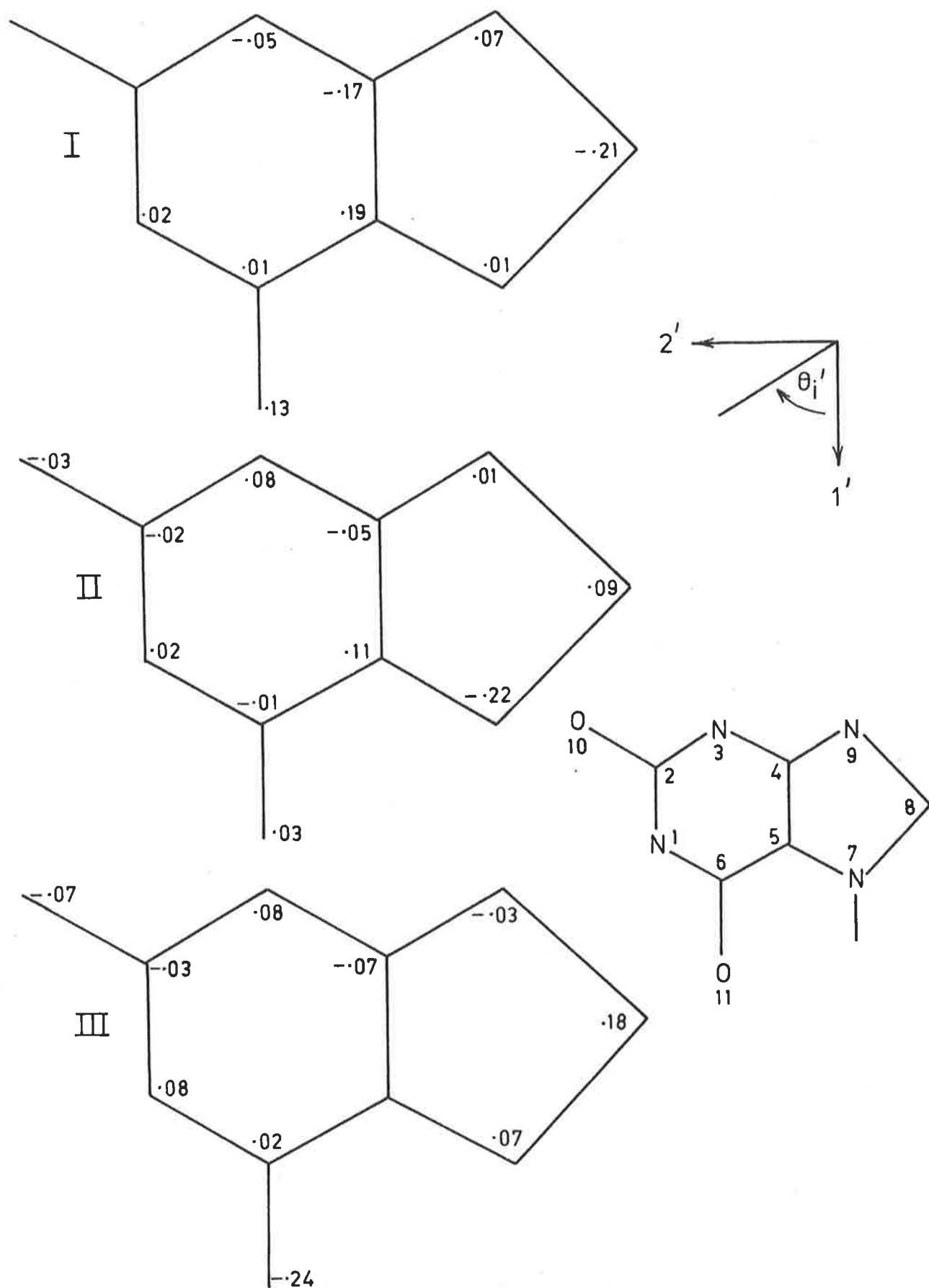
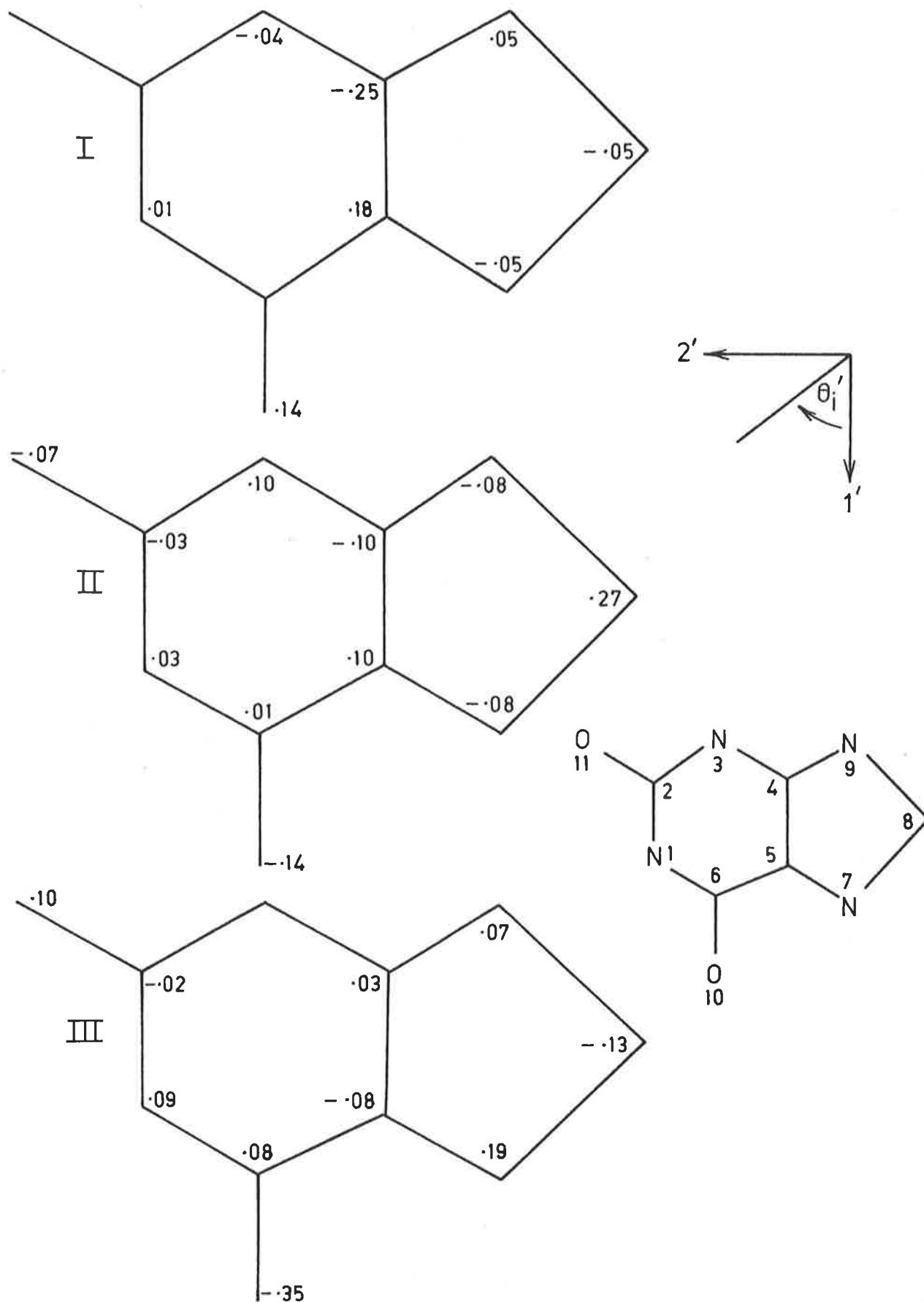


FIG 7.7 CALCULATED TRANSITION MONOPOLES FOR 9-H-XANTHINE



selection between the two possible values of  $\theta_{III}'$  for caffeine, or the possible values of  $\theta_{II}'$  and  $\theta_{III}'$  for 1-methylxanthine, and the results show them to be between  $-51$  and  $-88^\circ$ ,  $17$  and  $49^\circ$ , and  $13$  and  $53^\circ$  respectively.

TABLE 7.3

POSSIBLE ORIENTATION AXIS AND TRANSITION MOMENT DIRECTIONS FOR

Molecule	<u>XANTHINE DERIVATIVES</u>			
	$\theta_1'$ (deg)	$\theta_I'$	$\theta_{II}'$	$\theta_{III}'$
Theophylline	$-86 \pm 2$	$-77 \pm 12$	$-58 \pm 4$	-
		$84 \pm 9$	$65 \pm 1$	
	$29 \pm 2$	$39 \pm 9$	$0 \pm 4$	-
		$19 \pm 12$	$57 \pm 1$	
Caffeine	$15 \pm 1$	$63$	$19 \pm 4$	$34 \pm 1$
		$-32 \pm 1$	$17 \pm 3$	$-3$
	$-70 \pm 1$	$63$	$-67 \pm 3$	$-51$ )
		$-22 \pm 1$	$-73 \pm 4$	$-88 \pm 1$ )
1-Methylxanthine	$89 \pm 2$	$-47 \pm 3$	$-83 \pm 10$	$72 \pm 2$
		$45 \pm 1$	$81 \pm 6$	$-75 \pm 5$
	$35 \pm 2$	$79 \pm 1$	$27 \pm 10$ )	$18 \pm 5$ )
		$-9 \pm 3$	$43 \pm 6$ )	$51 \pm 2$ )

The orientation axis direction of caffeine,  $-70 \pm 1^\circ$ , is close to the theoretical value given in table 5.2. Unfortunately the optical data for theophylline in the literature are in conflict, as seen in that table, and therefore no comparison of theory and

experiment can be made in this case. In spite of the similarity of their structures, the orientation axes of theophylline and caffeine are seen to be almost at right angles: this shows the impossibility of predicting orientation properties from molecular shape for molecules such as these.

Comparison of the calculated and observed spectra of the 7-H- and 9-H-xanthine tautomers provides an excellent means of judging the effectiveness of the parametrisation of the Bailey-type PPP-CI calculations. The tautomers are distinguished by the use of different parameters for "pyrimidine" and "pyrrole" type nitrogen atoms in the calculations. These correctly predict the change of intensity of transition II, but the fact that they do not predict the lowering in energy indicates that the change in the electronic structure caused by tautomerism is not accounted for very convincingly. Transition II is not localised in either the pyrimidine or the imidazole ring: if it were confined to the imidazole ring only, tautomerism would have no effect on the spectrum, since the tautomers of imidazole are identical, and if it were confined solely to the pyrimidine portion of the molecule there would, of course, be no effect either. The calculations are in agreement on this point, showing the transition to be spread over atoms 3, 4, 5, 7 and 8. It was mentioned in section 6.5 that the calculations did not seem capable of predicting the correct contribution of the atomic orbitals of the oxygen atoms to the various molecular orbitals of uracil. This comment can be extended to the xanthenes, for the calculations predict a transfer of charge between oxygen atom  $O_{11}$  and the aromatic system in transition I, whilst it has been seen that this transition is most probably localised at atoms 4 and 5, as with uracil derivatives. The effect of vibronic

coupling on the calculated transition moments of 7-H-xanthenes may be judged by comparing results for theophylline and caffeine, since the only difference in the two sets of calculations is the molecular geometry, the largest difference in bond lengths in the two molecules being  $.07 \text{ \AA}$  (Sutor, 1958b). The figures in table 7.1 show that, once again, the calculations cannot be expected to give accurate results if vibronic coupling is not taken into account.

APPENDICESA.1 Resolution of a Dichroic Spectrum into Components Polarised  
Along Orthogonal Axes

Suppose that  $A_Y$  and  $A_Z$  are the dichroic absorbances of a solute in a stretched polymer film, and that  $A_1$  and  $A_2$  are the total absorbances along orthogonal molecular axes for all molecules in the sample. The component along the third axis is assumed to be negligible. It follows from eqn 1.1 that

$$\begin{aligned} A_Z &= l_{1Z}^2 A_1 + l_{2Z}^2 A_2 \\ &= K_1 A_1 + K_2 A_2 \end{aligned}$$

and

$$\begin{aligned} A_Y &= l_{1Y}^2 A_1 + l_{2Y}^2 A_2 \\ &= \frac{1}{2}(1 - K_1)A_1 + \frac{1}{2}(1 - K_2)A_2 \end{aligned}$$

where  $l_{1Z}$  etc. are direction cosines as used in the text. By inverting these equations, one obtains:

$$\begin{aligned} A_1 &= \frac{1 - K_2}{K_1 - K_2} A_Z - \frac{2K_2}{K_1 - K_2} A_Y \\ A_2 &= \frac{-(1 - K_1)}{K_1 - K_2} A_Z + \frac{2K_1}{K_1 - K_2} A_Y \end{aligned}$$

A.2 Derivation of Equation 2.9

By expanding eqn 2.8, and making use of the approximations discussed in section 2.5, one obtains the following expression for the dispersion potential:

$$\begin{aligned}
 U = & -\frac{1}{4} \frac{\epsilon_s \epsilon_p}{\epsilon_s + \epsilon_p} \cdot \frac{1}{r^6} [(b_z - b_y) \{(b_1 - b_3) l_{1z}^2 + (b_2 - b_3) l_{2z}^2\} \\
 & + 3b_y \{(b_1 - b_3) (\underline{1} \cdot \underline{\lambda})^2 + (b_2 - b_3) (\underline{2} \cdot \underline{\lambda})^2\} + b_1 b_y + b_2 b_y \\
 & + 3b_3 b_y + b_3 b_z]
 \end{aligned}$$

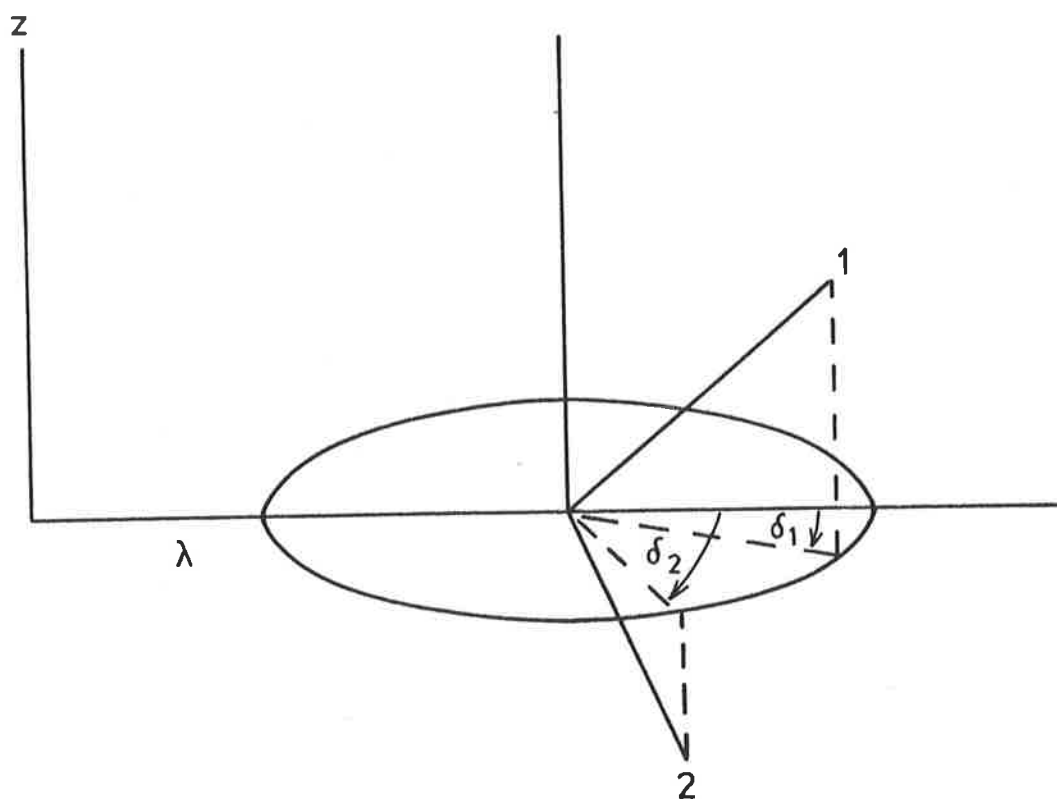
It is seen from fig A.1 that by varying  $\delta_1$  and  $\delta_2$ ,  $(\underline{1} \cdot \underline{\lambda})$  and  $(\underline{2} \cdot \underline{\lambda})$  may be varied independently of  $l_{1z}$  and  $l_{2z}$ . Since the only terms in the expression which are of concern in evaluating  $\langle l_{1z}^2 \rangle$  and  $\langle l_{2z}^2 \rangle$  are those containing  $l_{1z}$  and  $l_{2z}$ , the expression for U may be abbreviated for present purposes to:

$$U = U_0 \{(b_1 - b_3) l_{1z}^2 + (b_2 - b_3) l_{2z}^2\}$$

where

$$U_0 = -\frac{1}{4} \frac{\epsilon_s \epsilon_p}{\epsilon_s + \epsilon_p} (b_z - b_y)$$

FIG A.1 RELATIVE ORIENTATIONS OF POLYMER AND SOLUTE AXIS SYSTEMS



### A.3 Derivation of Series Expansions of the Functions A and B

It is noted firstly that the state density function  $\Omega$  is equal to  $\sin\beta$ .

The integral in the expression for A is expanded as follows:

$$\begin{aligned} & \sin\beta \cos^2\beta \exp(a_1 \cos^2\beta + a_2 \sin^2\beta \cos^2\gamma) \\ &= \sum_{i=0}^{\infty} \frac{(a_1 \cos^2\beta + a_2 \sin^2\beta \cos^2\gamma)^i}{\Gamma(i+1)} \\ &= \sum_{i=0}^{\infty} \sum_{j=0}^i \frac{a_1^{i-j} a_2^j}{\Gamma(j+1)\Gamma(i-j+1)} (\cos^2\beta)^{i-j} (\sin^2\beta)^{j+\frac{1}{2}} (\cos^2\gamma)^j d\gamma d\beta \end{aligned}$$

The infinite series is uniformly convergent if  $a_1$  and  $a_2$  are bounded; consideration of the definitions of  $a_1$  and  $a_2$  in section 2.5 shows that the physically meaningful values of  $a_1$  and  $a_2$  are bounded if  $T$  does not approach zero. Therefore it is permissible to integrate the series term by term giving

$$\begin{aligned} A &= \sum_{i=0}^{\infty} \sum_{j=0}^i \frac{a_1^{i-j} a_2^j}{\Gamma(j+1)\Gamma(i-j+1)} \int_0^{\frac{\pi}{2}} (\cos^2\beta)^{i-j} (\sin^2\beta)^{j+\frac{1}{2}} d\beta \times \\ & \quad \int_0^{\frac{\pi}{2}} (\cos^2\gamma)^j d\gamma \\ &= \frac{1}{4} \sum_{i=0}^{\infty} \frac{\Gamma(\frac{1}{2})}{\Gamma(i+\frac{3}{2})} \sum_{j=0}^i a_1^{i-j} a_2^j \frac{\Gamma(i-j+\frac{1}{2})\Gamma(j+\frac{1}{2})}{\Gamma(i-j+1)\Gamma(j+1)} \\ &= \frac{1}{4} \sum_{i=0}^{\infty} \frac{\Gamma(\frac{1}{2})}{\Gamma(i+\frac{3}{2})} I_i(a_1, a_2) \end{aligned}$$

where

$$\begin{aligned} I_i &= \sum_{j=0}^i a_1^{i-j} a_2^j A_{i,j} \\ A_{i,j} &= \frac{\Gamma(i-j+\frac{1}{2})\Gamma(j+\frac{1}{2})}{\Gamma(i-j+1)\Gamma(j+1)} \end{aligned}$$

A similar treatment gives

$$B = \frac{1}{4} \sum_{i=0}^{\infty} \frac{\Gamma(\frac{1}{2})}{\Gamma(i+\frac{3}{2})} \cdot \frac{1}{2i+3} \cdot \{I_i + 2a_1 \frac{\partial I_i}{\partial a_1}\}$$

Recursion formula for  $I_n$ 

Using the formulae above it is found that

$$I_0 = \pi; \quad I_1 = \pi \frac{a_1 + a_2}{2}; \quad I_2 = \pi \left( \frac{3}{4}(a_1 + a_2)I_1 - \frac{1}{2}a_1 a_2 I_0 \right)$$

This suggests the recursion formula

$$I_n = \frac{2n-1}{2n}(a_1 + a_2)I_{n-1} - \frac{n-1}{n}a_1 a_2 I_{n-2}$$

The truth of this formula may be established by induction.

Since

$$(a_1 + a_2)I_{n-1} = \sum_{j=1}^{n-1} A_{n,j} a_1^{n-j} a_2^j \left\{ \frac{n-j}{n-j-\frac{1}{2}} + \frac{j}{j-\frac{1}{2}} \right\} + \frac{\Gamma(\frac{1}{2})\Gamma(n-\frac{1}{2})}{\Gamma(n)} (a_1^n + a_2^n)$$

and

$$a_1 a_2 I_{n-2} = \sum_{j=1}^{n-1} A_{n,j} a_1^{n-j} a_2^j \left\{ \frac{(n-j)j}{(n-j-\frac{1}{2})(j-\frac{1}{2})} \right\}$$

then

$$\frac{2n-1}{2n}(a_1 + a_2)I_{n-1} - \frac{n-1}{n}a_1 a_2 I_{n-2} = \sum_{j=0}^n a_1^{n-j} a_2^j A_{n,j} = I_n$$

To illustrate the convergence of the series for A and B the partial sums for a typical example to 15 terms are shown in table A.1. The values of  $(b_1 - b_2)$ ,  $(b_1 - b_3)$  and  $U_0$  are as for the naphthalene entry in table 2.5.

The correctness of the expansions was also checked against direct, numerical evaluation of the integrals.

TABLE A.1

CONVERGENCE OF SERIES FOR A AND B

i	$U_0/kT = -.20 \times 10^{+24}$				
	A(a <sub>1</sub> , a <sub>2</sub> )	B(a <sub>1</sub> , a <sub>2</sub> )	B(a <sub>2</sub> , a <sub>1</sub> )	k <sub>1</sub>	k <sub>2</sub>
0	2.000	.667	.667	.334	.334
1	4.107	1.648	1.371	.401	.334
2	5.510	2.437	1.784	.442	.324
3	6.209	2.883	1.959	.464	.316
4	6.489	3.079	2.019	.475	.311
5	6.584	3.150	2.036	.478	.309
6	6.612	3.171	2.040	.480	.309
7	6.619	3.177	2.041	.480	.308
8	6.620	3.178	2.041	.480	.308
9	6.621	3.179	2.041	.480	.308
10	6.621	3.179	2.041	.480	.308
11	6.621	3.179	2.041	.480	.308
12	6.621	3.179	2.041	.480	.308
13	6.621	3.179	2.041	.480	.308
14	6.621	3.179	2.041	.480	.308

A.4 Proof of Some Identities Resulting from Equation 2.2(i) Proof that  $K_3 \leq R_Z \leq K_1$ 

By writing

$$m_1^2 = \cos^2 \beta, \quad m_2^2 = \sin^2 \beta \cos^2 \gamma \quad \text{and} \quad m_3^2 = \sin^2 \beta \sin^2 \gamma$$

in eqn 2.2, and differentiating, one obtains

$$dR_Z = -2\sin\beta\cos\beta d\beta (K_1 - K_2 \cos^2 \gamma - K_3 \sin^2 \gamma) - 2\sin\gamma\cos\gamma \sin^2 \beta d\gamma (K_2 - K_3).$$

Since  $K_1 > K_2 > K_3$

the expressions in parentheses are non-zero, and extrema of  $R_Z$  occur when

$$\beta = 0 \text{ or } \frac{\pi}{2} \text{ and } \gamma = 0 \text{ or } \frac{\pi}{2}.$$

When these conditions hold, the values of  $R_Z$  are  $K_1$  and  $K_3$ . A similar proof can be given to show that

$$K_2 \leq R_Z \leq K_1$$

for  $(\pi^*, \pi)$  transitions of a planar molecule.

(ii) Maximum and Minimum Values of Orientation Axis and Transition Moment Angles

It is seen from eqn 6.4 that

$$\frac{\partial \theta_i}{\partial K_1} = \frac{1}{\sin 2\theta_i} \frac{R_Z^i - K_2}{(K_1 - K_2)^2}$$

$$\frac{\partial \theta_i}{\partial K_2} = \frac{1}{\sin 2\theta_i} \frac{K_1 - R_Z^i}{(K_1 - K_2)^2}$$

The two differentials have zeros only when  $R_Z^i$  is equal to  $K_1$  or  $K_2$ , but these cases need not be considered because  $\theta_i$  then has a fixed value regardless of the values of  $K_1$  and  $K_2$ .

Suppose firstly that  $i = 1'$ .  $\theta_1$  is then equal to the orientation axis angle in the molecular  $(1', 2', 3')$

axis system. It is clear from the equations that this angle has its maximum and minimum values only when  $K_1$  and  $K_2$  also have their maxima or minima.

A similar result may be obtained for the angle  $\theta_{i'}$  of an electronic transition moment  $i$  in the system  $(1', 2', 3')$ . Since

$$\theta_{i'} = \theta_i - \theta_{1'}$$

one has

$$\frac{\partial \theta_{i'}}{\partial K_1} = \frac{1}{(K_1 - K_2)^2} \left\{ \frac{R_Z^i - K_2}{\sin 2\theta_i} - \frac{R_Z^{1'} - K_2}{\sin 2\theta_{1'}} \right\}$$

with a similar expression for  $\frac{\partial \theta_{i'}}{\partial K_2}$ . Unless the angles  $\theta_i$  and  $\theta_{1'}$  are identical, the quantity in brackets is non-zero, and  $\theta_{i'}$  has its greatest and least values only when  $K_1$  and  $K_2$  have their greatest or least values. This result is also true if  $\theta_i = \theta_{1'}$ , since  $\theta_{1'} = -\theta_{1'}$ , and the argument of the preceding paragraph would then apply.

REFERENCES

- A. Albert (1966), "The Acridines", 2nd Ed., (Edward Arnold)
- A.C. Albrecht (1961), J. Mol. Spectr., 6, 84
- J.F. Archard and A.M. Taylor (1948), J. Sci. Instr., 25, 407
- M.L. Bailey (1969), Theoret. Chim. Acta, 13, 56
- M.L. Bailey (1970), Theoret. Chim. Acta, 16, 309
- D.L. Barker and R.E. Marsh (1964), Acta Cryst., 17, 1581
- C.J. Ballhausen and A.E. Hansen (1972), Ann. Rev. Phys. Chem.,  
23, 15
- G.H. Beaven, E.R. Holiday and E.A. Johnson (1955) in E. Chargaff  
and J.N. Davidson, Eds., "The Nucleic Acids", Vol. 1,  
(Academic Press)
- L.J. Bellamy, B.R. Connelly, A.R. Philpotts and R.L. Williams  
(1960), Z. Elektrochem., 64, 563
- L.J. Bellamy (1973), "Advances in Infrared Group Frequencies",  
(Chapman and Hall)
- F. Bergmann, D. Lichtenberg and Z. Niemann (1972), in E.D.  
Bergmann and B. Pullman, Eds., "The Purines, Theory and  
Experiment", (Israel. Acad. of Sciences and Humanities)
- J.A. Biles, N.F. Witt and C.F. Poe (1951), Mikrochem., 38, 591
- E.R. Blout and M. Fields (1950), J. Am. Chem. Soc., 72, 479
- M. Born and E. Wolf (1970), "Principles of Optics", 4th Ed.,  
(Pergamon)
- C.C. Bott (1972), Honours Thesis, Adelaide University
- C.C. Bott and T. Kurucsev (1975), J. Chem. Soc. Farad. II, 71,  
749
- J. Brandrup and E.H. Immergut, Eds. (1966), "Polymer Handbook",  
2nd Ed., (Interscience)

- A. Bree, A.R. Lacey, I.G. Ross and R. Zwarich (1974), Chem. Phys. Lett., 26, 329
- B.J. Bridge and L.P. Gianneschi (1976), J. Chem. Soc. Farad. II, 72, 1622
- F.C. Brooks (1952), Phys. Rev., 86, 92
- J.N. Brown, L.M. Trefonas, A.F. Fucaloro and B.G. Anex (1974), J. Am. Chem. Soc., 96, 1597
- P.R. Callis, E.J. Rosa and W.T. Simpson (1964), J. Am. Chem. Soc., 86, 2293
- P.R. Callis and W.T. Simpson (1970), J. Am. Chem. Soc., 92, 3593
- P.R. Callis, B. Fanconi and W.T. Simpson (1971), J. Am. Chem. Soc., 93, 6679
- L.F. Cavalieri, J.J. Fox, A. Stone and N. Chang (1954), J. Am. Chem. Soc., 76, 1119
- Q. Chae and P.-S. Song (1974), J. Am. Chem. Soc., 97, 4176
- P.J. Chappell and I.G. Ross (1976), Chem. Phys. Lett., 43, 440
- H.H. Chen and L.B. Clark (1969), J. Chem. Phys., 51, 1862
- H.H. Chen and L.B. Clark (1973), J. Chem. Phys., 58, 2593
- C.L. Cheng, R.J.W. Lefevre, G.L.D. Ritchie, P.H. Gore and M. Yusuf (1971), J. Chem. Soc. B, 1579
- L.B. Clark and I. Tinoco (1965), J. Am. Chem. Soc., 87, 11
- A. Davidsson and B. Norden (1972), Tetr. Lett., 30, 3093
- A. Davidsson and B. Norden (1974), Chem. Phys. Lett., 28, 221
- H. Devoe and I. Tinoco (1962), J. Mol. Biol., 4, 500
- H. Devoe (1965), J. Chem. Phys., 43, 3199
- H. Devoe (1971), J. Phys. Chem., 75, 1509
- M.J.S. Dewar and S.D. Worley (1969), J. Chem. Phys., 51, 263
- F. Doerr (1966), Angew. Chem. Int. Ed., 5, 478

- J. Downing and J. Michl (1972), *Int. J. Q. Chem.*, 6, 311
- W.A. Eaton and T.P. Lewis (1970), *J. Chem. Phys.*, 53, 2164
- C. Fayat and A. Foucauld (1970), *Bull. Soc. Chim. France*,  
12, 4491
- R.D.B. Fraser (1958), *J. Chem. Phys.*, 28, 1113
- A.F. Fucaloro (1969), Doctoral Dissertation, (University of  
Arizona)
- A.F. Fucaloro and L.S. Forster (1971), *J. Am. Chem. Soc.*, 93,  
6443
- A.F. Fucaloro and L.S. Forster (1974), *Spectr. Acta*, 30A, 883
- S. Furberg, C.S. Petersen and C. Romming (1965), *Acta Cryst.*,  
18, 313
- N.S. Gangakhedkar, A.V. Namjoshi, P.S. Tamhane and  
N.K. Chaudhuri (1974), *J. Chem. Phys.*, 60, 2584
- R. Gerdil (1961), *Acta Cryst.*, 14, 333
- V. Gilpin and W.C. McCrone (1950), *Anal. Chem.*, 22, 368
- M.L. Gulrajani and M.R. Padhye (1971), *Ind. J. Technol.*, 9, 211
- F. Gutman and L.E. Lyons (1967), "Organic Semiconductors",  
(Wiley)
- A.E. Hansen (1967), *Mol. Phys.*, 13, 425
- J.F. Harrison (1968), *J. Chem. Phys.*, 49, 3321
- K.A. Hartman (1967), *Biochem. Biophys. Acta*, 138, 192
- H. Hiratsuka, Y. Tanizaki and T. Hoshi (1972), *Spectr. Acta*,  
28A, 2375
- R.M. Hochstrasser (1966), "Molecular Aspects of Symmetry",  
(Benjamin)

- K. Hoogsteen (1963), *Acta Cryst.*, 16, 28
- H. Horak and J. Gut (1961), *Coll. Czech. Chem. Commun.*, 26, 1680
- T. Hoshi and Y. Tanizaki (1970), *Z. Phys. Chem. N.F.*, 71, 230
- T. Hoshi, Y. Yoshino, H. Funami, H. Kadoi and H. Inoue (1972),  
*Ber. Bunsenges. Phys. Chem.*, 76, 888
- F.B. Howard and H.T. Miles (1965), *J. Biol. Chem.*, 240, 801
- W. Hug and I. Tinoco (1973), *J. Am. Chem. Soc.*, 95, 2803
- H. Inoue, T. Hoshi, T. Masamoto, J. Shiraishi and Y. Tanizaki  
(1971), *Ber. Bunsenges. Phys. Chem.*, 75, 441
- W.H. Inskeep, D.W. Miles and H. Eyring (1972), *J. Chem. Phys.*,  
57, 2736
- J.H. Jaffe, H. Jaffe and K. Rosenbeck (1967), *Rev. Sci.*  
*Instrum.*, 38, 935
- G.A. Jeffrey and Y. Konoshita (1963), *Acta Cryst.*, 16, 20
- H. Jensen and M. Friedrich (1927), *J. Am. Chem. Soc.*, 49, 1049
- W.C. Johnson and I. Tinoco (1969), *Biopolymers*, 7, 727
- D.E. Joyce and T. Kurucsev (1974), *Biophysical Chem.*, 2, 273
- W. Kauzmann (1957), "Quantum Chemistry", (Academic Press)
- G.R. Kelly (1974), Ph.D. Thesis, Adelaide University
- G.R. Kelly and T. Kurucsev (1975), *Europ. Polymer J.*, 11, 581
- G.R. Kelly and T. Kurucsev (1976), *Biopolymers*, 15, 1481
- J.N. Kikkert, G.R. Kelly and T. Kurucsev (1973), *Biopolymers*,  
12, 1459
- T. Kitagawa (1968), *J. Mol. Spectr.*, 26, 1
- J. Kolc and J. Michl (1974), *J. Mol. Spectr.*, 51, 298
- S. Konev (1967), "Fluorescence and Phosphorescence of Proteins  
and Nucleic Acids", (Plenum)

- O. Kratky (1933), *Kolloid-Z.*, 64, 213
- S. Krimm, C.Y. Liang and G.B.B.M. Sutherland (1956), *J. Polymer Sci.*, 22, 227
- W. Kuhn and F. Gruen (1942), *Kolloid-Z.*, 101, 248
- T. Kurucsev and J.R. Zdysiewicz (1971), *Biopolymers*, 10, 593
- Y. Kyogoku, S. Higuchi and M. Tsuboi (1967), *Spectr. Acta*, 23A,  
969
- M. Lamotte, J. Jousset-Dubien, M.J. Mantione and P. Clauerie  
(1974), *Chem. Phys. Lett.*, 27, 515
- M. Lamotte (1975), *J. Chim. Phys.*, 71, 803
- G. Lancelot (1975), *Mol. Phys.*, 29, 1099
- M.A. Lasheen and I.H. Ibrahim (1975), *Acta Cryst.*, A31, 136
- P.D. Lawley (1971), in D.J. Brown, Ed., "Fused Pyrimidines.  
Part II: Purines", (Wiley)
- C.G. Lefevre and R.J.W. Lefevre (1955), *Rev. Pure Appl. Chem.*,  
5, 261
- R.J.W. Lefevre, L. Radom and G.L.D. Ritchie (1968), *J. Chem.  
Soc. B*, 775
- T.P. Lewis and W.A. Eaton (1971), *J. Am. Chem. Soc.*, 93, 2054
- D. Lichtenberg, F. Bergmann and Z. Niemann (1971), *J. Chem.  
Soc. C*, 1676
- V.A. Lipasova and R.N. Nurmukhametov (1976), *Opt. Spectr.*, 40, 228
- F. London (1937), *Trans. Farad. Soc.*, 33, 8
- R.C. Lord and G.J. Thomas (1967), *Spectr. Acta*, 23A, 2551
- G.R. Luckhurst and R.N. Yeates (1976), *Mol. Cryst. Liq. Cryst.*,  
34, 57
- R. Mason (1970), *Perspectives in Structural Chemistry*, 3, 59

- S. Mataga and N. Mataga (1959), Z. Phys. Chem. N.F., 19, 231
- E. Matzat (1972), Acta Cryst., B28, 415
- J. Michl, E.W. Thulstrup and J.H. Eggers (1970, J. Phys. Chem.,  
74, 3878
- J. Michl, E.W. Thulstrup and J.H. Eggers (1974), Ber. Bunsenges.  
Phys. Chem., 78, 575
- J. Michl and J.H. Eggers (1974), Tetrahedron, 30, 813
- D.W. Miles, R.K. Robins and H. Eyring (1967), Proc. Nat. Acad.  
Sci. U.S.A., 57, 1139
- H.T. Miles (1964), Proc. Nat. Acad. Sci. U.S.A., 51, 1104
- J.F. Muller, D. Cagniant, O. Chalvet, D. Lavalette, J. Kolc  
and J. Michl (1974), J. Am. Chem. Soc., 96, 5038
- J.N. Murrell (1963), "The Theory of the Electronic Spectra of  
Organic Molecules", (Methuen)
- J. Nehring and A. Saupe (1969), Mol. Cryst. Liq. Cryst., 8, 403
- B. Norden (1971), Chem. Scripta, 1, 145
- B. Norden and A. Davidsson (1972), Acta Chem. Scand., 26, 842
- B. Norden (1975), Chem. Scripta, 7, 167
- B. Norden and A. Davidsson (1976), Chem. Phys. Lett., 37, 433
- K. Ozeki, N. Sakabe and J. Tanaka (1969), Acta Cryst., B25, 1038
- R.G. Parr (1964), "The Quantum Theory of Molecular Electronic  
Structure", (Benjamin)
- W. Pfleiderer and G. Nuebel (1961), Annalen, 647, 155
- N.V. Platonova, K.R. Popov, I.I. Shamolina and L.V. Smirnov (1970)  
Opt. Spectr., 29, 254
- J.A. Pople and D.L. Beveridge (1970), "Approximate Molecular  
Orbital Theory", (McGraw-Hill)

- K.R. Popov and L.V. Smirnov (1962), *Opt. Spectr.*, 13, 155
- K.R. Popov and L.V. Smirnov (1971), *Opt. Spectr.*, 30, 341
- K.R. Popov (1975a), *Opt. Spectr.*, 38, 102
- K.R. Popov (1975b), *Opt. Spectr.*, 39, 142
- K.R. Popov (1975c), *Opt. Spectr.*, 39, 285
- K.R. Popov (1975d), *Opt. Spectr.*, 39, 368
- J.G. Pritchard (1970), "Polyvinylalcohol", (MacDonald, London)
- A. Pullman and B. Pullman (1968), *Adv. Quantum Chem.*, 4, 263
- W. Rhodes and M. Chase (1967), *Rev. Mod. Phys.*, 39, 348
- C.C.J. Roothaan (1951), *Rev. Mod. Phys.*, 23, 69
- I.G. Ross, P.J. Chappell and M.J. Robey (1976), Papers given  
at 10th Australian Spectroscopy Conference, Perth
- E. Sackmann and H. Moehwald (1972), *Chem. Phys. Lett.*, 12, 467
- E. Sackmann and H. Moehwald (1973), *J. Chem. Phys.*, 58, 5407
- W. Saenger (1973), *Ang. Chem. Int. Ed.*, 12, 591
- A.M. Sarzhevskii (1963), *Opt. Spectr. Suppl.* 1, 34
- G.W. Schael (1968), *J. Appl. Polymer Sci.*, 12, 903
- T. Shimanouchi, M. Tsuboi and Y. Kyogoku (1964), *Adv. Chem.  
Phys.*, 7, 447
- J. Siodmiak and D. Frackowiak (1972), *Photochem. Photobiol.*,  
16, 173
- L.V. Smirnov (1952), *Zh. Eksp. Teor. Fiz.*, 23, 68
- L.C. Snyder, R.G. Shulman and D.B. Neumann (1970), *J. Chem.  
Phys.*, 53, 256
- R.S. Stein and B.E. Read (1969), *Appl. Polymer Symp.*, 8, 255
- R.F. Stewart and N. Davidson (1963), *J. Chem. Phys.*, 39, 255
- R.F. Stewart and L.H. Jensen (1964), *J. Chem. Phys.*, 40, 2071
- R.F. Stewart and L.H. Jensen (1967), *Acta Cryst.*, 23, 1102

- H. Susi and J.S. Ard (1971), *Spectr. Acta*, 27A, 1549
- D.J. Sutor (1958a), *Acta Cryst.*, 11, 83
- D.J. Sutor (1958b), *Acta Cryst.*, 11, 453
- Y. Tanizaki (1959), *Bull. Chem. Soc. Japan*, 32, 75
- Y. Tanizaki (1965), *Bull. Chem. Soc. Japan*, 38, 1798
- Y. Tanizaki and S. Kubodera (1967), *J. Mol. Spectr.*, 24, 1
- Y. Tanizaki, M. Kobayashi and T. Hoshi (1972), *Spectr. Acta*,  
28A, 2351
- Y. Tanizaki, H. Hiratsuka and T. Hoshi (1972), *Spectr. Acta*,  
28A, 2367
- G. Temple (1960), "Cartesian Tensors", (Methuen)
- E.W. Thulstrup, J. Michl and J.H. Eggers (1970), *J. Phys. Chem.*, 74, 3868
- E.W. Thulstrup, M. Vala and J.H. Eggers (1970), *Chem. Phys. Lett.*, 7, 31
- E.W. Thulstrup, P.L. Case and J. Michl (1974), *Chem. Phys.*, 6,  
410
- E.W. Thulstrup, J. Michl and C. Jutz (1975), *J. Chem. Soc. Farad. II*, 71, 1618
- E.W. Thulstrup, M. Nepras, V. Dvorak and J. Michl (1976), *J. Mol. Spectr.*, 59, 265
- I. Tinoco (1967), *J. Chim. Phys.*, 65, 91
- M. Tsuboi, S. Takahashi and I. Harada (1973), in J. Duchesne, Ed., "Physico-Chemical Properties of Nucleic Acids", Vol. 2, (Academic Press)
- M. Tsuboi (1974) in P.O.P. Ts'o, Ed., "Basic Principles in Nucleic Acid Chemistry", Vol. 1, (Academic Press)
- T. Tsunoda and Y. Yamaoka (1965), *J. Polymer Sci.*, A3, 3691

- W. Voelter, R. Records, E. Bunnenberg and C. Djerassi (1968),  
J. Am. Chem. Soc., 90, 6163
- D. Voet, W.B. Graetzer, R.A. Cox and P. Doty (1963),  
Biopolymers, 1, 193
- M.F. Vuks (1966), Opt. Spectr., 20, 361
- D.G. Watson, R.M. Sweet and R.E. Marsh (1965), Acta Cryst.,  
19, 573
- R.C. Weast, Ed. (1971), "Handbook of Chemistry and Physics",  
52nd Ed., (Chemical Rubber Co.)
- A.N. Winchell (1954), "Optical Properties of Organic Compounds",  
2nd Ed., (Academic Press)
- A. Wittwer and V. Zanker (1959), Z. Phys. Chem. N.F., 22, 417
- A. Yogev, L. Margulies and Y. Mazur (1971), Chem. Phys. Lett.,  
8, 157
- A. Yogev, L. Margulies, J. Sagiv and Y. Mazur (1974), Rev. Sci.  
Instr., 45, 386
- D.W. Young, P. Tollin and H.R. Wilson (1969), Acta Cryst., B25,  
1423
- V. Zanker and A. Wittwer (1960), Z. Phys. Chem. N.F., 24, 183
- V. Zanker and J. Preuss (1969), Bull. Soc. Roy. Liege, 38, 673
- R. Zbinden (1964), "Infrared Spectroscopy of High Polymers",  
(Academic Press)
- N.V. Zheltovskii and V.I. Danilov (1974), Biophysics, 19, 802
- L. Ziegler and A.C. Albrecht (1974), J. Chem. Phys., 60, 3558
- H. Zimmerman and N. Joop (1961), Z. Elektrochem., 65, 61